سُورَةُ الْعَلَقِ مَكِّيَّةٌ وَهِيَ تِسْعَ عَشْرَةَ آيَةً

بِسْمِ اللّٰهِ الرَّحْمٰنِ الرَّحِيْمِ

اِقْرَاْ بِاسْمِ رَبِّكَ الَّذِيْ خَلَقَ ۚ ﴿١﴾ خَلَقَ الْاِنْسَانَ مِنْ عَلَقٍ ۚ ﴿٢﴾
اِقْرَاْ وَرَبُّكَ الْاَكْرَمُ ۙ ﴿٣﴾ الَّذِيْ عَلَّمَ بِالْقَلَمِ ۙ ﴿٤﴾ عَلَّمَ
الْاِنْسَانَ مَا لَمْ يَعْلَمْ ۚ ﴿٥﴾

(صدق الله العظيم)

ProQuest LLC.
789 East Eisenhower Parkway
P.O. Box 1346
Ann Arbor, MI 48106 – 1346

To my father, mother, father in law, mother in law,
brothers and sisters
with a special note of thanks.
To my Wife Ghada and my Son Omar
With Love.

A Two Parameter Characterisation of Defects (With Reference to Pipe Work)

By

Abduladeim Mohamad Al-Ani

Submission for Degree of
Doctor of Philosophy
(Ph.D.)

University of Glasgow
Department of Mechanical Engineering
Glasgow
Scotland

March-1991

Table of Contents

Chapter (4) : Elastic-Plastic Fracture Mechanics: (Two Parameter Characterisation)

Chapter (5) : Three Term Boundary Layer Formulation Characterisation of the Crack Tip Field.

Chapter (6) :Elastic-Plastic Fracture Toughness Parameter (Experimental Tests)

Acknowledgements.

I am pleased to be able to express my indebtedness and my sincere thanks to my supervisor, Professor J.W. Hancock. I owe my deepest gratitude and appreciation for his invaluable supervision advice, and constant encouragement throughout the work.

Acknowledgements are due to Hibbitt Karlsson and Sorensen in access to ABAQUS under Academic license.

I am pleased to thank the staff of the Mechanical Engineering Department, Mr Alex Torry and Mr Neil Flaherty for their valuable help in the experimental work.

A special note of thanks is due to my family, in particularly my father, my mother my father in law, my mother in law, my wife, my brothers and my sisters, for their boundless patience and continual encouragement.

A special note of thanks is due to my brothers Motlak and Naser for their encouragement and support.

Finally, great thanks are reserved for the government of the Republic of IRAQ for their continual financial support.

Summary:

The work described in this thesis comprises an investigation into the effect of the non-singular elastic stresses (T and S) on elastic-plastic crack tip deformation.

A necessary preliminary of the present work involved calculating the T stress for a wide range of single edge cracked geometries loaded in tension and bending. Direct stress and displacement methods have been used to calculate the T stress. The effect of the T stress on J dominance for these geometries has been investigated and the stress fields ahead of the crack tip were compared with modified boundary layer formulations involving K and T, following Larsson and Carlsson (1973) and Betegón and Hancock (1990).

Part of the work presented in this thesis comprises of an experimental investigation on the effect of the crack depth on fracture toughness and a (J-T) and (δ-T) locus for three point bend specimens has been produced. Experimental tests were carried out on a carbon-manganese structural steel grade 50D under a range of temperatures from room temperature (+23C) to liquid nitrogen temperatures (-196C).

Previous investigations involved two dimensional plane strain geometries in which only the effect of the T stress was considered. However for three dimensional geometries such as those involving semi-elliptical cracks and circumferential cracks, it is important to understand the effect of the out of plane (S) stress on the crack tip stress field. The effect of the out of plane stress (S stress) has been investigated using both modified boundary layer formulations and full field solutions. For modified boundary layer formulations the displacement

field associated with the elastic singular term K and the two non-singular terms T and S were imposed as a boundary condition at a distance remote from the crack tip. Modified boundary layer formulations were compared with full field solutions involving two different types of axisymmetric geometries, namely the circumferential crack in a round bar and central crack in a round bar. These geometries were chosen to represented different values of the S and T stress.

The present work also includes an estimation of the non-singular terms S and T for circumferential crack in pipes. Two analyses were considered, a continuum model and line spring model. The results of the two models were in a good agreement with each other.

As a first attempt to provide a completely workable fracture design approach based on the J -T locus curve, the T stress for a semi-elliptical crack has been derived using a line spring analysis. The geometry chosen for this calculation was an internal circumferential and longitudinal semi-elliptical cracks allocated in an internally pressurised cylinder.

Chapter (1)

Linear Elastic Fracture Mechanics

1.1. Introduction:

The purpose of fracture mechanics is to provide a fundamental understanding of the processes causing fracture in solids and to predict the critical condition at which failure occurs. This is complemented by an engineering requirement to provide measurable parameters which characterise fracture, and which can be evaluated from a knowledge of the geometry and loading of the structure.

Fracture mechanics is divided into two areas; linear elastic fracture mechanics (LEFM) and elastic-plastic fracture mechanics (EPFM). In the first section of this thesis the basic concepts of linear elastic fracture mechanics and its application to the prediction of failure are presented. The review is given in the form of a discussion of the fundamental concepts of the elastic strain energy release rate and stress intensity factor which form the foundation of linear elastic fracture mechanics.

1.2. The elastic strain energy release rate:

The energetics of crack advance were first considered by Griffith (1920). Griffith derived a fracture criterion based on the concept, that as a crack extends, elastic strain energy is released to create the new surface which absorbs the energy. If the energy release rate is greater than or equal to the energy consumption rate, crack propagation is energetically favourable. In his analytical model Griffith considered an infinite plate with unit thickness having fixed boundary conditions

and containing a through thickness crack of length 2a, loaded with a remote tensile stress, σ. Griffith calculated the elastic energy release of the system U_e as

$$U_e = \frac{1}{2} \frac{\sigma^2 \pi a^2}{E'} \tag{1}$$

where a is the half crack length, σ is the nominal applied stress. $E' = E$, for plane stress while $E' = E/(1-\upsilon^2)$ for plane strain, where υ is Poisson's ratio and E is Young's modulus.

The work W to create the surfaces of the crack is

$$W = 2a\gamma \tag{2}$$

where γ is the surface energy per unit area. Fracture occurs when

$$\frac{\partial U_e}{\partial a} \geq \frac{\partial W}{\partial a} \tag{3}$$

i.e

$$\frac{\partial U_e}{\partial a} \geq 2\gamma \tag{4}$$

$\partial U_e/\partial a$ is known as the strain energy release rate and given the symbol G

$$G = \frac{\partial U_e}{\partial a} = \frac{\sigma^2 \pi a}{E'} \tag{5}$$

The strain energy release rate is a fracture characterising

parameter such that fracture can take place when G reaches a critical value G_c, related to the critical stress at fracture σ_c by :

$$\sigma_c = \sqrt{\frac{E\,G_c}{\pi\,a}} \qquad (6)$$

As pointed out by Irwin (1948), Griffith's theory strictly applies to a perfectly brittle material in which there is no plasticity at the crack tip. In order to apply the strain energy criterion to materials which exhibit plastic deformation, one has to modify the energy balance to account for the effect of plastic deformation. This modification follows a suggestion of Irwin (1948) by replacing the surface energy by a term denoting the total work done against the resistance of material to fracture which consists of both surface energy and plastic terms γ_e and γ_p .

$$G_c = \frac{\partial U_e}{\partial a} = \frac{\sigma^2\,\pi\,a}{E} = 2\,(\gamma_e + \gamma_p) \qquad (7)$$

The validity of this modification is restricted to conditions in which the plastic zone developed at the crack tip is significantly smaller than the dimensions of the cracked body. Linear elastic fracture mechanics is therefore concerned with fracture at a stress level very much less than the yield stress when the body is largely elastic and crack tip plasticity is still small enough to be viewed and treated as a small perturbation of the local stress field.

Irwin and Kies (1952) demonstrated that if a crack extends by an infinitesimal amount (da) the work done by the stress field is equivalent to the change in strain energy (G B da). Fracture occurs if

the elastic strain energy release rate U_e is equal to the work done by a remotely applied load P to create an incremental displacement Δ

$$U_e = \frac{P\Delta}{2} = \frac{P^2 C}{2} \tag{8}$$

If C is the linear elastic compliance of the specimen, the strain energy release rate is then given as:

$$G_c = \frac{\partial U_e}{\partial a} = \frac{P^2}{2}\frac{dc}{da} \tag{9}$$

This now allows the critical strain energy release rate to be determined either experimentally or numerically from the rate of change of the compliance of a cracked body

1.3. The Stress Intensity Factor:

In linear elastic fracture mechanics the stress ahead of the crack tip can be written as a series following Willams(1957).

$$\sigma_{ij} = A_{ij}(\varnothing)\ r^{-1/2} + B_{ij}\ (\varnothing) + C_{ij}(\varnothing)\ r^{1/2} + ... \tag{10}$$

The first term in the expansion is singular at the crack tip, whereas the remaining terms are finite and bounded. By considering an analysis due to Westergaard (1939), Irwin (1957) noted that the asymptotic linear elastic solution for all cracks can be written in a general form by considering only the first term in the series, and ignoring higher order terms as,

$$\sigma_{ij} = \frac{K}{\sqrt{2\pi r}} f_{ij}(\phi) \tag{11}$$

Here $f_{ij}(\phi)$ are universal functions of ϕ which are independent of the overall geometry of the problem. K is a parameter called the stress intensity factor which measures the strength of the elastic singularity. Dimensional analysis shows that K must linearly related to the stress and directly proportional to the square root of a characteristic dimension such as the crack length.

There are three modes to describe the displacements of the crack surface during crack growth, see Fig (1.1). These comprise of an opening mode, in which the crack surfaces move directly apart, an edge sliding mode in which the crack surfaces move normal to the crack front while remaining in the crack plane and a shear mode in which the crack surface moves parallel to crack front while remaining in the crack plane. In practice mode I is usually the most important and further discussion is limited to mode I. For mode I loading under plane strain conditions, the stresses and displacements in the vicinity of the crack tip can be expressed in terms of the stress intensity factor K by.

$$\begin{bmatrix} \sigma_{xx} \\ \sigma_{yy} \\ \tau_{xy} \end{bmatrix} = \frac{K}{\sqrt{2\pi r}} \cos\frac{\phi}{2} \begin{bmatrix} 1-\sin\frac{\phi}{2}\sin\frac{3\phi}{2} \\ 1+\sin\frac{\phi}{2}\sin\frac{3\phi}{2} \\ \sin\frac{\phi}{2}\cos\frac{3\phi}{2} \end{bmatrix} \tag{12}$$

For plane strain $\sigma_{zz} = \upsilon(\sigma_{xx} + \sigma_{yy})$ while for plane stress condition

$\sigma_{zz} = 0$. Similarly the displacements (u,v,w) can be written as :

$$\begin{bmatrix} u \\ v \\ w \end{bmatrix} = \frac{(1+\upsilon)\,K}{E}\sqrt{\frac{r}{2\pi}}\begin{bmatrix} \cos(\frac{\phi}{2})\,[2-4\upsilon+2\,\sin^2(\frac{\phi}{2})] \\ \sin(\frac{\phi}{2})\,[4-4\upsilon-2\,\cos^2(\frac{\phi}{2})] \\ 0 \end{bmatrix} \tag{13}$$

In plane stress the displacements can be written as :

$$\begin{bmatrix} u \\ v \end{bmatrix} = \frac{(1+\upsilon)\,K}{E}\sqrt{\frac{r}{2\pi}}\begin{bmatrix} \cos(\frac{\phi}{2})[\frac{3-\upsilon}{1+\upsilon} - 1 + 2\,\sin^2(\frac{\phi}{2})] \\ \sin(\frac{\phi}{2})[\frac{3-\upsilon}{1+\upsilon} + 1 - 2\,\cos^2(\frac{\phi}{2})] \end{bmatrix} \tag{14}$$

$$w = -\frac{\upsilon Z}{E}(\sigma_{xx} + \sigma_{yy}) \tag{15}$$

It is to be noted that the critical stress intensity indicates that crack extension occurs when K attains a critical value K_c known as the fracture toughness of material. For example for a central crack in an infinite plate K is equal to ($\sigma\sqrt{(\pi a)}$) and crack extension occurs when

$$\sigma\sqrt{\pi a} \geq \sigma_c\sqrt{\pi a} = K_c \tag{16}$$

A more general expression for K is given by

$$K = f(\frac{a}{W})\,\sigma\sqrt{\pi a} \tag{17}$$

f(a/W) is a function which is dependent on the specimen geometry,

crack shape and boundary conditions. There are many methods to determine stress intensity factors, including experimental, theoretical and finite element methods. As a result a wide range of solutions for two and three dimensional configuration are now available in the literature eg. Rooke and Cartwright (1976) and Tada et al (1973).

The strain energy release rate G fundamental to Griffith's work can be identified with the stress intensity factor K through the relation

$$G = \frac{1 + \kappa}{8\mu} K^2 \qquad (18)$$

where μ is the shear modulus and κ is a function of Poisson's ratio (υ)

$$\kappa = 3 - 4\upsilon \qquad \text{for plane strain}$$

$$\kappa = \frac{3 - \upsilon}{1 + \upsilon} \qquad \text{for plane stress}$$

1.4. Crack Tip Plasticity

Linear elastic fracture mechanics is limited by the requirement that crack tip plasticity is surrounded by a controlling elastic field. The regime in which crack tip plasticity is small compared to crack length or ligament length is known as contained or small scale yielding (SSY).

Irwin (1960) pointed out that at a first estimate the radius of the plastic zone r_y can be made by applying the Tresca or Von Mises yield criterion to the elastic field ahead of the crack. This can be done conveniently if the stress in the Westergaard equations are given as principal stresses σ_1 , σ_2 and σ_3 .

$$\sigma_1 = \frac{K}{\sqrt{2\pi r}} \cos\frac{\phi}{2}\left(1+\sin\frac{\phi}{2}\right)$$

$$\sigma_2 = \frac{K}{\sqrt{2\pi r}} \cos\frac{\phi}{2}\left(1-\sin\frac{\phi}{2}\right) \qquad (19)$$

The third principal stress depends on whether plane stress or plane strain conditions apply.

For plane stress $\sigma_3 = 0$ and the Tresca yield criterion becomes

$$\sigma_1 - \sigma_3 = \frac{K}{\sqrt{2\pi r}} \cos\frac{\phi}{2}\left(1+\sin\frac{\phi}{2}\right) = \sigma_o \qquad (20)$$

Here σ_o is the yield stress in uniaxial tension.

The radius of the plastic zone r_y can then be given as :

$$r_y = \frac{1}{2\pi}\left(\frac{K}{\sigma_o}\right)^2 \cos^2\frac{\phi}{2}\left(1+\sin\frac{\phi}{2}\right)^2 \qquad (21)$$

In plane strain the Tresca yield criterion is

$$\sigma_1 - \sigma_2 = \sigma_o \qquad (22)$$

From which the plastic zone radius r_y can be written as

$$r_y = \frac{1}{2\pi}\left(\frac{K}{\sigma_o}\right)^2 \sin^2\phi \qquad (23)$$

A comparison of the size and shape of the plastic zone for plane stress and plane strain is shown in Fig (1.2). It is clear that the plastic

zone in plane strain is smaller than that in plane stress. The ratio of the plastic zone radius r_y to the thickness of the specimen B, determines whether plane stress or plane strain is applicable. If (r_y/B) is very much less than unity, a plane strain state exists. As the material thickness increases, plane strain conditions dominate and lead to a minimum plane strain fracture toughness K_{Ic} ,which is a material constant. Detailed methods for determining K_{Ic} experimentally are given by ASTM (1974) and BS 5447(1978) who have defined standard methods for plane strain fracture toughness testing. These standard test methods require that certain conditions must be met to ensure that both small scale yielding and plane strain conditions apply. Both are determined by reference to the maximum radius of the plastic zone. To ensure that both plane strain and small scale yielding condition apply, the specimen dimensions are required to be large compared to the size of the plastic zone. The standards give the size requirements as:

$$B,\ a\ > 2.5\ (\frac{K}{\sigma_o})^2$$

$$B,\ a,\ W\text{-}a\ > 2.5\ (\frac{K}{\sigma_o})^2 \qquad (24)$$

Here a, (W-a), and B are the crack length, the ligament length and the thickness of the specimen respectively. Although the value of K_{Ic} can be determined from a wide range of specimen geometries, certain types of specimen are preferred because they require smaller loads than others. Preferred specimen geometries include the three and four point bend tests and compact tension specimens illustrated in Fig (1.3). Whatever the geometry, the specimen has to contain a sharp crack

which is produced by fatigue loading under standard conditions.

The critical stress intensity factor K_{Ic} characterises the condition at which crack extension starts. Theoretically, in a perfectly brittle solid, crack extension is expected to continue as long as the stress intensity factor K, resulting from the applied loading, is greater than, or equal to the critical value K_{Ic}.

1.5. References

American Society for Testing and Materials ASTM., (1974), 'Standard Method for Plane Strain Fracture Toughness Testing, E399-74.

British Standard (1978)' A Method For Test For Plane Strain Fracture Toughness Testing Of Metallic Material. The British Standards Institution 5447.

Griffiths, A. A., (1920), Phil Trans Roy Soc, A221, 163.

Irwin, G. R. (1948), "Fracture Dynamics., Fracturing of Metal,147, ASM Publ.

Irwin, G. R. and Kies J. A., (1952), Weld Res Suppl., 17and 95S.

Irwin, G. R. (1957), J. Appl. Mech., 24, 361

Irwin, G. R. (1960), in "Structural Mechanics" 557, Pergamon, New York.

Rooke, D. P and Cartwright, D. J., (1976), Compendium of stress intensity factor,London, H. M. S. O.

Tada, H., Paris, P. and Irwin, G., (1973), The Stress Analysis of Cracks Handbook, Hellertown, Pennsylvania, Del Research Corporation.

Westergaard; H. M., (1939), J. Appl. Mech., 61, 49.

Williams, M. L., (1957), J. Appl. Mech., 24, 111.

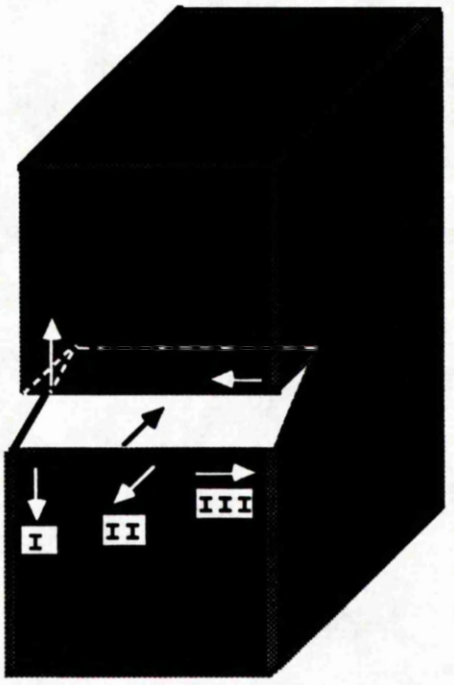

I Opening Mode

II Edge Sliding Mode

III Shear Mode

Fig (1.1) : Basic modes of the crack surface displacement.

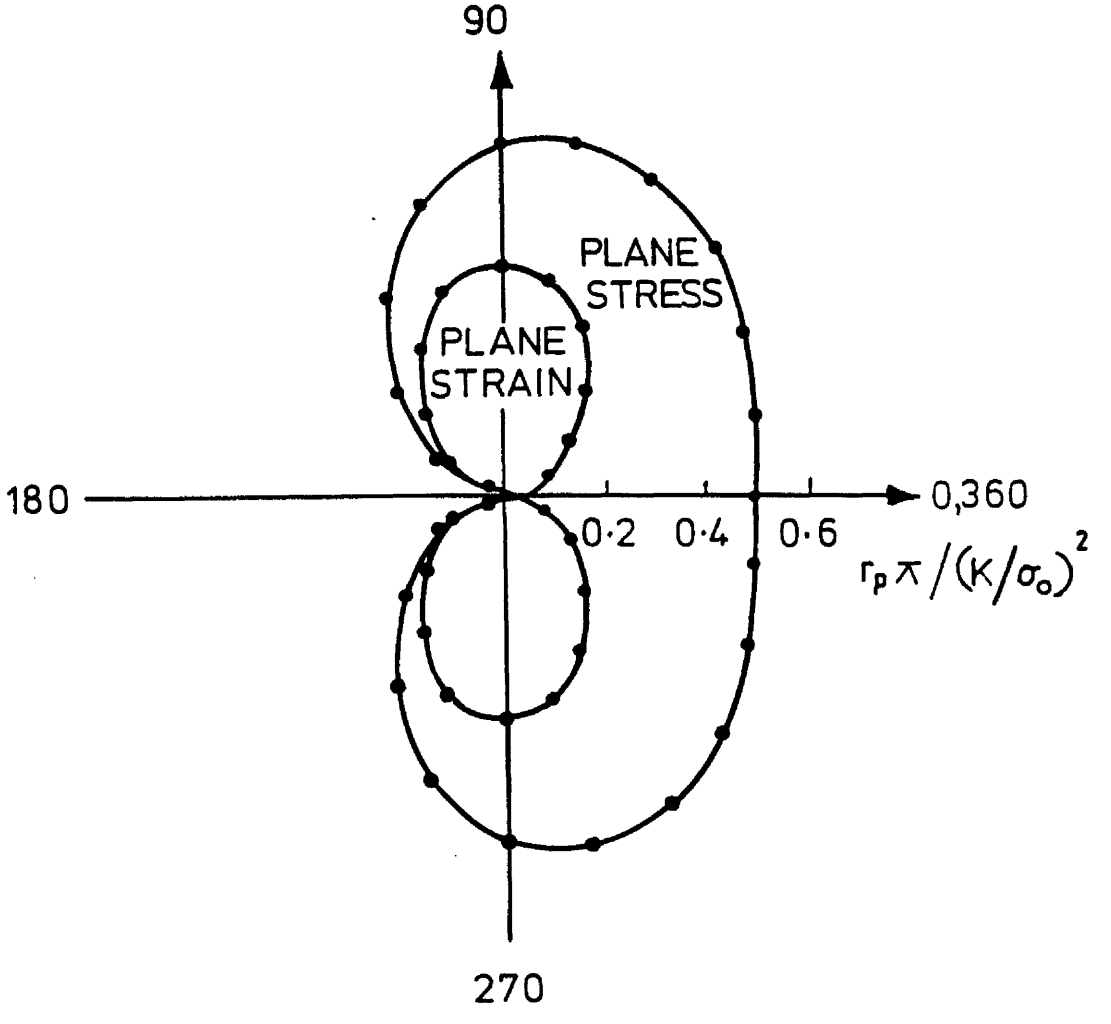

Fig (1.2) : Plane strain plastic zone

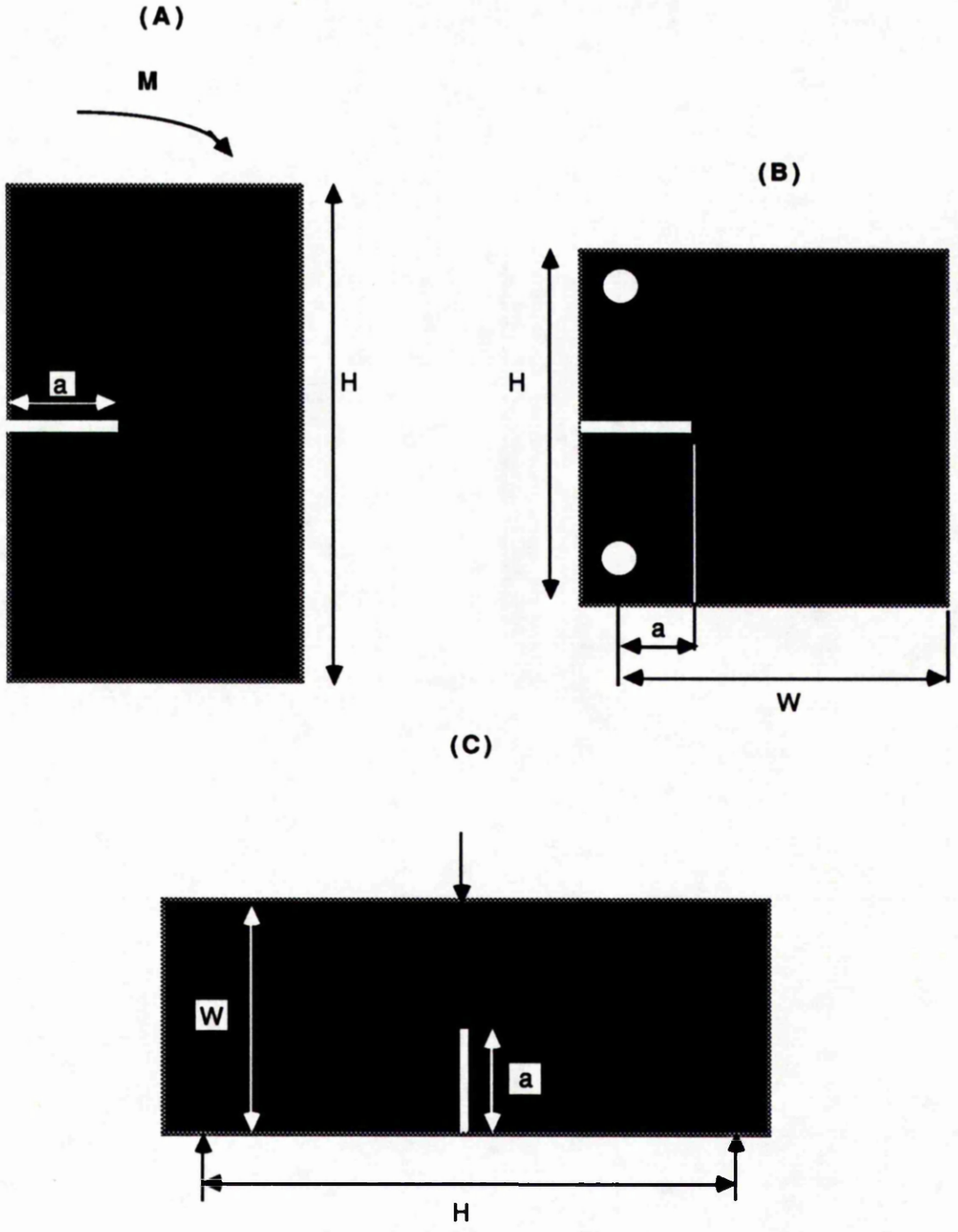

Fig (1.3) : Some Fracture specimen geometries:
(A) Single edge notched bend bar (SENB).
(B) Compact tension (CT).
(C) Three point bend (3PB).

Chapter (2)

The Elastic T-Stress

2.1. Introduction

Larsson and Carlsson (1973) determined the plastic zone size and shape for compact tension, bend, double edge-cracked and centre-cracked specimens using a finite element method. Their plane strain elastic-plastic finite element calculations, demonstrated that the plastic zone size differed between the various geometries by 10 to 30 per cent, even within the ASTM limits. Following a suggestion of Rice (1972) they attributed these results to the role of the first non-singular term in the Willams (1957), expansion.

$$\sigma_{ij} = \frac{K}{\sqrt{2\pi r}} f(\phi) + B_{ij}(\phi)\, r^{0} + C_{ij}(\phi)\, r^{1/2} + \cdots \tag{1}$$

Rice (1974) denoted the first non-singular term $B_{ij}(\phi)\, r^{0}$ as the T-stress

$$\begin{bmatrix} \sigma_{11} & \sigma_{12} \\ \sigma_{21} & \sigma_{22} \end{bmatrix} = \frac{K}{\sqrt{2\pi r}} \begin{bmatrix} f_{11}(\phi) & f_{12}(\phi) \\ f_{21}(\phi) & f_{22}(\phi) \end{bmatrix} + \begin{bmatrix} T & 0 \\ 0 & 0 \end{bmatrix} \tag{2}$$

Close to the crack tip, the non-singular terms can be separated into two parts. The first part ($B_{ij}(\phi)\, r^{0}$), is independent of r and finite at the crack tip, while the higher order terms ($C_{ij}(\phi)\, r^{1/2} + \cdots$), which are dependent on r, disappear at the crack tip (r=0).

$$\lim_{r \to 0} \quad C_{ij}(\varnothing)\, r^{1/2} = 0 \tag{3}$$

The only non-singular component remaining at the crack tip is ($B_{ij}(\varnothing)$ r^0), which is the T-stress.

Solutions for the elastic T-stress for a range of geometries have been given by Leevers and Radon (1983), Kfouri (1986), and Sham (1989) and Al-Ani (1988). The results are usually expressed in terms of a biaxiality parameter ß

$$\beta = \frac{T\sqrt{\pi a}}{K} \tag{4}$$

Published results for single edge cracked geometries in tension and bending as a function of a/W ratio given by Sham (1989) are presented in Table (2.1). The biaxiality parameter of a single edge crack in a semi-infinite plate is given by Harlin and Willis (1988) and Betegón and Hancock (1990) as (-0.485). The latter also gave the β value for a crack approaching the edge of a semi-infinite half space using a form involving the ligament c.

$$\beta = \frac{T\sqrt{\pi c}}{K} \tag{5}$$

For this limiting problem pure stretch conditions give rise to negative biaxialties β which changed from negative to positive when the moment become the controlling term in the ligament.

A necessary preliminary of the present work involved calculating the T-stress for a wide range of single edge crack geometries loaded in tension and bending. The present results are compared with those given

by Leevers and Radon (1983), Kfouri (1986), and the contemporaneous results obtained independently by Sham (1989).

2.2. Methods of Calculating the T- Stress:

A number of numerical procedures have been proposed to evaluate the non-singular terms in the Williams expansion. Larsson and Carlsson (1973) determined the T-term directly from an elastic finite element calculation of the stress field in the crack tip region of a full specimen. For a crack lying on the x axis, the stress parallel to the crack flank in the specimen σ_{xx}, and the stress σ_{xx}, for a boundary layer formulation with T= 0, were compared. The boundary layer formulation solution is obtained by modelling the crack tip deformation by a focused mesh of the type shown in Fig (2.1). The displacement field corresponding to the singular elastic field (K field) is imposed as a boundary condition at a distance remote from the tip.

The T-stress for each specimen was obtained as the difference between the stress in the specimen σ_{xx} and the corresponding σ_{xx} in the boundary layer formulation directly ahead of the crack.

$$T = \sigma_{xx}{}_{SPEC} - \sigma_{xx}{}_{BLF} \qquad (6)$$

A method for calculating the T-stress based on a theorem due to Eshelby was suggested by Cardew et al. (1985). It is based on the evaluation of the J contour integral for various combined loadings. The specimen is loaded by an external force system applied at the remote boundary and a point force applied at the crack tip Fig (2.2). The external force produces a deformation field as does the point force. Let J(F) be the value of J when the specimen is loaded by the external force F, J(f,t) the J-integral when the point force f is applied

at the crack tip and is resisted by tractions t applied at the remote boundary and J(F,f,t) is the value of the J-integral corresponding to F,f and t. If the tractions t_0 denote the remote tractions which are statically equivalent to -f in an infinite body, the first form of Eshelby's theorem gives :

$$J(F,f,t_0) = J(F) + \frac{Tf}{E'} \tag{7}$$

When the point force f is resisted by tractions t which differ from tractions t_0, the theorem takes a second form:

$$J(F,f,t) = J(F) + J(f,t) + \frac{Tf}{E'} + \frac{2K_I K_f}{E'} \tag{8}$$

K_I is the stress intensity factor when the load F is applied and K_f is the stress intensity factor when the tractions $(t-t_0)$ are applied on the boundary without the point force f. When $t_0=t$, $J(f,t_0)=0$ and the second form reverts to the first form. The full evaluation and proof of this theorem is given by Kfouri (1986). The T-stress can then be evaluated from the combined and separate load cases.

$$T = \frac{E'}{f}\,[J(F,f,t) - J(F) - J(f,t)] \tag{9}$$

A difficulty arises with this method using ABAQUS as, J can not be determined by the virtual crack extension method when the crack tip is loaded with a force f.

In (1989) Sham used higher order weight functions, in which the elastic T-term can be determined by a work-conjugate integral in the same spirit as determination of the stress intensity factor. These

higher order functions are a generalisation of the Bueckner-Rice function Bueckner (1973) and Rice (1972). The displacements and the stresses of the second term of the expansion are generated by the complex functions $\phi_2(z)$ and $\rho_2(z)$

$$\phi_2(z) = a_2 z, \qquad \rho_2(z) = -a_2 z \tag{10}$$

The complex variable z is defined as x +iy where i is the imaginary unit. The displacement u_2 and v_2 corresponding to the second term are

$$u_2 = \frac{1}{2\mu} a_2 r (\kappa + 1) \cos \phi \tag{11}$$

$$v_2 = \frac{1}{2\mu} a_2 r (\kappa - 3) \sin \phi \tag{12}$$

Here $\kappa = (3-4\upsilon)$ for plane strain and $[(3-\upsilon)/(1+\upsilon)]$ for plane stress.

Similarly the stress components are :

$$(\sigma_{xx})_2 = 4 a_2$$

$$(\sigma_{yy})_2 = 0$$

$$(\sigma_{xy}) = 0 \tag{13}$$

where a_2 is equal to T/4, υ is Poisson's ratio and μ is the shear modulus.

The displacements and stresses for the third term are given by :

$$\phi_3(z) = a_3 z\sqrt{z}\ , \qquad \rho_3(z) = a_3 z\sqrt{z}$$

$$u_3 = -\frac{1}{2\mu} a_3 r\sqrt{r}\ [(\kappa+\frac{1}{2})\cos\frac{3\phi}{2} - \frac{3}{2}\cos\frac{\phi}{2}] \tag{14}$$

$$v_3 = -\frac{1}{2\mu} a_3 r\sqrt{r}\ [(\kappa-\frac{1}{2})\sin\frac{3\phi}{2} - \frac{3}{2}\sin\frac{\phi}{2}] \tag{15}$$

$$(\sigma_{xx})_3 = 3 a_3\sqrt{r}\ \frac{1}{4}[5\cos\frac{\phi}{2} - \cos\frac{3\phi}{2}] \tag{16}$$

$$(\sigma_{yy})_3 = 3 a_3\sqrt{r}\ \frac{1}{4}[3\cos\frac{\phi}{2} + \cos\frac{3\phi}{2}] \tag{17}$$

$$(\sigma_{xy})_3 = -3 a_3\sqrt{r}\ \frac{1}{4}[\sin\frac{\phi}{2} + \sin\frac{3\phi}{2}] \tag{18}$$

The values of a_1, a_2, and a_3 for a single edge cracked bar under tension given by Sham (1989) and are given in Table (2.1).

2.3. Numerical Analyses

Edge cracked bars with a/W ratios varying between 0.03 and 0.9 have been analysed, where a is the crack length and W is the width of the specimen as illustrated in Fig (2.3). Taking advantage of symmetry of the configuration, only half of the specimen above the crack surface was modelled. The crack tip was represented with a focussed mesh of eight noded plane strain isoparametric elements provided by the finite element code ABAQUS (1984). 8 8-noded elements were collapsed at the crack tip to provide 17 initially coincident but independent nodes. Poisson's ratio υ was set at 0.3. The geometries were loaded using uniform tensile stress or a pure moment.

The J value for these geometries was calculated using the virtual crack extension method of Parks (1974) as modified by Li et al (1985)

and implemented in ABAQUS (1984).

As an example, the mesh for an a/W ratio of 0.5 is shown in Fig (2.4). The details of the other finite element geometries are given in Table (2.2).

2.4. Present method of Calculating T-Stress

2.4.1. Stress method

The T-stress can be evaluated directly from the stress or the displacement fields. The crack is located on the x axis of a set cartesian axes (x,y) with its tip at x=0. Alternatively it is some times is convenient to work in cylindrical co-ordinates (r,ø) which are centred at the crack tip, such that the crack lies on the line ø=±π. In this method the stress σ_{xx} in the y=0 plane was determined from an elastic finite element analysis. As r tends to zero, the higher order non-singular terms tend to zero and the only non-singular term left has order r^0. This comprises a uniform stress field parallel to the flanks of the crack. Directly ahead of the crack (ø=0) $f_{ij}(ø)$ is equal to unity, and the T stress can be identified as :

$$T = \lim_{r \to 0} (\sigma_{xx} - \sigma_{yy}) \qquad (ø=0) \tag{19}$$

The biaxiality β is then given by :

$$\beta = \lim_{r \to 0} \frac{(\sigma_{xx} - \sigma_{yy})\sqrt{\pi a}}{K} \qquad (ø=0) \tag{20}$$

The biaxiality parameter ß is obtained by extrapolating a plot of $[(\sigma_{xx} - \sigma_{yy})\sqrt{\pi a}/K]$ to the crack tip. On the flanks of the crack, the

stress σ_{yy} should be zero because it is a free surface, the only term left is the stress σ_{xx}, which is the T- stress.

$$T = \lim_{r \to o} \sigma_{xx} \qquad (\varnothing = \pm \pi) \tag{21}$$

Using equation (20), $[\sigma_{xx} \sqrt{\pi a}/K]$, at each node behind the crack was calculated and plotted as a function of distance r, allowing the biaxiality parameter to be obtained by extrapolation to the crack tip.

2.4.2. Displacement Method:

The displacement in the x and y directions comprises two terms. The first term is related to the singular term in the Williams expansion and is denoted here by u^k. The second term corresponds to the first non-singular term in the William's expansion u^T. The total displacement in x and y directions under plane strain deformation can be written in the form:

$$u = u^k + u^T$$

$$u_x = \frac{K}{E}(1+\upsilon)\sqrt{\frac{r}{2\pi}}\, f_x(\varnothing) + (1-\upsilon^2)\frac{\beta}{E\sqrt{\pi a}} K r \cos(\varnothing) \tag{22}$$

$$u_y = \frac{K}{E}(1+\upsilon)\sqrt{\frac{r}{2\pi}}\, f_y(\varnothing) - \upsilon(1+\upsilon)\frac{\beta}{E\sqrt{\pi a}} K r \sin(\varnothing) \tag{23}$$

The stress intensity factor was calculated by virtual crack extension. Subsequently subtracting u^K from u_x and extrapolating the second term to the crack tip, the biaxiality parameter ß was calculated for each geometry.

2.5. Results

Fig (2.5a) illustrates the difficulties of obtaining biaxiality parameters by direct extrapolation to the crack tip. One of the reasons behind these problems is that due to the finite size of the elements on the crack flank, σ_y is not exactly equal to zero in the numerical solutions, even though it is a free surface. The value of σ_y decreases with increasing distance from the tip as shown in Fig (2.6)

In order to avoid this problem the (*EQUATION) option available in ABAQUS has been used. This technique was used to ensure the correct form of displacement function for the non-singular term. This allows the displacements at the nodes behind the crack tip to be written as a series of linear equations such that the displacement in the flank increases linearly with distance r behind the crack tip, as shown in Fig (2.5b). Fig (2.7) shows the biaxiality parameter ß as a function of a/W for 8 edge cracked specimens with a/W ratios between 0.03 and 0.9 in bending and tension. All the geometries have the same height to width ratio H/W=3. The biaxiality parameter ß was calculated using the stress methods discussed in section 2.3. The present ß values for edge cracked geometries in bending, are plotted against a/W and compared with those given by Kfouri (1986) and Leevers and Radon (1983) Fig (2.8). The comparison shows a good correlation for cracks with an a/W ratio less than 0.4, which have a negative biaxiality ß. Kfouri (1986) and Leevers and Radon (1983) presented the β values corresponding to a/W ratios of between 0.2 and 0.6, with H/W equal to 2. The calculations given in this chapter relate to a whole range of a/W ratios between a 0.03 and 0.9, with an H/w value of 3. Nevertheless it is to be expected that for H/W>2, the data will be insensitive to (H/W) and correspond to an infinitely long bar.

Sham (1989) has also given the biaxiality parameter β for a wide

range of a/W ratios, in tension and bending. These confirm the results shown in Fig (2.9). The results show that cracked geometries with a/W values of less than 0.35 in bending and 0.55 in tension exhibit negative biaxialities, whereas deeply cracked geometries show a positive β value. The effect of the T-stress on elastic-plastic crack tip field will be discussed in detail in chapter (4).

2.6. Conclusion:

Direct stress and displacement methods provide simple methods for calculating the biaxiality parameter β. In the present work a direct stress method has been used. The results show that single edge cracked bars with a/W ratios of less than 0.35 in bending and 0.55 in tension exhibit positive biaxialities β, while geometries with values of a/W less than 0.35 in bending and 0.55 in tension exhibit a negative biaxialities β.

2.7. References:

Al-Ani A.M. (1988) Ms.C thesis Department of Mechanical Engineering University of Glasgow

Betegón, C., and Hancock J., W.,(1990) J. Appl. Mech. in press.

Bueckner, H. F., (1973) in Mechanics of Fracture I, G. C.Sih. (ed), Noordhoff, Leyden, 239-314.

Cardew, G. E., Goldthorpe, M. R. Howard, I. C. and Kfouri, A. P., (1985), (Eshelby Memorial Symposium), Cambridge University Press, 465.

Harlin, G. and Willis, J. R., (1988), Proc. R. Soc. Lond. A415,197.

Hibbitt, Karlsson and Sorensen Inc, (1984), ABAQUS User Manual, Providence., Rhode Island.

James Watt G. U. (1989) Internal report , Mechanical Engineering Department. Glasgow University.

Kfouri, A. P.,(1986), Int. J. Fracture., 30,301.

Larsson, S. G. and Carlsson, A. J., (1973), J. Mech. Phys. Solids, 21, 263.

Leevers, P. S. and Radon, J. C., (1983), Int. J. Fracture.,19,13.

Parks, D. M., (1974), Int. J. of Fracture., 10, 487.

Rice, J. R., (1972), Int. J. Solids. Structures., 8, 751.

Rice, J. R., (1974), J. Mech. Phys. Solids, 22, 17.

Sham, T.-L. (1989), The Determination of the Elastic T-Term using Higher Order Weight Functions. Department of Mechanical Engineering. Troy, New York 12180-3590 ,U.S.A

Williams, M. L., (1957), J. Appl. Mech., 24, 111.

a/W	$\frac{K}{\sigma\sqrt{\pi a}}$	$\frac{T}{\sigma}$	$\frac{H\sqrt{a}}{\sigma}$
Tension			
0.1	1.18784	-0.551628	0.350216
0.3	1.65781	-0.614720	0.127945
0.4	2.10856	-0.585921	-0.393172
0.5	2.82099	-0.432127	-1.712530
0.6	4.02602	0.026811	-5.185730
0.7	6.34693	1.331830	-15.62940
0.8	11.9298	5.972600	-58.03318
0.9	34.5250	35.55360	-419.1170
Pure Bending			
0.1	1.04594	-0.379295	0.11481
0.3	1.12211	-0.826161	-0.52705
0.4	1.25873	0.115729	-1.10974
0.5	1.49507	0.390871	-2.12377
0.6	1.91026	0.827309	-4.18050
0.7	2.72150	1.660700	-9.30452
0.8	4.66564	3.919080	-27.3206
0.9	12.4210	15.73050	-163.410

Table (2.1)

Values of K , T and the Third Term in the Elastic Expansion for SEN Specimen

a/w	No. of Nodes	No. of Element	Degree of Freedom
0.03	1391	414	2782
0.1	577	170	1834
0.2	589	174	1874
0.3	731	218	2334
0.5	699	208	2230
0.7	731	218	2334
0.8	589	174	1874
0.9	577	170	1834

Table (2.2)

Details of the Finite Elements Mesh for SEN Specimens

Pure Bending

a/W	Present Results H/W=3	Kfouri (1985) H/W=2	Leevers & Radon (1982) H/W=2	Betegon (1989) H/W=3	Harlin & Wills (1988)	Sham 1898
0				-0.48	-0.48	
0.03	-0.45					
0.1	-0.425					-0.3626
0.2	-0.27	-0.25	-0.27			-0.228
0.3	-0.125	-0.15	-0.14			-0.0073
0.4		-0.032	+0.02			+0.0092
0.5	+0.25	+0.087	+0.18			+0.2616
0.6		+0.216	+0.38			+0.433
0.7	+0.625					+0.6104
0.8	+0.90					+0.8386
0.9	+1.25					+1.26
1.0						

TENSION

a/W	Present Results H/W=3	Kfouri (1985) H/W=2	Lveers & Radon (1982) H/W=2	Betegon (1989) H/W=3	Harlin & Wills (1988)	Sham 1898
0				-0.48	-0.48	
0.03	-0.45					
0.1	-0.50					-0.463
0.2	-0.475					-0.433
0.3	-0.40					-0.3707
0.4		-0.382	-0.370			-0.277
0.5	-0.125	-0.287	-0.270			-0.152
0.6		-0.172	-0.145			+0.0069
0.7	+0.215	-0.029	+0.013			+0.210
0.8	+0.45					+0.501
0.9	+1.00					+1.03
1.0				-0.73		

Table (2.3)

Results for SENB and SENT Specimens

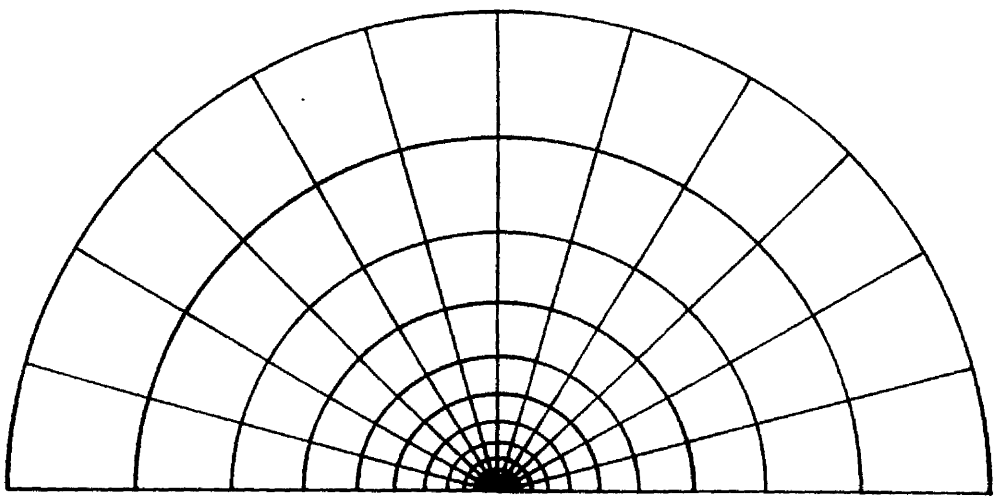

Fig (2.1) : The mesh of the boundary layer formulation

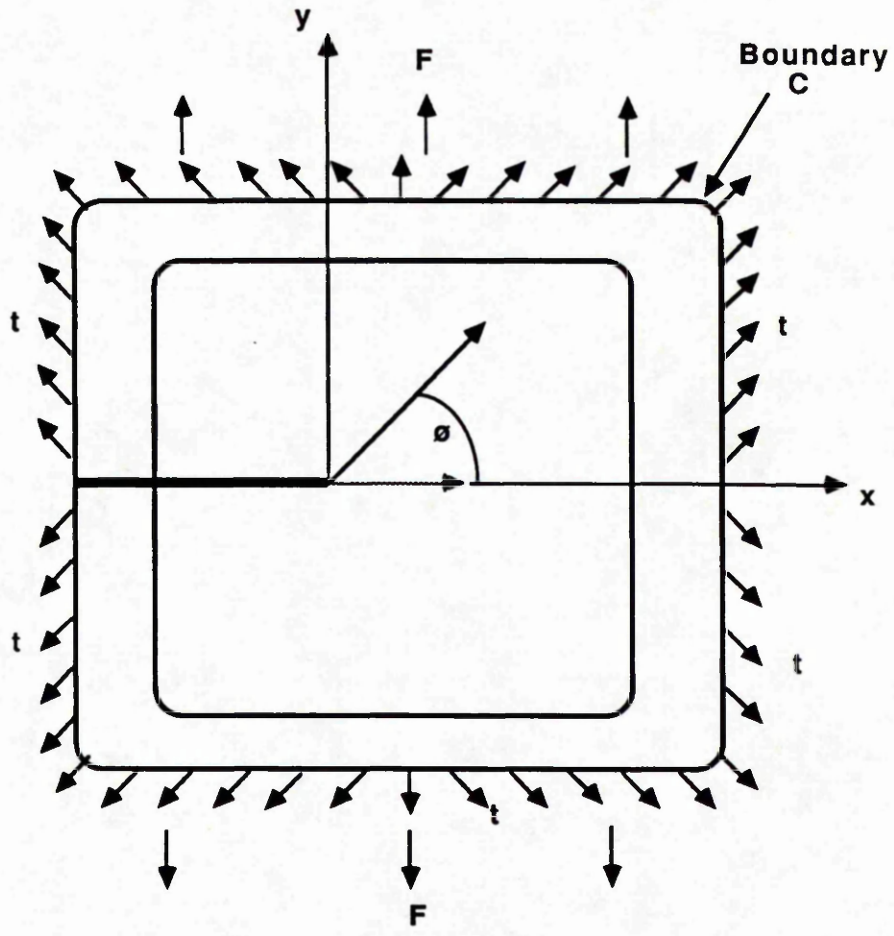

Fig. (2.2): Cracked body subjected to external force F, and a point force f applied at the crack tip resisted by tractions t

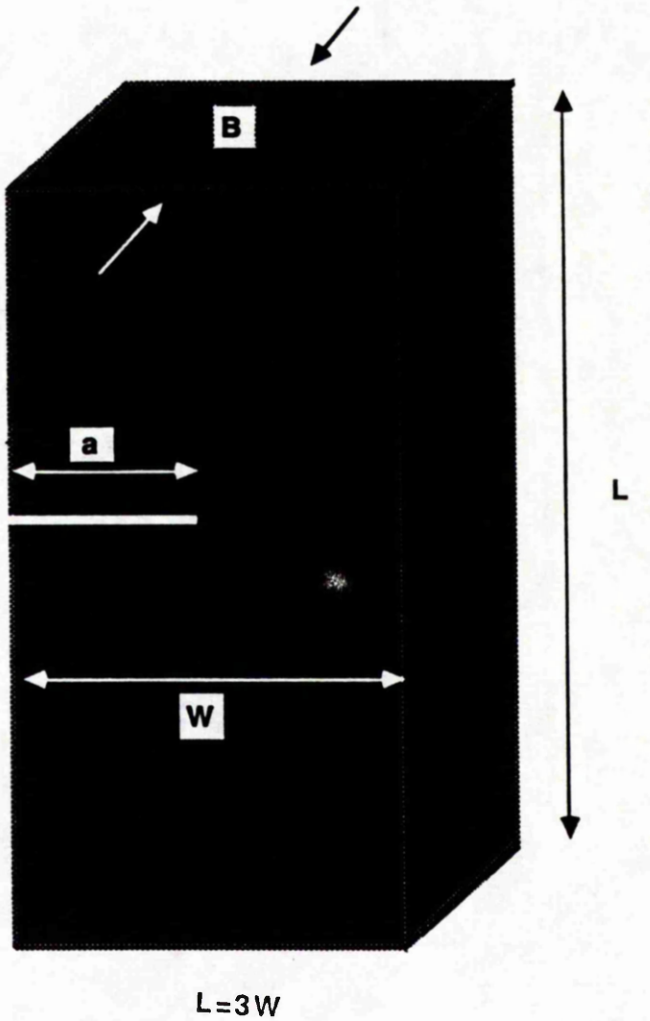

Fig (2.3): Single-edge-notched bend (SENB) specimen

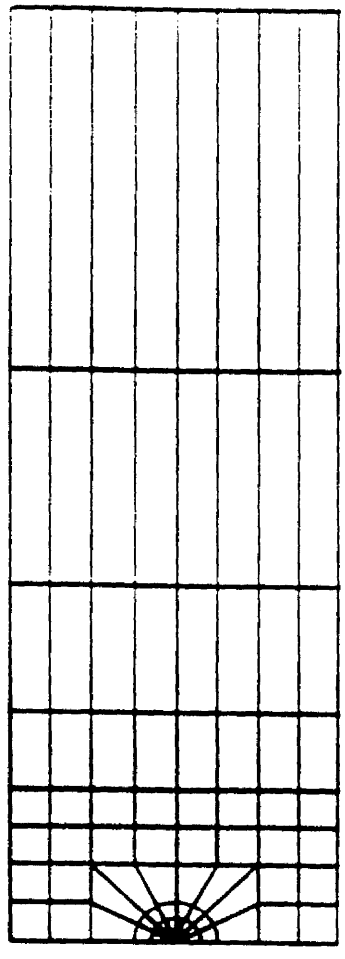

Fig (2.4): Finite element mesh for (a/W=0.5) representing one half of the geometry

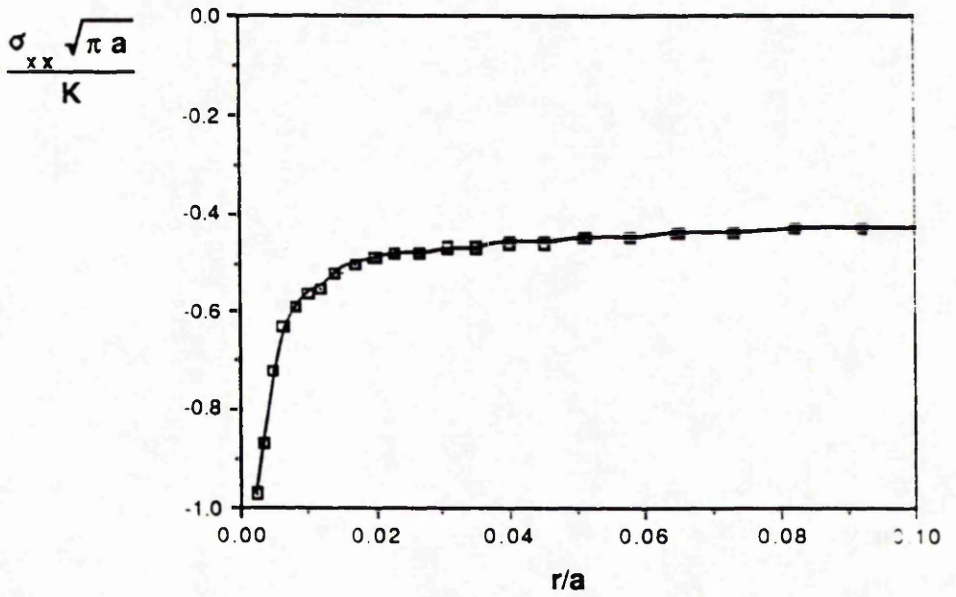

Fig (2.5a): The extrapolation of non-singular term to the crack tip biaxiality B before using (*EQUATION).

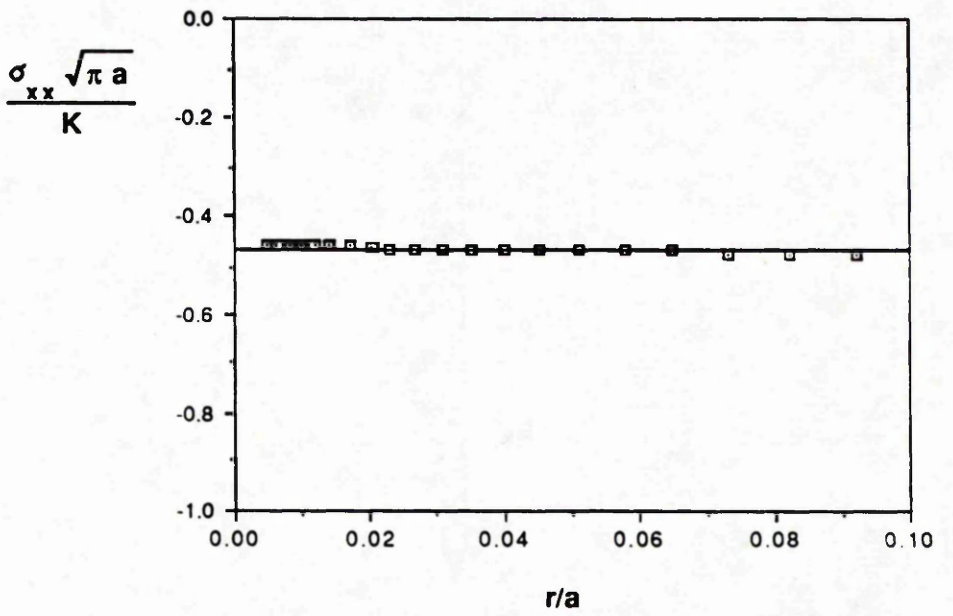

Fig (2.5b): The extrapolation of the non-singular term to the crack tip with (*EQUATION).

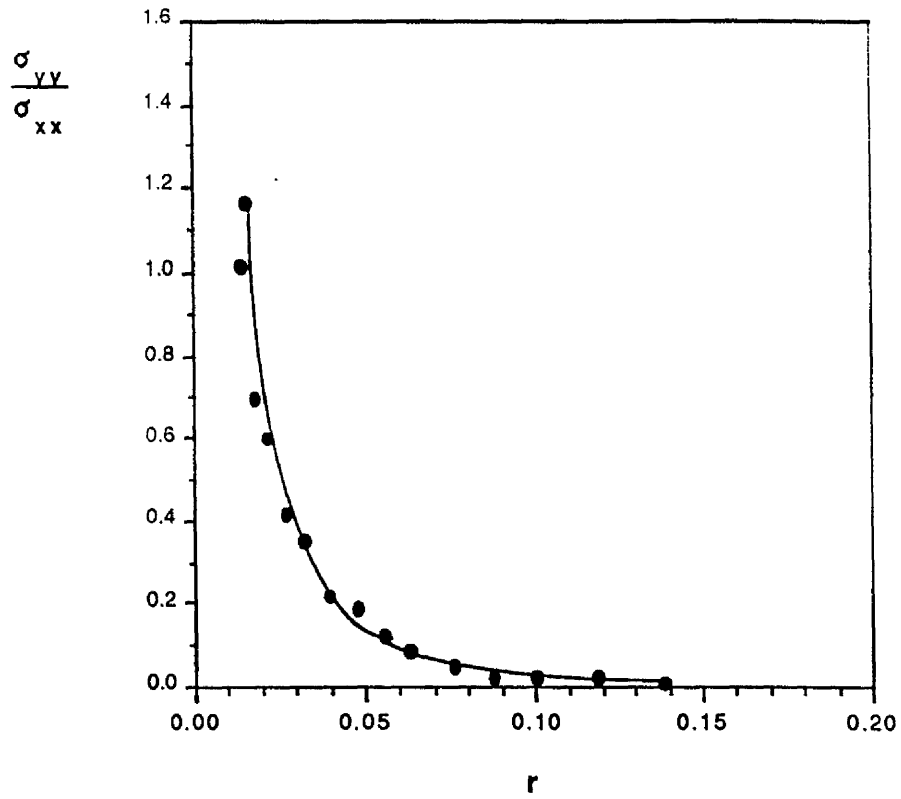

Fig (2.6): The ratio of $\sigma_{yy} / \sigma_{xx}$ as a function of the distance r behind the crack tip

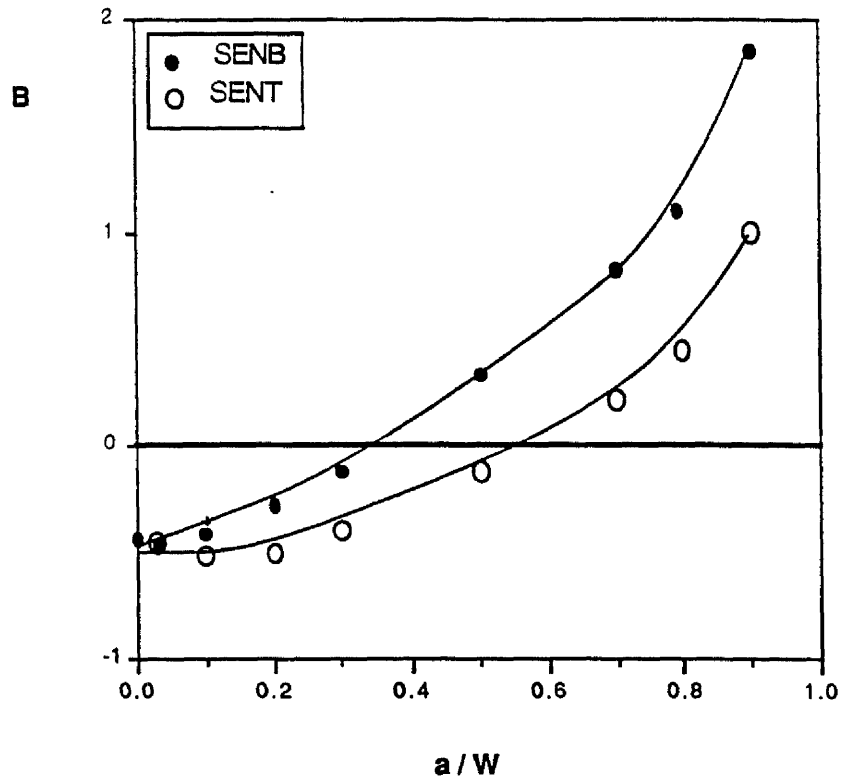

Fig (2.7): The biaxiality parameter B as a function of (a/W) for single edge cracked bars in tension and bending.

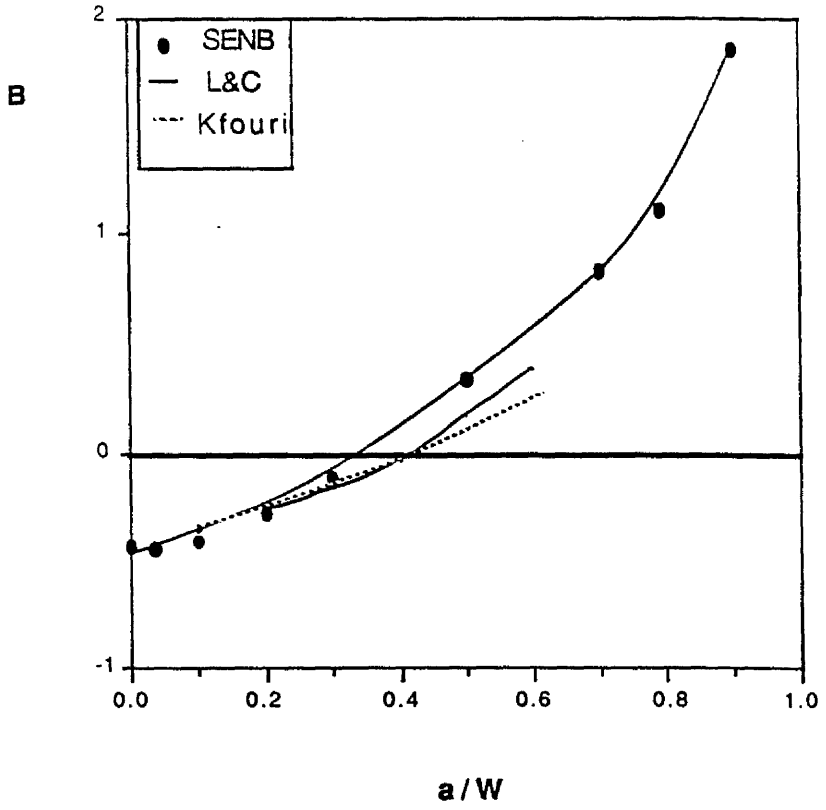

Fig (2.8): Values of the biaxiality parameter B for SENB specimens as a function of a/W compared with values given by Kfouri (1986) and Leevers and Radon (1983).

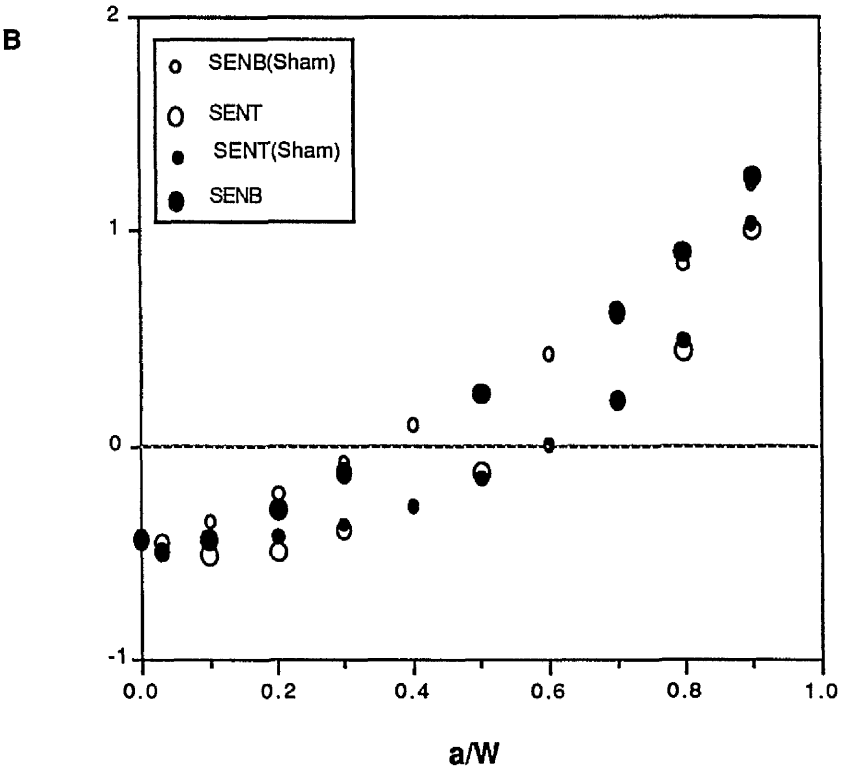

Fig (2.9) : Values of the biaxiality parameter B for single edge cracked bars in tension and bending as a function of (a/W) compared with B values calculated by Sham (1989)

Chapter (3)

Elastic-Plastic Fracture Mechanics: (Single Parameter Characterisation)

3.1. Introduction

Linear elastic fracture mechanics (LEFM) attempts to predict fracture, when the plastic zone is small compared to the dimensions of the cracked body. Elastic-plastic fracture mechanics is concerned with failure when the plastic zone size is large compared to the relevant dimensions of the cracked body, invalidating LEFM procedures.

Elastic-plastic fracture mechanics is based on the development of suitable characterising parameters. Among these characterising parameters are the crack opening tip displacement (δ) and the J-integral. The J-integral was introduced independently by Cherepanov (1967), Eshelby (1968) and Rice (1968), but its application to fracture is largely attributable by Rice (1968). Fig (3.1) shows an arbitrary contour from the lower crack face to the upper face around the crack tip. On each small element ds of this surface there is a force F which is a vector. If the crack, advances by a small amount Δa the surface also moves and the element ds moves by a small displacement Δu. As the crack advances, the stress field only changes by a negligibly small amount and because both the force F and the displacement Δu are vectors the work done on the element ds is $F.\Delta u$ where the dot or scalar product takes care of the fact that Δu and F may not be in the same direction. The total work done on the material inside the contours is obtained by integrating around the circuit.

$$\int_r (F.\ \Delta u)\ ds \tag{1}$$

The displacement vector Δu can be written in terms of the crack advance in the x direction.

$$\Delta u = \frac{du}{dx} . \Delta a \tag{2}$$

thus the work done by the external force is

$$\Delta a \int (F. \frac{du}{dx}) \ ds \tag{3}$$

As the crack advances the contour moves, and the material inside the contour loses and gains energy from the shaded regions. If W is the strain energy per unit volume, the change of strain energy in the small strip.

$$W\ \Delta a\ dy \tag{4}$$

The net loss in strain energy of the material inside the contour is obtained by integration around the path.

$$\Delta a \int_r W\ dy \tag{5}$$

The material inside the contour loses strain and external force does work so the net loss in energy is :

$$\Delta U = \Delta a \int_{r} W\, dy - \Delta a \int (F. \frac{du}{dx})\, ds \qquad (6)$$

The important feature of this integral is that Rice (1968) has shown it to be independent of the path chosen, and is applicable to both linear and non-linear elasticity.

For linear elastic fracture mechanics J is thus identical to the potential energy release rate G and establishes contact with the stress intensity factor K :

$$J = G = \frac{K^2}{E'} \qquad (7)$$

Where E' is the Young's modulus which equals E for plane stress and $E/(1-\upsilon^2)$ for plane strain.

The crack tip opening displacement, δ, is related to the potential energy release rate G.

$$\delta = d_n \frac{G}{\sigma_o} \qquad (8)$$

As J and G are identical in LEFM.

$$\delta = d_n \frac{J}{\sigma_o} \qquad (9)$$

Values of d_n, which are dependent on the hardening rat n and the yield strain ε_o, are given in tabulated form by Hutchinson (1978) and Shih (1978).

It has been noted that the J-integral can be used as an energy based fracture criterion, however Rice and Rosengren (1968) and Hutchinson (1968) have also shown that J has a role in characterising the deformation field ahead of stationary cracks. The material behaviour is taken to be described by a plastic power law.

$$\frac{\varepsilon}{\varepsilon_o} = \alpha \left(\frac{\sigma}{\sigma_o}\right)^n \tag{10}$$

Here σ_o is a reference stress, ε_o is a reference strain, α is a material constant and n is the strain hardening exponent.

Using J_2 deformation theory with

$$\sigma_e^2 = \frac{3}{2} S_{ij} S_{ij} \tag{11}$$

The uniaxial stress-strain may be generalised to multi-axial states as

$$\frac{\varepsilon_{ij}}{\varepsilon_o} = \frac{3}{2} \alpha \left(\frac{\sigma_e}{\sigma_o}\right)^{n-1} \frac{S_{ij}}{\sigma_o} \tag{12}$$

Here S_{ij} and σ_e are the stress deviators and the effective stress respectively. The method of solution employed by Hutchinson (1968) used the minimum complementary energy theorem, under which of all the stress distributions which satisfy equilibrium and the stress boundary conditions, the correct distribution is the one which minimizes the complementary energy U_c over the volume v.

$$U_c = \int_V \int \varepsilon_{ij} \, d\, \sigma_{ij} \, dv \tag{13}$$

In plane stress or plane strain the complementary energy can be written in terms of the stress as :

$$U_c = \int_A \left(\frac{1}{3} (1+\upsilon) \, \sigma_e\right)^2 + \left(1+\frac{2\upsilon}{\sigma}\right) \sigma_{kk}^2 + \left(\frac{\alpha}{n+1}\right) \sigma_e^{n+1} \tag{14}$$

Equilibrium is satisfied by a non-dimensional stress distribution Σ, which in cylindrical co-ordinates satisfies the following relations.

$$\sigma_{rr} = \frac{1}{r} \frac{\partial \Sigma}{\partial r} + \frac{1}{r^2} \frac{\partial^2 \Sigma}{\partial \varnothing^2} \tag{15}$$

$$\sigma_{\varnothing\varnothing} = \frac{\partial^2 \Sigma}{\partial r^2} \tag{16}$$

$$\sigma_{r\varnothing} = - \frac{\partial \left(\frac{1}{r} \frac{\partial \Sigma}{\partial \varnothing}\right)}{\partial r} \tag{17}$$

On this basis a solution is sought in the vicinity of the crack which satisfies the equilibrium equations, and the local boundary conditions.

$$\Sigma = \frac{\partial \Sigma}{\partial \varnothing} = 0 \qquad (\varnothing = -\pi, +\pi) \tag{18}$$

The solution is assumed to take the form of an asymptotic expansion whose dominant term is

$$\Sigma = K r^{s} \Sigma (\emptyset) \tag{19}$$

With this form of solution the complementary energy can be evaluated and minimised by using the amplitude K and the exponent s. The solution is given by :

$$s = \frac{2n+1}{n+1} \tag{20}$$

Hence the crack tip stress, strain and displacement fields can be obtained in terms of J as :

$$\sigma_{ij} = \sigma_o \left[\frac{J}{\alpha \varepsilon_o \sigma_o I_n r}\right]^{\frac{1}{n+1}} \sigma_{ij} (\emptyset, n) \tag{21}$$

$$\varepsilon_{ij} = \alpha \varepsilon_o \left[\frac{J}{\alpha \sigma_o \varepsilon_o I_n r}\right]^{\frac{n}{n+1}} \varepsilon_{ij} (\emptyset, n) \tag{22}$$

$$u_1 = \alpha \varepsilon_o \left[\frac{J}{\alpha \sigma_o \varepsilon_o I_n}\right]^{\frac{n}{n+1}} r^{\frac{1}{n+1}} u_1 (\emptyset, n) \tag{23}$$

Here I_n is an integration constant which is a function of n only, σ_{ij} and ε_{ij} are dimensionless functions which depend on ø and n.

The basis of the one parameter characterisation of the crack tip stress and strain fields, by J, is that the region ahead of the crack tip over which the HRR field singularity dominates completely encompass the fracture processes zone. McClintock (1971) pointed out that the

fully plastic slip-line field solution for the centre-cracked panel (CCP) and the deeply double edge cracked panel (DECP) subjected to tensile loading and the cracked bend bar (CBB) subjected to bending are completely different as illustrated in Fig (3.2). For the limit of non-hardening material and in the fully plastic state, McClintock (1971) indicated that there is no unique stress and strain in the crack tip region and these field are dependent on the crack geometry. For the anti-plane shear problems Rice (1976) showed that for contained yielding the distance in which the HRR field dominated decreases with decreasing hardening rate. In the fully plastic state Amazigo(1978) found the same effect, that increasing (n), (decreasing the hardening rate), decreases the distance ahead of the crack tip over which the HRR field dominates. These observations by McClintock (1971), Rice (1976) and Amazigo (1978) emphasise the role of the specimen configuration and material properties on the size of the HRR dominated field.

The conditions under which the crack tip stress and strain fields maintain the character of the HRR field has been defined as J dominance and the size requirements for J dominance as expressed by Rice (1976) take the form

$$(W\text{-}a) \geq M(\varepsilon_o, n)\,\frac{J_c}{\sigma_o}$$

equivalently

$$(W\text{-}a) \geq M(\varepsilon_o, n)\,\frac{\delta_c}{dn} \qquad (24)$$

Paris (1972) suggested a value of M ranging from 25 to 50 to

ensure plane strain conditions in the process zone and hence a valid J test. By testing different cracked geometries Hancock and Cowling (1978) found that the value of J_c and δ varied with a change in the flow field configuration for a tempered and quenched steel similar to HY80.

The limits of J dominance were studied by McMeeking and Parks (1979), using a large deformation plane strain finite element method for a deeply cracked centre-cracked panel (CCP) and single edge cracked bend bar (CBB). For a weakly hardening material, they compared the fully plastic field with the normalised small scale yielding stress distribution obtained by McMeeking (1977), as the standard field associated with a J dominated crack tip region. The solution for the single edge cracked bend bar was characterised by J into large scale yielding. Hence the proposed a size requirement for a J toughness test indicated that the ligament (W-a) must exceed 25 J/σ_o to ensure a valid J characterisation of the crack tip field.

For the centre cracked panel McMeeking and Parks (1979) demonstrated that the crack tip field deviated from the standard field beyond contained plasticity. From this observation they concluded that to ensure J dominance for the CCP, the ligament has to exceed 200 J/σ_o. The limitations of J dominance are most clearly seen in the fundamental difference form the slip line field for these geometries Fig (3.2) McClintock (1971)

Shih and German (1981) carried out a detailed finite element analysis of deeply cracked and center cracked panel geometries using small strain theory. The stress and strain fields obtained from the finite element analysis for the cracked bend bar (CBB), the single edge cracked bar (SENB) and the centre cracked panel (CCP) were compared with the singular HRR field. The comparison showed that

when the plastic zone size is small compared to the ligament size the stress and the strain fields are in a good agreement with the HRR field. Increasing the deformation (large scale yielding), the stress and strain fields for CCP fell below the HRR field. However for the CBB geometry, the stress and strain fields remained in good agreement with the HRR field until $(W-a)=25J/\sigma_0$. Shih and German (1981) pointed out that under large scale yielding the stress field is dependent on the specimen geometry and material hardening rate. Their results confirmed the size requirements proposed by McMeeking and Parks (1979).

The work of Shih and German (1981) and of McMeeking and Parks (1979) was concerned with deeply cracked geometries in which the ligament is the controlling dimension. However when a crack is formed in components it usually begins at a surface defect or the root of a notch and is initially very short, Miller (1982). There are two different viewpoints from which a crack can be defined as short. From a micro-structural viewpoint, the crack can be considered as short if it's length is of the order of the grain size. This regime is of most interest to investigators concerned with the fatigue life as exemplified by Miller and Ibrahim (1979), Miller and Kfouri (1981), Wang and Miller (1982) and Miller (1982). However from a continuum mechanics viewpoint crack can be considered as a short if the crack length is the controlling dimension of the body and the crack length is very much greater than the grain size.

Wang and Miller (1982) have presented elastic-plastic finite element calculations in which the stress and strain fields ahead of the crack tip which were compared with the small scale yielding solution

of McMeeking (1977). In their conclusion Wang and Miller (1982) pointed out that the plastic zone develops rapidly in a short crack compared to a deep crack, and at the same equivalent stress intensity factor short cracks show greater equivalent plastic strain than deep cracks. They also concluded that a single parameter such as J or δ is not sufficient to characterise the crack tip stress field ahead of the crack tip in a short crack.

Al-Ani (1988) performed detailed finite element analyses of short and deeply edge cracked bars with a/W between 0.03 and 0.5 in bending and a/W between 0.1 and 0.3 in tension. Elastic-plastic small geometry change solutions with an initially sharp crack and large geometry change solutions in which the tip utilised a small but finite crack tip radius were presented as, illustrated in Fig (3.3a,b).

The stress field of the small geometry change solutions was compared with the HRR field in contained yielding. For shallow cracked geometries with a/W less than 0.3 in bending and a/W<0.5 in tension, the stress field ahead of the tip fell below the HRR field. With increasing deformation, the results indicated that the stress field continued to fall below the HRR field until at extensive levels of plasticity, the stress field converged to a fully plastic field which was geometry dependent. Following Green (1953) the full plastic slip line field for deep cracks in bending is shown in Fig (3.4). For shallow cracks ($a/W \leq 0.3$) plasticity breaks back to the cracked surface, following modification to the slip line field proposed by Ewing (1968). This feature was confirmed by the numerical solutions of Al-Ani (1988), illustrated in Fig (3.5a,b). The results of the stresses ahead of the crack tip for shallow cracks ($a/W \leq 0.3$) in bending and tension specimens are shown in Figs (3.6 to 3.8).

For deeply cracked geometries with a/W $\geq$ 0.3, plasticity is confined to the ligament and the stress field ahead of the crack tip is closely similar to the HRR field. This similarity was maintained as plasticity extended from small scale yielding into full plasticity of the uncracked ligament as illustrated in Figs (3.9 and 3.10).

In the large geometry change solution Al-Ani (1988) investigated the deformation within one or two crack tip opening δ in the spirit of the work by McMeeking (1977). The results showed that the stress field ahead of the crack tip for the geometry with a/W=0.3 approaches the small scale yielding (SSY) solution over a distance about 2δ, however, the stress field for the geometry with a/W less than 0.3 did not achieve the full value of the J dominated field, but reached a maximum stress at distance of less than δ.

Based on these observations Al-Ani (1988) and Al-Ani and Hancock (1991) pointed out that for short crack geometries with a/W $\leq$ 0.3 in bending and a/W$\leq$ 0.5 in tension, there is a marked loss of J dominance with crack length which occurs before a =200 J/σ_o Deeply cracked geometries with a/W $\geq$ 0.3 in bending and a/W$\geq$ 0.5 in tension follow the criteria described by Shih and German (1981) and McMeeking and Parks (1978) in which the ligament is the controlling dimension.

3.2. References:

Al-Ani A. M. and Hancock, J. W.,(1991) J. Mech. Phys. Solids, 39, 23.

Al-Ani A. M. (1988), MSc Thesis. Mech. Eng. Dept., Glasgow Unviersity.

Amazigo, J. C., (1978), " Some Mathmetical Problems of Elastic-Plastic Growth" Presented at AMS/SIAM Symposium on Mathmetical Problems in Fracture Mechanics.

Cherepanov, G. P., (1967), J Appl Math Mech., 31, 503.

Eshelby, J. D., (1968), "Stress Analysis of Cracks, ISI publication, 121,13.

Ewing, D. J., (1968), J. Mech. Phys. Solids, 16, 305.

Green, A. P., (1953), Q J Mech Appl Math, 6, 223.

Hancock, J. W and Cowling, M. J. (1980), Met Sci, 14, 293.

Hutchinson, J. W, (1978), J. Mech. Phys. Solids ,26, 163.

Hutchinson, J. W, (1968), J. Mech. Phys. Solids, 16, 13.

McClintock, F. A.,(1971), in Fracture: An Advanced Treatise (H.Leibowitz,ed.), 3,47, Academic Press.

McMeeking ,R. M. and Parks, D. M.,(1979), ASTM. STP 668, 175.

McMeeking ,R. M., (1977), J. Mech. Phys. Solids, 25, 37.

Miller, K. J., (1982), Fatigue Engng Mater. 5, 223.

Miller, K. J., and Ibrahim, M. F. E., (1979), Fatigue Engng Mater 4, 236.

Miller, K. J., and Kfouri, A. P., (1981), STM. STP 668, 214.

Paris, P. C., (1972), ASTM STP 514, 210.

Rice, J. R., (1967), J Appl Mech, 34,287.

Rice, J. R. and Rosengren, G. F. ,(1968), J. Mech. Phys. Solids, 16, 1.

Rice, J. R., (1968), J Appl Mech, 35,379.

Rice, J. R., (1976), J Appl Mech, 19, 23.

Shih, C. F., and German, M. G. (1981), Int. J of Fracture, 17, 27.

Shih, C. F., (1978), "The Relation Between Initation and Growth Parameter Based On The J Integral and Crack Opening Displacement.

Wang TZU and Miller, K. J.,(1982), Fatigue Engng Mater 5, 249.

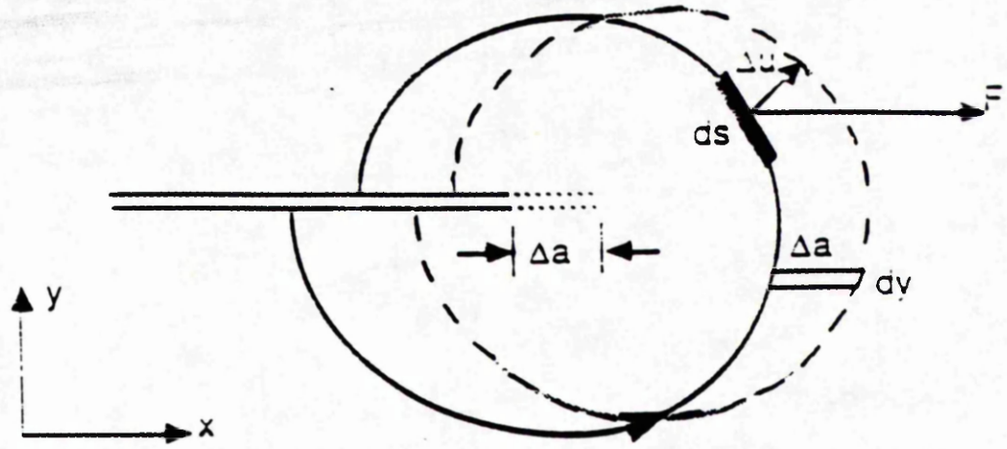

$$J = \int_{\Gamma} (W dy - (F - \frac{du}{dx}) ds)$$

Fig (3.1) : Crack tip coordinate system and an arbitrary line integral

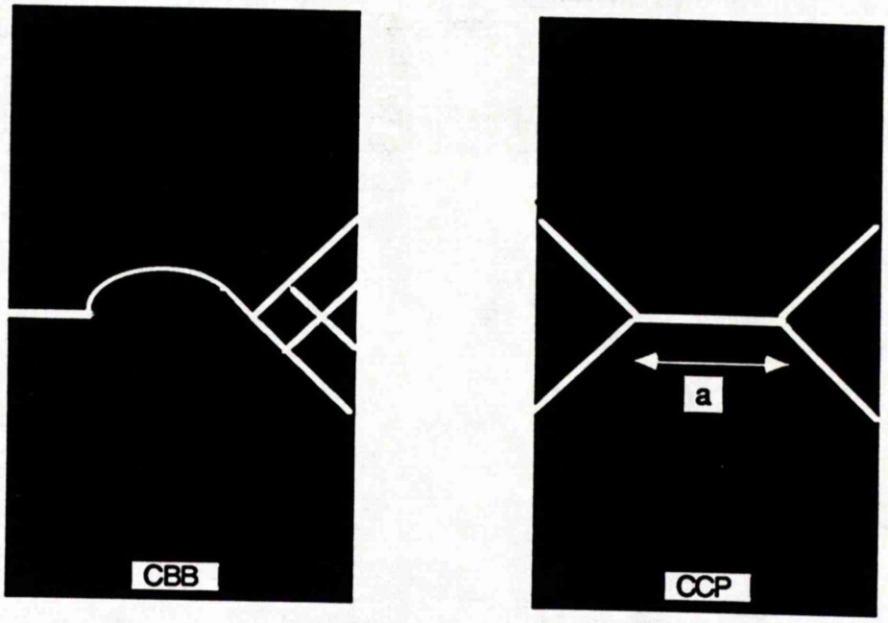

Fig (3.2) : The slip line field of CCP and CBB

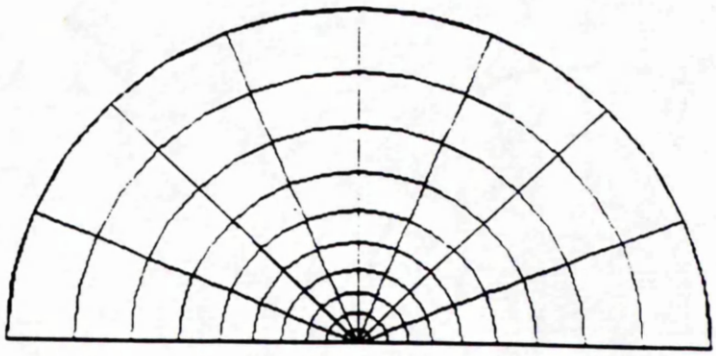

Fig (3.3a) : A focussed mesh at a sharp crack

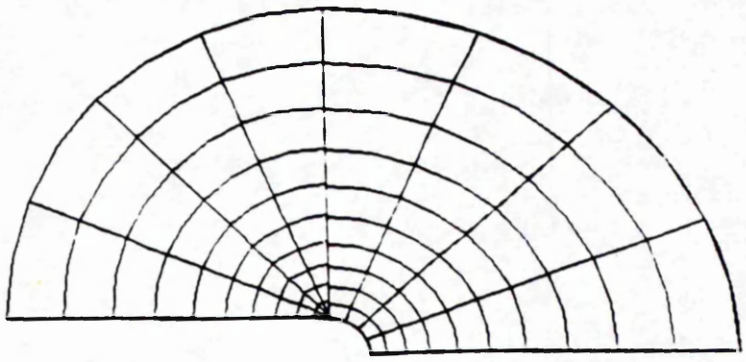

Fig (3.3b) : A blunt crack with a small initial radius

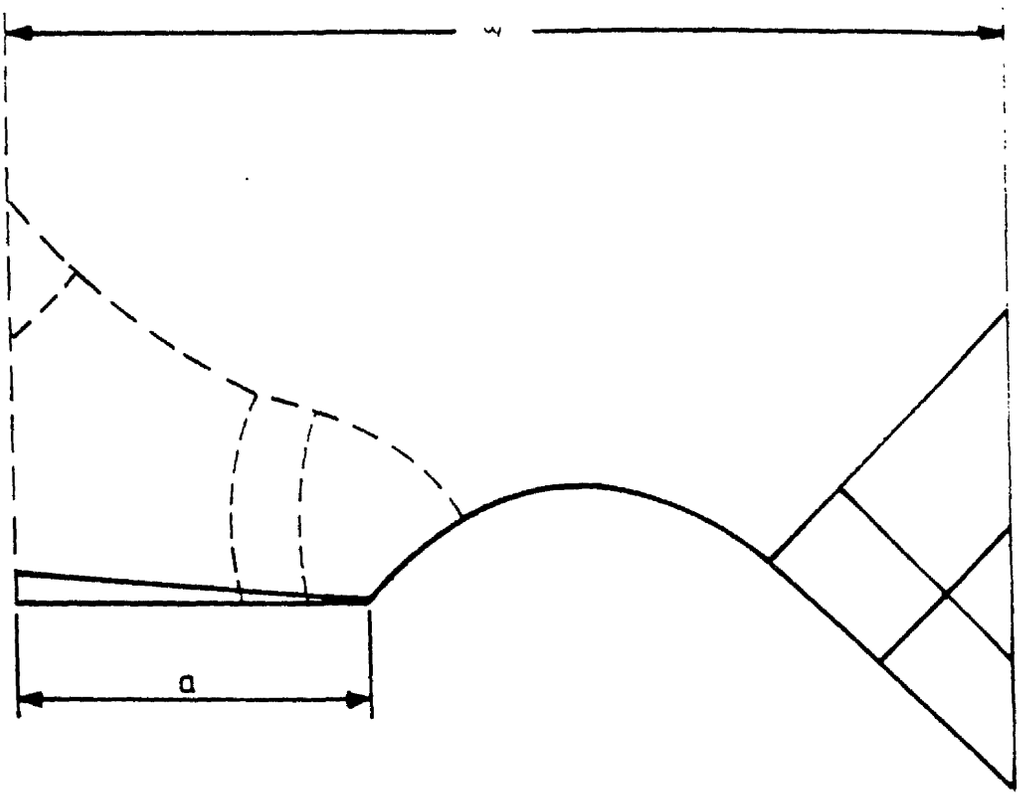

Fig (3.4) : The slip line field of deep and shallow cracks following Green (1956) and Ewing (1968)

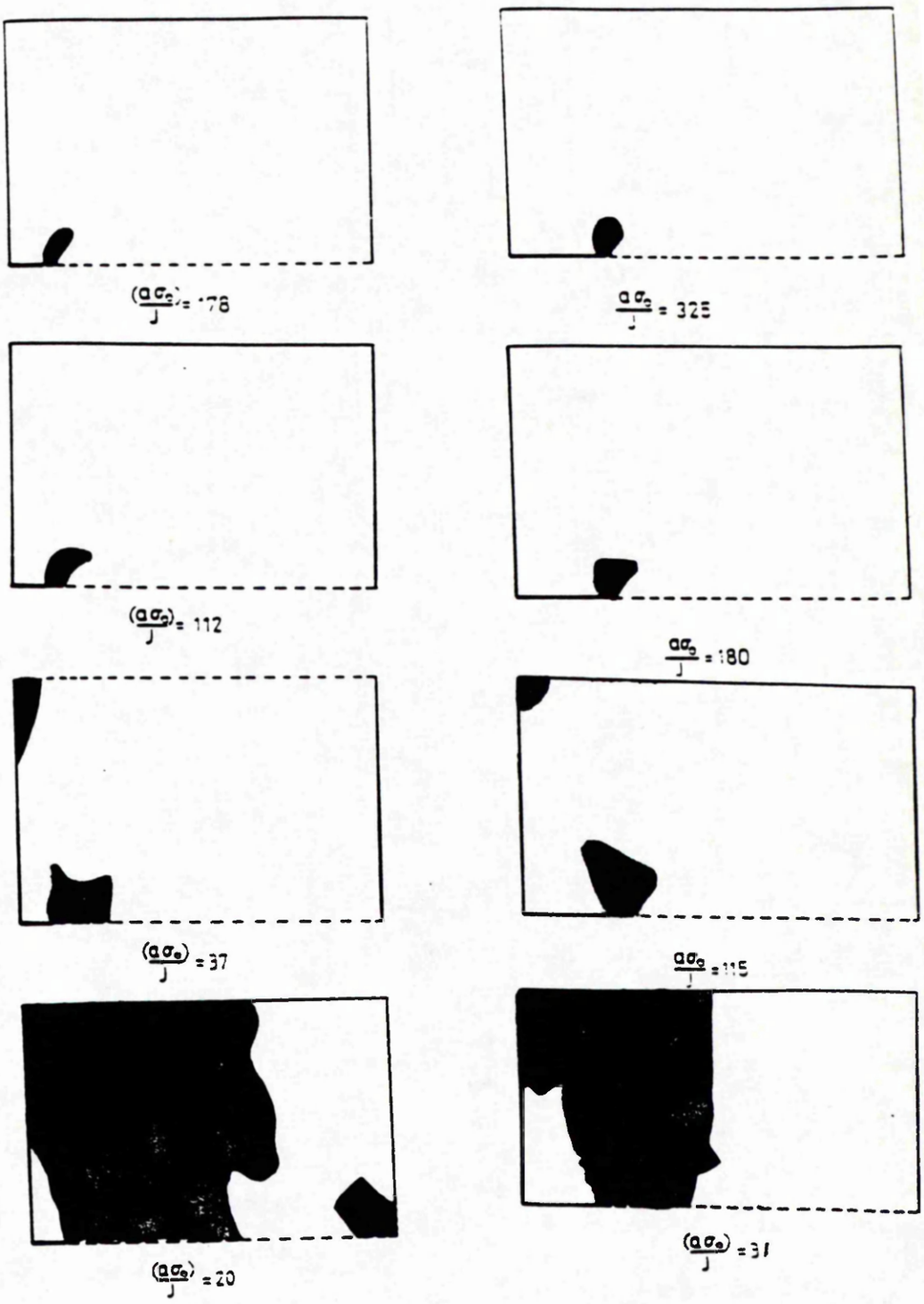

Fig (3.5) : The development of the plastic zone for a shallow cracked bar (a/W<0.3) in bending

(a) a/W=0.1

(b) a/W=0.2

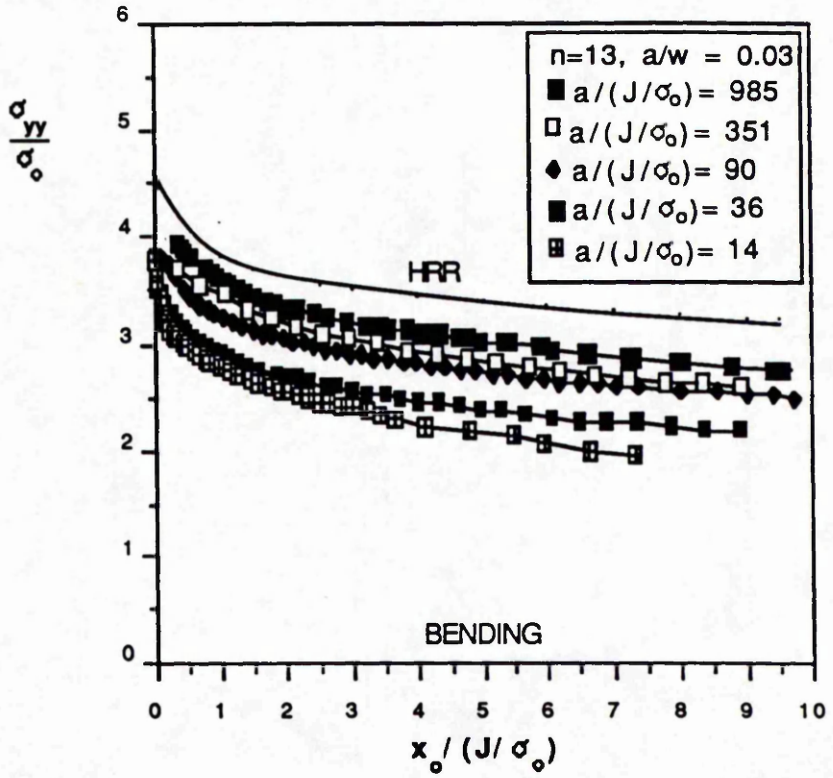

Fig (3.6) : The stress field ahead of a crack in bending (a/W=0.03)

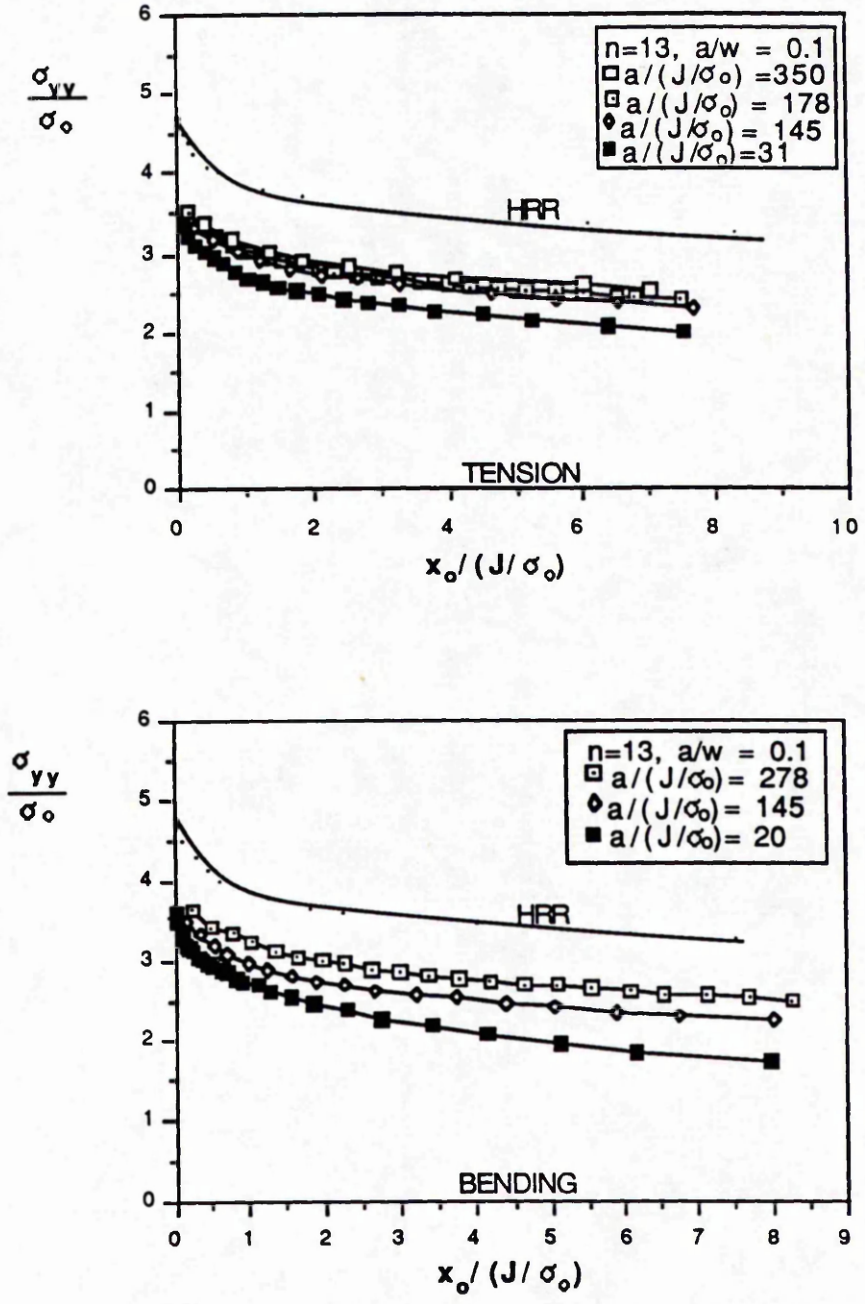

Fig (3.7) : The stress field ahead of a crack in bending and tension (a/W=0.1)

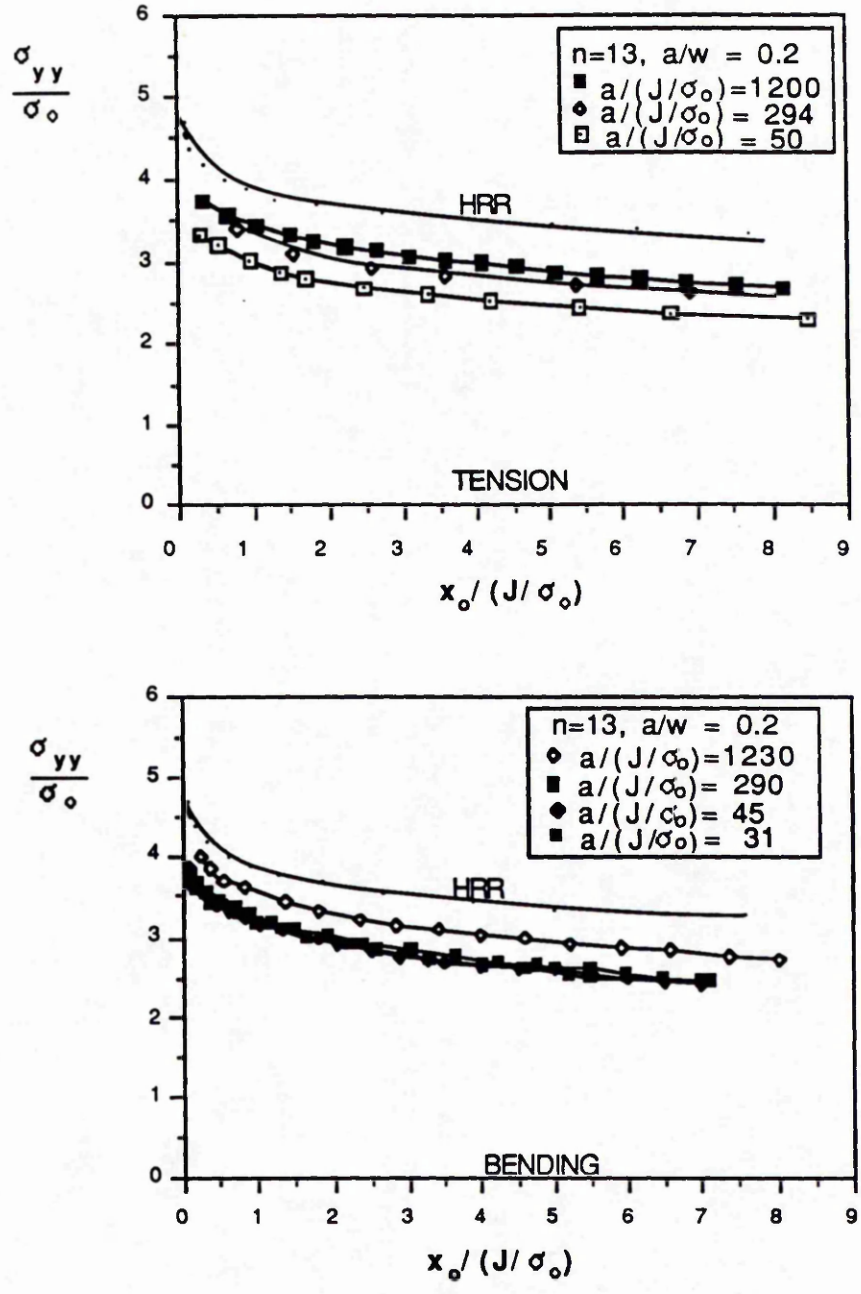

Fig (3.8) : The stress field ahead of a crack in bending and tension (a/W=0.2)

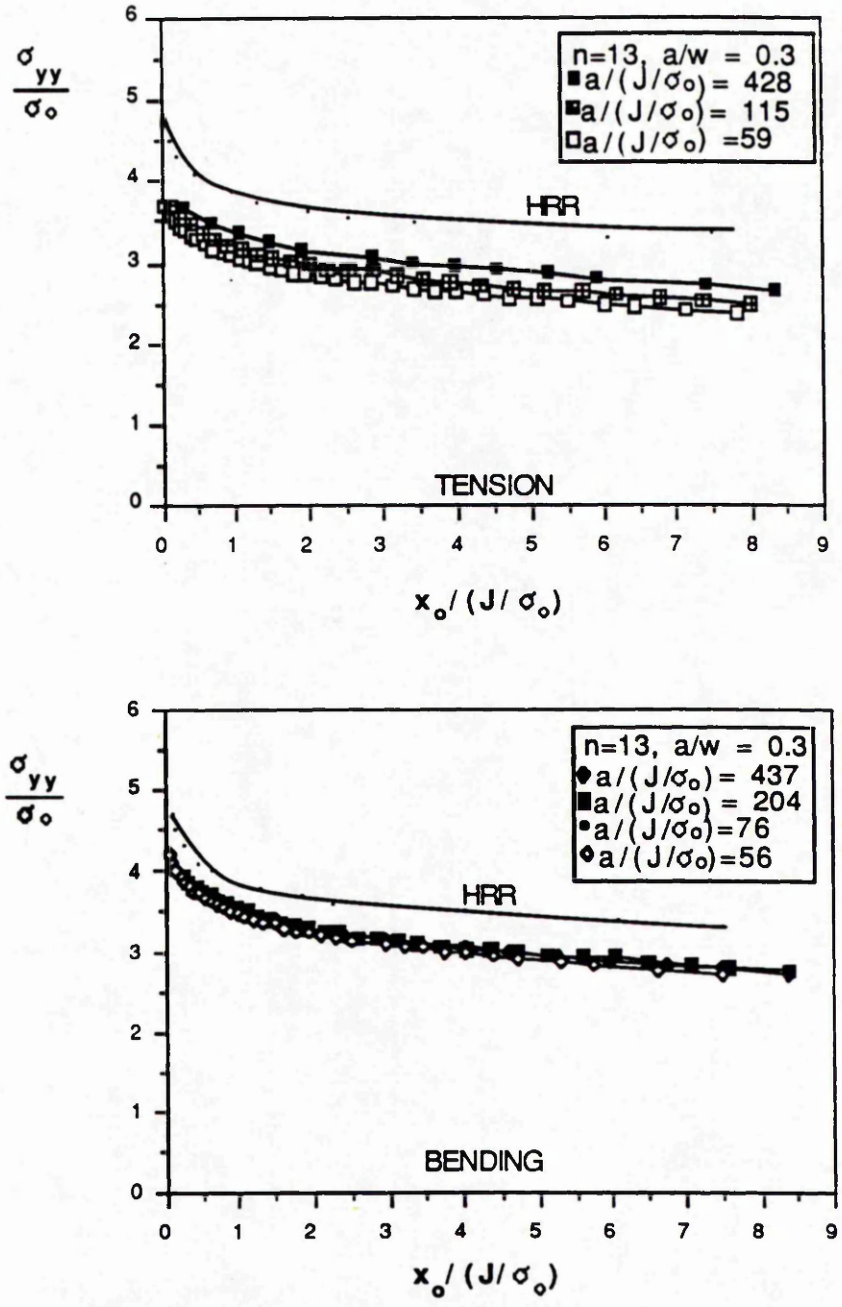

Fig (3.9) : The stress field ahead of a crack in bending and tension (a/W=0.3)

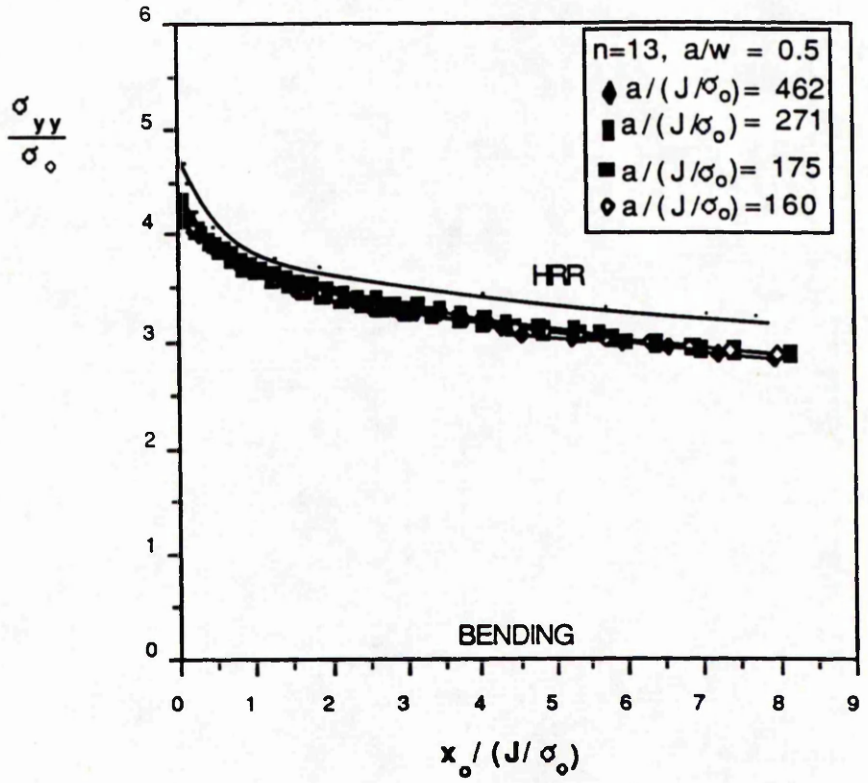

Fig (3.10) : The stress field ahead of a crack in bending (a/W=0.5)

Chapter (4)

Elastic-Plastic Fracture Mechanics : (Two Parameter Characterisation)

4.1. Introduction

Fracture mechanics attempts to maintain the structural integrity of engineering structures which contain defects by establishing a relation between the loading conditions under which the crack extends, and the geometry of the defect and the structure. Hutchinson (1968) and Rice and Rosengren (1968) developed the leading term in elastic-plastic asymptotic solutions for the stresses near the crack tip (known as the HRR field) in which the stress field ahead of the crack tip is characterised by J or δ.

The validity of the HRR field is subjected to size requirements, so that one parameter characterisation is dependent on geometric criteria. The basis of the one parameter approach to fracture using J or δ, is that the stress field ahead of the crack tip must be uniquely characterised by J or δ for different cracked geometries with different loading patterns. Analyses of shallow cracked bend and tension bars by Al-Ani (1988) have shown that there is no such unique relationship, and a single parameter such as J or δ is unable to characterise the stress field ahead of the crack tip. The results indicate that even under small scale yielding conditions ($a\sigma_0/J \geq 1000$), the stress field ahead of the crack tip for shallow cracks was less severe than those in deeply cracked bend geometries and the HRR field.

Li and Wang (1986) have investigated a two term asymptotic expansion of the near tip plastic solution of a plane strain crack in a homogeneous material. The problem was formulated in terms of a

function of the form:

$$\sigma_{ij} = K_{S1}\, r^{S1} f_{ij}\,(\varnothing,n) + K_{S2}\, r^{S2}\, g_{ij}\,(\varnothing,n) \qquad (1)$$

where the first term was identified with the HRR field. The strength of the second term was however very much weaker than the first term. They suggested the magnitude of the second term of the asymptotic expansion of the small strain plastic crack tip field as a second parameter to be used together with J-integral in the fracture criteria.

The effect of the second term in the elastic expansion (T) on the near crack tip distribution was recognised by Larsson and Carlsson (1973) who performed boundary layer solutions of the crack problem. In their full field solutions for different geometries they found significant discrepancies between full field solution of various geometries even at the ASTM limit. Larsson and Carlsson (1973) suggested that the boundary layer formulations based on the K field can be modified to represent the stresses field ahead of the crack tip. The modification amounts to an addition of the tractions corresponding to the non-singular T term in addition to the K field.

Bilby et al (1986) examined the effect of the T stress on the large geometry change crack tip field assuming that the crack blunts smoothly into a circular arc. The large geometry change numerical results for shallow crack-cracked bar with a/W=0.2 showed that the stresses field ahead of the crack tip are lower than that for the deeply-cracked specimen although they have identical ligaments. The results indicated that a two-parameter description of the fields ahead of the crack is reasonable for the range concerned. Recently Betegón and Hancock (1991) correlated the loss of J dominance with the second

term in the elastic expansion using modified boundary layer formulations. Their results were compared with the HRR field and a single term boundary layer formulation, in which the displacements corresponding to the K field were imposed at the remote boundary. The results for positive T stresses show that early in the deformation, the stresses are comparable to the $\beta=0$ field. Increasing the deformation caused the stress to rise slightly until the data closely approximated to the HRR field Fig (4.1). For negative T stresses the field is close to the $\beta=0$ field, but as the T-stress became more negative the stress fell and diverged from the HRR field as illustrated in Fig (4.2).

The effect of the non-singular T stress on non-hardening plasticity has been investigated by Du and Hancock (1990) who also used modified boundary layer formulations. The results showed agreement with results given by Larsson and Carlsson (1973), in that tensile T stresses decrease the size of the plastic zone, while compressive T stress increase the maximum radius of the plastic zone and caused the plastic lobes to swing forward as illustrated in Fig (4.3). Their results show that a positive T-stress produced deformation, corresponding to the full Prandtl field (Rice 1968a,b) and the limit of the HRR field for non-hardening material. In contrast a compressive T-stress decreased the angular span of the centered fan and gave an incomplete Prandtl field in which the plasticity does not envelop the crack. The effect of the T stress is to reduce the hydrostatic stress by T and this causes a loss of J dominance. These results have been given by Du and Hancock (1990) and can be summarised by the following equations.

$$\left(\frac{\sigma_m}{\sigma_o}\right)_{(r)} = \left(\frac{\sigma_m}{\sigma_o}\right)_{(r,T=0)} + \left(\frac{T}{\sigma_o}\right) \qquad -0.5 \geq \frac{T}{\sigma_o} \leq 0 \tag{2}$$

$$\left(\frac{\sigma_m}{\sigma_o}\right)_{(r)} = \left(\frac{\sigma_m}{\sigma_o}\right)_{(r,T=0)} + 0.712\,\frac{T}{\sigma_o} - 1.1\left(\frac{T}{\sigma_o}\right)^2 \qquad \frac{T}{\sigma_o} \leq 0 \tag{3}$$

The slip line fields corresponding to positive ,T=0 and negative, are illustrated in Fig (4.4.a,b,c,d)

O´Dowd and Shih (1990) investigated the limitation of a one-parameter approach by considering two parameter approach.They outlined a two-parameter fracture mechanics approach in which the fracture toughness depend on a parameter named Q which is a dimensionless amplitude factor of the second order field. For the small strain formulation and for power-law material which deforms under Ramberg-Osgood uniaxial tension relationship, they show that the stresses follow the asymptotic expansion :

$$\frac{\sigma_{ij}}{\sigma_o} = \left(\frac{J}{\alpha\,\varepsilon_o\,\sigma_o\,I_n\,r}\right)^{\frac{1}{n+1}} \sigma_{ij}(\varnothing) + \frac{Q}{r/r_p}\,\sigma_{ij}(\varnothing) + \text{higher order terms} \tag{4}$$

The first term is the HRR field singularity which is a function of J, While the second term has a dimensionless parameter Q as its amplitude, r_p is the plastic zone size, $\sigma_{ij}(\varnothing)$ are angular functions which depend on the strain hardening rate n. Based on the full field solution they suggested the following two term asymptotic expansion.

$$\frac{\varepsilon_{ij}}{\alpha\varepsilon_o} = \left(\frac{J}{\alpha\varepsilon_o\sigma_o I_n r}\right)^{\frac{n}{n+1}}\varepsilon_{ij}(\varnothing) + \left(\frac{J}{\alpha\varepsilon_o\sigma_o r}\right)^{\frac{n-1}{n+1}} Q\,\varepsilon_{ij}(\varnothing) \tag{5}$$

$$\frac{u_i - u_i^0}{\alpha\varepsilon_o} = \left(\frac{J}{\alpha\varepsilon_o\sigma_o I_n}\right)^{\frac{n}{n+1}} r^{\frac{1}{n+1}} u_i(\varnothing) + \left(\frac{J}{\alpha\varepsilon_o\sigma_o}\right)^{\frac{n-1}{n+1}} Q r^{\frac{2}{n+1}} u_i(\varnothing) \tag{6}$$

The second order field was obtained by substracting the HRR field scaled by applied J from the full field solution($J=(1-\upsilon^2)K/E$). In conclusion O'Dowd and Shih (1990) correlated the loss of J dominance with the value of the amplitude of the second term. For highly constrained geometries such as deeply cracked bend geometries, their results show that Q reaches a steady state value at a small amount of plastic yielding and the stress field corresponds to, or slightly exceeds the HRR field. In these circumstances the fracture toughness value meets the required size limitation for the J dominance discussed in ASTM E813. For shallow cracked tension and bending geometries which show low constraint and have negative value of Q, the stress field falls below the HRR field and J integral can no longer be used as a fracture criterion.

Sharma and Aravas (1990) developed an alternative methodology for the determination of higher order terms in asymptotic elastic-plastic crack tip solutions of the HRR type. To avoid the algebraic complications arising when the stress function approach is used Sharma and Aravas (1990) formulated the problem in terms of fundamental quantities, such as stresses and displacements. The formulation can be used for plane stress and plane strain. The

behaviour of the material was described by J_2-deformation theory. For the case of a plane strain crack in a homogeneous material Sharma and Aravas (1990), pointed out that when the hardening capacity of the material is small, the effect of the elasticity enters the asymptotic solution in the third term or higher in the expansion, however when the hardening capacity of material is large, elastic effects enter the solution to second order and the magnitude of the second term the expansion of the solution is controlled by the J-integral. By considering a polar coordinate system r and (ø) they attempted an asymptotic expansion of the solution in the form.

$$\frac{\sigma(r,\text{ø})}{\sigma_o} = r^s\sigma^{(0)}(\text{ø}) + r^t\sigma^{(1)}(\text{ø}) + \text{---} \quad \text{as } r\rightarrow 0 \tag{7}$$

Based on the assumption that the first and second terms in the stress expansion equation (3) are separable in polar co-ordinates r and ø, at the crack tip, Sharma and Aravas (1990) attempted to normalise the stress/strain and displacements in such a way to enable direct comparsion with the asymptotic solution developed by Hutchinson (1968). For t<(n-2)/(n+1) and as r→0 they suggested the following asymptotic form :

$$\frac{\sigma(r,\text{ø})}{\sigma_o} = \left(\frac{J}{\alpha\,\varepsilon_o\sigma_o I_n\, r}\right)^{\frac{1}{n+1}} \sigma^{(0)}(\text{ø}) + K^{(1)}r^t\sigma^{(1)}(\text{ø}) + \text{---} \tag{8}$$

$$\frac{\varepsilon(r,\theta)}{\alpha\varepsilon_o} = \left(\frac{J}{\alpha\varepsilon_o\sigma_o I_n r}\right)^{\frac{n}{n+1}} \varepsilon^{(0)}(\theta) + K^{(1)}\left(\frac{J}{\alpha\varepsilon_o\sigma_o I_n}\right)^{\frac{n-1}{n+1}} r^{s(n-1)+t}\varepsilon^{(1)}(\theta) + \cdots \tag{9}$$

$$\frac{u(r,\theta)}{\alpha\varepsilon_o} = \left(\frac{J}{\alpha\varepsilon_o\sigma_o I_n}\right)^{\frac{n}{n+1}} r^{\frac{1}{n+1}} u^{(0)}(\theta) + K^{(1)}\left(\frac{J}{\alpha\varepsilon_o\sigma_o I_n}\right)^{\frac{n-1}{n+1}} r^{s(n-1)+t+1} u^{(1)}(\theta) + \cdots \tag{10}$$

$K^{(1)}$ is the amplitude of the second term. They also presented a solution for the case of t=(n-2)/(n+1) as well as plane stress and plane strain solutions for a crack in homogenous material.

Betegón and Hancock (1991) investigated the limit of the two term boundary layer formulation J and T characterisation of elastic-plastic crack tip fields. They pointed out that in the case of bending deformation which introduced tensile T-stress, the limits of a single parameter characterisation is consistent with $25J/\sigma_0$ proposed by McMeeking and Parks (1979) and Shih and German (1981). For largely tensile stress states which feature negative T-stresses J-dominance is lost at an early stage in the deformation for example $b\sigma_0/J$ =2400 compared to the HRR field and $b\sigma_0/J$ =550 when it is compared with the β=0 field. In comparison J-T characterisation extended beyond $b\sigma_0/J$ =10, when the stress level was approximately two thirds of the HRR value. The extent of single and two parameter characterisation of plane strain elastic -plastic crack tip field are summarised in Table (4.1).

An initial aim of the present work was to investigate the effect of the T-stress on J dominance for single edge cracked geometries in bending and tension. The stress field of these geometries are compared with modified boundary formulation involving both K and

T following Larsson and Carlsson (1973) and Betegón and Hancock (1991).

4.2. Modified Boundary Layer Formulation

Modified boundary layer solutions have been obtained using an elastic-plastic, plane strain, small scale yielding solution, in which the crack tip has been modelled using a focused mesh at the crack tip. The finite element model consisted of 144, eight-noded isoparametric hybrid elements and 471 nodes with twelve rings of 12 elements concentric with the crack tip, which consisted of 25 independent but initially coincident nodes shown in Fig(2.1). At the remote boundaries the displacement field associated with elastic singular K and the non-singular elastic T was imposed as a boundary condition at a distance remote from the crack tip.

$$u = \frac{K}{E}(1+\upsilon)\, f_1(\varnothing) + (1-\upsilon^2)\frac{\beta}{E\sqrt{\pi a}} K\, r \cos(\varnothing) \tag{13}$$

$$v = \frac{K}{E}(1+\upsilon)\sqrt{\frac{r}{2\pi}}\, f_2(\varnothing) - \upsilon\,(1+\upsilon)\frac{\beta}{E\sqrt{\pi a}} K\, r \sin(\varnothing) \tag{14}$$

where the universal angular functions $f_1(\varnothing)$ and $f_2(\varnothing)$ are given in equation (14).on the chapter (1).

The plastic stress-strain response was represented by a Ramberg-Osgood power law of the form :

$$\frac{\varepsilon}{\varepsilon_o} = \frac{\sigma}{\sigma_o} + \alpha \left(\frac{\sigma}{\sigma_o}\right)^n \tag{15}$$

The material constants α and n were set at 3/7 and 13 respectively. Poisson's ratio υ and σ_0/E were 0.3 and 0.002 respectively. The J-integral was determined by the virtual crack extension method of Parks (1974) as implemented in ABAQUS (1984) and from the K component of the outer field. As the T-stress is an elastic concept it was always calculated from the remote K field using the biaxiality parameter. In the full field solutions which involved extensive plasticity the T-stress is calculated from the elastic component of the J-integral.

4.3. Results and Discussion

The loss of J-dominance for short cracks is clearly seen by referring to the appropriate slip line field in Fig (3.45). The slip line field for a deeply cracked bar under bending, given by Green (1953) shows that the deformation is confined to the uncracked ligament, and independent of notch depth and J-dominance thus applies for extensive plasticity. The finite element calculations for a weakly hardening material in bending and tension obtained by Al-Ani and Hancock (1991) are consistent with these observations, in that plasticity is confined to the uncracked ligament for $a/W \geq 0.5$ in tension and $a/W \geq 0.3$ in bending. Both of these geometries thus essentially behave as deeply cracked bars, and the stress straight ahead of the crack in small geometry change solutions is closely similar to the HRR fields. This feature is maintained as plasticity extends from small-scale yielding into full plasticity of the uncracked ligament. For these geometries the size of the ligament is clearly the controlling dimension, and the results are consistent with J-dominance criteria of

McMeeking and Parks (1979) and Shih and German (1981). In contrast, analysis of the sub-critical geometries (a/W< 0.3 in bending and 0.5 in tension Al-Ani and Hancock (1991) indicated that the plasticity spreads to the surface of the bar and the stresses ahead of the crack tip fall below the HRR field. These geometries lose J dominance. Deep crack geometries in tension and bending exhibit positive biaxiality parameters, which introduce tensile T-stresses, while shallow crack geometries exhibit negative biaxiality parameters which introduce compressive T-stresses. There is a remarkable correlation between the change in the fully plastic field and the elastic biaxiality parameter that for shallow cracked geometries which exhibited negative T stresses the plasticity breaks back to the crack surface, while for deep cracked geometries which show positive T stress as illustrated in Fig (3.5), plasticity is confined to the ligament. This has also been observed in double edge cracked bars.

In the present work modified boundary layer formulations, following Betegón and Hancock(1991), have been correlated with fully plastic solutions of real geometries. In order to pursue this approach, the stress σ_{yy} at a distance $r=2J/\sigma_o$ has been plotted against the T-stress normalised by the yield stress as shown in Fig (4.5). For all the geometries examined, the stresses were described by the boundary layer formulation characterised by J and T until full plasticity. Geometries with negative T-stresses show that the stress field decreases in accord with predictions of the boundary layer formulation into full plasticity. As an example the short crack in bending (a/W=0.03) shows agreement with stress field predicted from the two term boundary formulation at plasticity level of $a\sigma_o/J = 14$, when the plastic zone is very much greater than the crack length, and the ligament is almost fully plastic.

4.4. Conclusions.

The present results on plane strain edge cracked bars are consistent with the results of Betegón and Hancock (1991). Compressive T-stresses which reduce the hydrostatic stress ahead of the crack tip causes the stress field to fall below the HRR field and lose single parameter characterisation. Geometries with positive T-stresses develop stress fields similar to the HRR field and are characterised by J. There is a remarkable correlation between the T-stress and the plastic deformation ahead of the crack tip, negative T-stresses increase the radius of the plastic zone and cause plasticity to spread to the back face of the crack, while positive T-stress caused the plastic deformation to confined to the uncracked ligament.

J dominance is a special case of two-parameter characterisation of crack tip fields, when the second term becomes insignificant, which occurs when the T-stress is tensile and the effect of higher order terms in the nonlinear asymptotic crack field is negligible, leaving the HRR field as the only significant term.

4.5. References:

Al-Ani A. M. and Hancock, J. W.,(1991) J. Mech. Phys. Solids, 39, 23.

Al-Ani A. M. (1988), MSc Thesis. Mech. Eng. Dept., Glasgow Unviersity.

Betegón, C., and Hancock J., W.,(1991), J. Appl. Mech. in press

Bilby, B. A. ,Cardew, G. E. a, Goldthrope, M. R. and Howard,I. C. (1986),"Size Effect in Fracture. I. Mech. Eng. London. 37.

Du, Z. Z. and Hancock, J. W J. (1990), J. Mech. Phys. Solids. in press

Hutchinson, J. W, (1968), J. Mech. Phys. Solids 16, 13.

Green, A. P. (1953), Q J.Mech. Appl. Math., 6, 223.

Hibbitt, Karlsson and Sorensen Inc, (1984), ABAQUS User Manual, Providance., Rhode Island.

Larsson, S. G. and Carlsson, A. J., (1973),c, 21,263

Li, Y. and Wang, Z., (1986), " High-Order Asymptotic Field of Tensile Plane -Strain Non-Linear Crack Problrm., Scienta Sinica (Series A), 29,942

McMeeking ,R. M. and Parks, D. M.,(1979), ASTM. STP 668,175.

O'Dowd, N. P. and Shih, C. F.,(1990), "Family of Crack Tip Fields Characterised by a Triaxiality Parameter. Part 1- Structure of Field. University of Brown. Division of Engineering

Parks, D. M., (1974), Int. J. of Fracture., 10,487.

Rice, J. R. and Rosengren, G. F.,(1968), J. Mech. Phys. Solids, 16, 1.

Sharma, S. M. and Aravas, A. (1990), "Determination of Higher Order Terms in Asymptotic Elastoplastic Crack Tip Solution. University of Phennsyvania. Mech. Eng. Dept.

Shih, C. F., and German, M. G. (1981), Int. J of Fracture, 17, 27.

Loading	J	J - T
Bending	$b \geq \frac{25\,J}{\sigma_o}$	$b \geq \frac{25\,J}{\sigma_o}$
	$a \geq \frac{200J}{\sigma_o}$	$a \geq \frac{10\,J}{\sigma_o}$
Tension	$b \geq \frac{500\,J}{\sigma_o}$	$b \geq \frac{10J}{\sigma_o}$
	$a \geq \frac{200J}{\sigma_o}$	$a \geq \frac{10\,J}{\sigma_o}$

Table (4.1)

The extent of single and two parameter characterisation of plane strain elastic-plastic crack tip field

After Betegon and Hancock (1991)

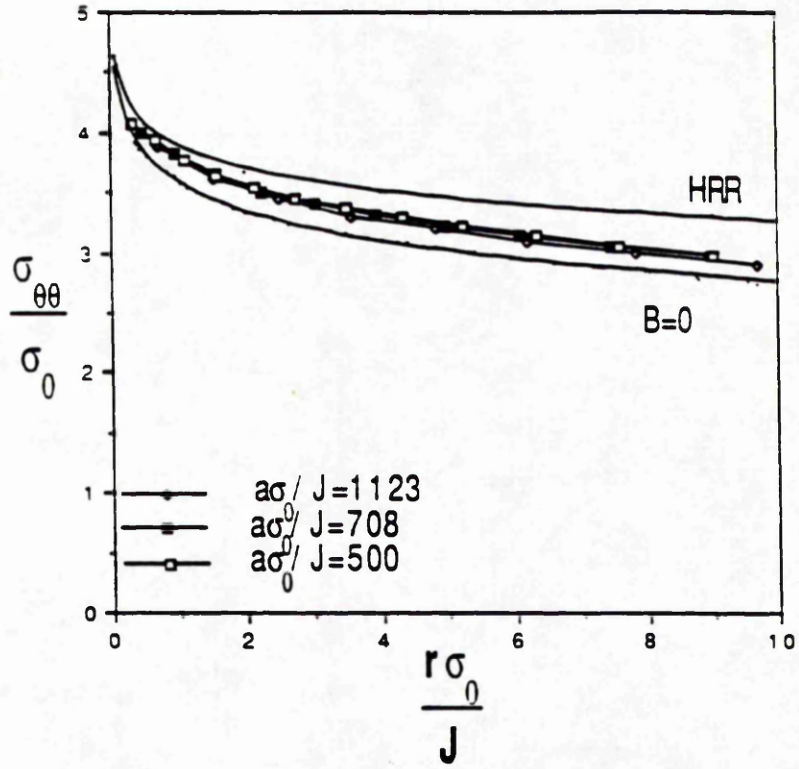

Fig (4.1) : The tangential stress directly ahead of the crack tip in boundary layer formulations, B=+1.06 and n=13.

After (Betegón and Hancock 1991)

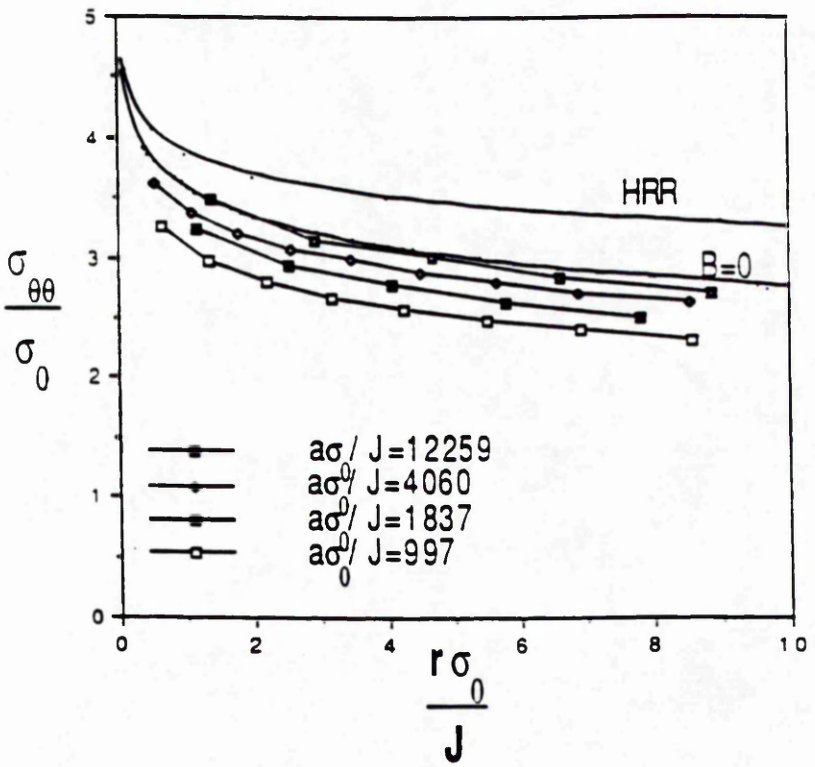

Fig (4.2) : The tangential stress directly ahead of the crack tip in a boundary layer formulation, B=-1.06 and n=13.

After (Betegón and Hancock 1991)

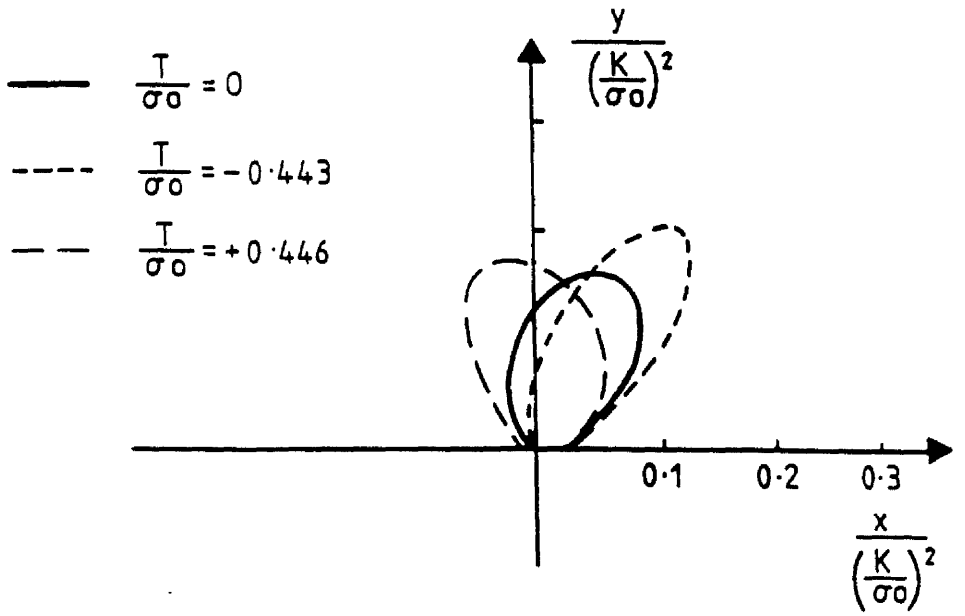

Fig (4.3) : The effect of the T-stress on the non-dimensionalised plastic zone

After (Du and Hancock 1990)

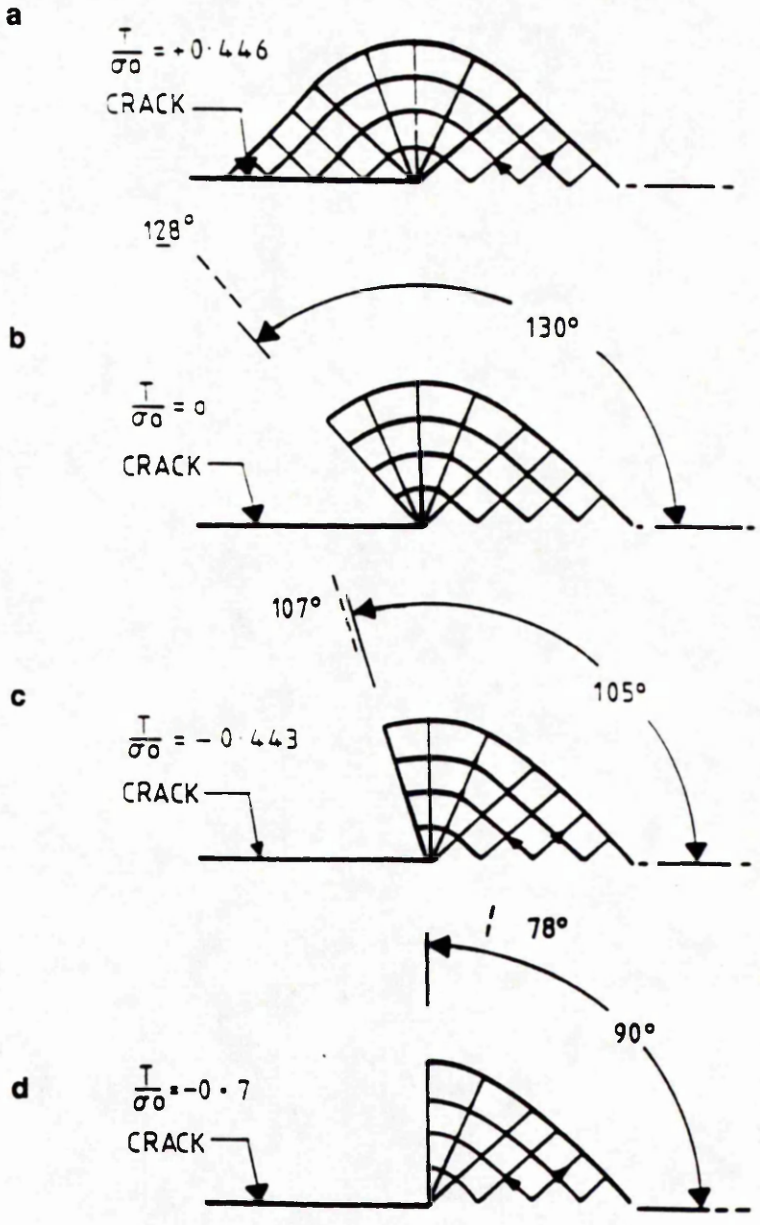

Fig (4.4) : A slip line filed represntation of the crack tip stress field for

(a) $T/\sigma_o = +0.446$

(b) $T/\sigma_o = 0$

(c) $T/\sigma_o = -0.443$

(d) $T/\sigma_o = -0.77$

After Du and Hancock (1990)

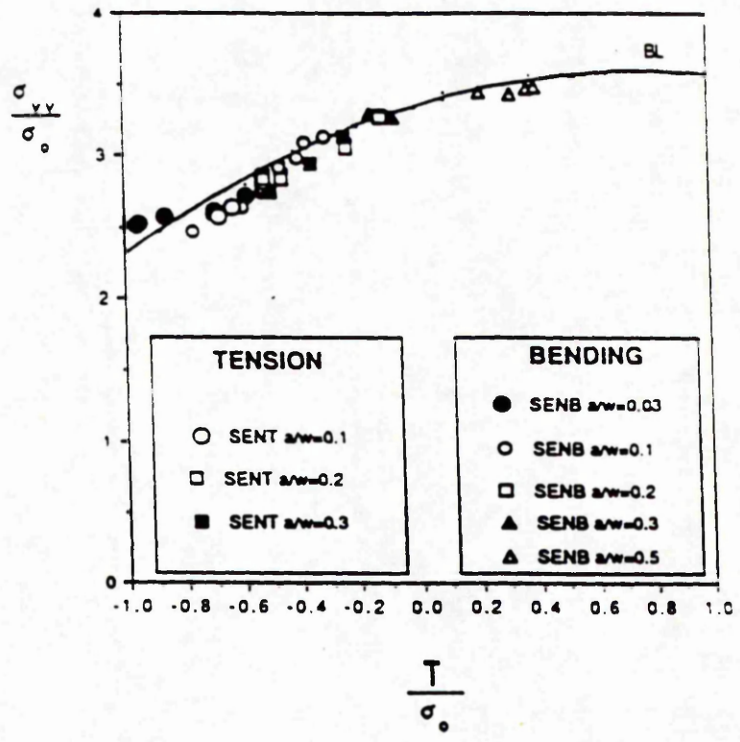

Fig (4.5) : The stress directly ahead at distance $2J/\sigma_o$ as a function of T/σ_o in edge cracked bars in tension and bending. The solid line is the modified boundary layer prediction.

Chapter (5)

Three Term Boundary Layer Formulation
Characterisation of the Crack Tip Field.

5.1. Introduction:

Given the importance of the in-plane non-singular stress, T, on crack tip deformation it is now important to understand and to consider the effect of the out of plane non-singular term. The out of plane stress σ_{33} comprises a singular K term and a non-singular term denoted S following Rice (1974). The asymptotic expansion of the stress about the crack tip for a three dimensional stress field can now be written as :

$$\begin{bmatrix} \sigma_{xx} & \sigma_{xy} & \sigma_{xz} \\ \sigma_{yx} & \sigma_{yy} & \sigma_{yz} \\ \sigma_{zx} & \sigma_{zy} & \sigma_{zz} \end{bmatrix} = \frac{K}{\sqrt{2\pi r}} \begin{bmatrix} f_{xx}(\varnothing) & f_{xy}(\varnothing) & f_{xz}(\varnothing) \\ f_{yx}(\varnothing) & f_{yy}(\varnothing) & f_{yz}(\varnothing) \\ f_{zx}(\varnothing) & f_{zy}(\varnothing) & f_{zz}(\varnothing) \end{bmatrix} + \begin{bmatrix} T & 0 & 0 \\ 0 & 0 & 0 \\ 0 & 0 & S \end{bmatrix} \tag{1}$$

Under plane strain conditions, the elastic stress-strain relation $e_{zz}=1/E\ [\sigma_{zz}-\upsilon(\sigma_{xx}-\sigma_{yy})]$ establishes the relations.

$$f_{zz}(\varnothing) = \upsilon\ (f_{yy}(\varnothing) + f_{xx}(\varnothing))$$

$$f_{xz}(\varnothing) = f_{yz}(\varnothing) = f_{zx}(\varnothing) = f_{zy}(\varnothing) = 0 \tag{2}$$

In plane strain these simplifications allow the stresses at the crack tip to be written in the form:

$$\begin{bmatrix} \sigma_{xx} \\ \sigma_{yy} \\ \sigma_{zz} \end{bmatrix} = \frac{K}{\sqrt{2\pi r}} \begin{bmatrix} f_{xx}(\phi) \\ f_{yy}(\phi) \\ \upsilon\,(f_{xx}(\phi) + f_{yy}(\phi)) \end{bmatrix} + \begin{bmatrix} T \\ 0 \\ S \end{bmatrix} \qquad (3)$$

On the flanks, $\sigma_{yy}=0$, $\sigma_{xx}=T$ and $\sigma_{zz}=S$, giving

$$e_{zz} = \frac{1}{E}(S - \upsilon T) = 0 \qquad (4)$$

The elastic plane strain condition thus establish a relation between the in plane and out of plane non-singular terms.

$$S = \upsilon T \qquad (5)$$

However, in general three dimensional problems, it is to be expected that a range of (S/T) ratios will be encountered. The purpose of the present chapter is thus to investigate the effect of the out of plane non-singular term, S.

5.2. Numerical Methods and Finite Element Model:

5.2.1. Boundary Layer Formulation.

Modified boundary layer solutions have been obtained under elastic-plastic plane strain small scale yielding with generalised plane strain boundary conditions. In generalised plane strain the out of plane

strain e_{zz} may be non-zero but must be independent of spatial co-ordinate (r,ø).

$$e_{zz} \neq 0$$
$$\gamma_{yz} = \gamma_{zx} = 0 \qquad (6)$$

The finite element model consisted of 144, ten-noded isoparametric hybrid elements comprising 12 rings of 12 elements concentric with crack tip. The crack tip was modelled with a focused mesh of collapsed elements, so that the tip consisted of 25 independent but initially coincident nodes. These elements were generated as a eight noded elements introducing two extra nodes without any coordinates to generate the ten noded elements. The first eight nodes of each element were conventional and determine the position and motion of the element in the two bounding planes. The two extra nodes were the same for all the generalised plane strain elements. The active degrees of freedom for the first eight nodes were degrees of freedom 1 and 2 representing the movements in the x and y directions. The first extra node had one degree of freedom which represented the change in length of an axial material fiber connecting this node with its image in the other bounding plane, while the active degrees of freedom for the second node of additional nodes are the relative rotations of one bounding plane with respect to the other and denoted by ϕ_x and ϕ_y in Fig (5.1). Positive rotation about the x axis causes increasing axial strain with respect to y coordinate in the cross section, and positive rotation about the y axis causes decreasing the axial strain with respect to the x coordinate in the cross section. In the current problem the bounding planes were initially parallel and prevented from rotating

with deformation. At the remote boundaries the displacements (u,v) in the x and y directions associated with the elastic singular term K and the two non-singular elastic terms T and S were imposed as boundary conditions at a distance remote from the crack tip.

$$u = \frac{K}{E}(1+\upsilon)\sqrt{\frac{r}{2\pi}}\left[\cos\left(\frac{\phi}{2}\right)\left(1-2\upsilon+\sin^2\left(\frac{\phi}{2}\right)\right)\right]+\frac{1}{E}(T-\upsilon S)\, r\cos\phi \tag{7}$$

$$v = \frac{K}{E}(1+\upsilon)\sqrt{\frac{r}{2\pi}}\left[\sin\left(\frac{\phi}{2}\right)\left(2-2\upsilon-\cos^2\left(\frac{\phi}{2}\right)\right)\right]+\frac{1}{E}(\upsilon(T+S)\, r\sin\phi \tag{8}$$

The out of plane displacements corresponding to the non-singular term S were applied to the extra nodes of the model elements.

$$w = \frac{Z}{E}(S-\upsilon T) \tag{9}$$

Here Z is the out -of-plane thickness of the model. If the applied displacement on two extra nodes is positive ($S>\upsilon T$) the planes move apart, so that there is a tensile axial direction strain in the model, while when the displacement is negative ($S<\upsilon T$) there is a compressive axial strain.

The plastic stress-strain response was represented by a Ramberg-Osgood power law of the form :

$$\frac{\varepsilon}{\varepsilon_o} = \frac{\sigma}{\sigma_o} + \alpha \left(\frac{\sigma}{\sigma_o}\right)^n \qquad (10)$$

The material constants α and n were set at 3/7 and 13 respectively. Poisson's ratio υ and σ_o /E were 0.3 and 0.002 respectively. The J-integral was determined both by the virtual crack extension method of Parks (1974) as modified by Li et al (1985) and implemented in ABAQUS (1984) and from the K component of the outer field.

5.2.2. Results of the Boundary Layer Formulation:

Results of the stress field for the boundary layer formulation corresponding to different (S/T) ratios are presented in Fig (5.2) in cylindrical co-ordinats (r,ø) centred at the tip. The hoop stress at distance ($2J/\sigma_o$) ahead the tip for the boundary layer formulation are plotted as a function of the T-stress. Both the hoop stress $\sigma_{øø}$ and the T stress were normalised by the yield stress σ_o. The T stress was calculated from the displacement in the radial direction, applied on the nodes located at the outer boundary at the crack flank (ø=180°).

$$\frac{T}{\sigma_o} = \frac{U_r E}{R \sigma_o} \frac{1}{1-(\upsilon \left(\frac{S}{T}\right))} \qquad (11)$$

The effect of the (S/T) ratio on the shape and the size of the plastic zone can be seen in Fig (5.3a,b), the stresses fields are insensitive to the ratio (S/T) and are similar to plane strain boundary layer formulations fields with the appropriate T stress.

5.3. Full Field Solutions:

Full field solutions are presented for penny shaped cracks located in the centre of round bars, as well as round bars with circumferential cracks. For both geometries a range of crack length (a) to width (W) ratios were investigated. The geometries shown in Fig (5.4),were chosen to represent different values of T and S. The finite element meshes utilised eight noded hybrid axisymmetric elements with reduced integration to prevent mesh locking. Symmetry allowed one quarter of the model to be represented. The details of the finite element mesh for each geometry is given in Table (2.2). In all cases the crack was modelled with a focused mesh with independent coincident nodes at the crack tip. All the specimens were subject to uniform tensile displacement boundary conditions. The plastic stress-strain response was represented by a Ramberg-Osgood power law of the form given in equation (10). The material constants α and n were set at 3/7 and 13 respectively. Poisson's ratio υ and σ_0 /E were 0.3 and 0.002 respectively. The J-integral was determined by the virtual crack extension method of Parks (1974) as modified by Li et al (1985) and implemented in ABAQUS (1984).

5.3.1. Elastic Analysis of T and S Stresses

The magnitude of the T-stress is defined through a biaxiality parameter β_T which depends on both the geometry and the loading :

$$\beta_T = \frac{T\sqrt{\pi a}}{K} \qquad (12)$$

The T-stress was evaluated directly from the stress on the crack flanks under perfectly elastic conditions using cylidrical co-ordinates (r,Ø,z) with origin at the center of the bar. On the crack flanks, the axial stress σ_{zz} must be equal to zero because it is a free surface, and the only in plane term left is the T stress σ_{rr}. The term $[\sigma_{rr}\sqrt{\pi a}/K]$, at each node behind the crack was determined and extrapolated to the crack tip. The out of plane non-singular term S can also be expressed in term of a biaxiality parameter β_S.

$$\beta_S = \frac{S\sqrt{\pi a}}{K} \tag{13}$$

On the flank the S-stress is taken to be equal to the out of plane stress $\sigma_{\theta\theta}$. The biaxiality parameter β_S corresponding to the non-singular term S was also determined by extrapolation to the crack tip.

The value of the biaxiality parameters β_T and β_S for both central and circumferential cracks are given in Figs (5.5) and (5.6) as a function of (a/W). For the central penny shaped cracks both β_T and β_S are consistently negative values for all (a/W) ratios paralleling the results for plane strain center cracked panels. Fig (5.6) shows the biaxiality parameters β_T and β_S for the circumferential crack. In this case the biaxiality parameter corresponding to the T term β_T is negative value for all values of (a/W) while the biaxiality parameter corresponding to the S term β_S is negative for (a/W)≤0.3 and positive value for (a/W)≥0.3.

5.3.2. Elastic-Plastic Results of the Full Field Solution:

5.3.2.1. Circumferential Crack in a Round Bar:

The stress distribution ahead of circumferential cracks with (a/W) ratios 0.1, 0.3, and 0.9 are shown in Figs (5.7,5.8 and 5.9). These ratios were chosen to represented different (S/T) ratios. For (a/W)=0.1, (S/T)=+0.5; (a/W)=0.3, (S/T=0), and for (a/W)=0.9, (S/T)=-2. The stresses are normalised by the yield stress σ_o, while the original distance X of a point ahead of the crack is non-dimensionalised by (J/σ_o). The numerical solutions were compared with both the HRR field and the unmodified plane strain boundary layer formulation (T=0, S=υT). For geometries with (a/W) ratios equal to 0.1 and 0.3, which have positive and zero (S/T) ratios, at all the levels of plasticity the stress fell below both the HRR field and plane strain T=0 field. For the geometry with (a/W) equal to 0.9, which has a negative (S/T) ratio, the stress field fell below the HRR field, but was close to the plane strain boundary layer formulation T=0 field. It is significant to note that for geometries with (a/W) ratios less than 0.3 plasticity extended initially to the cracked face and finally to the uncracked ligament as illustrated by the the plastic zone for (a/W=0.1) shown in Fig (5.10a). These geometries exhibited negative biaxialities β_T and β_S. In contrast for geometries with (a/W>0.3), which exhibited a negative biaxiality β_T and positive β_S, the full plastic slip field is confined to the uncracked ligament as illustrated by the plastic zones shown in Fig (5.11a,b). For the axisymmetric circumferential cracks the change in the nature of the fully plastic flow field, is coincident with change in the biaxiality parameter β_S from negative to positive.

5.3.2.2. Central Penny Shaped Crack in a Round Bar:

Although all the geometries with penny shaped cracks had similar (S/T) ratios, the stress distribution ahead of the crack for three geometries with ratios of (a/W) equal to 0.1,0.3 and 0.9 are presented in Figs (5.12, 5.13, and 5.14). The stresses are normalised by the yield stress σ_0, while the original distance X of a point ahead of the crack is non-dimensionalised by (J/σ_0). For all the geometries, at all levels of plasticity the stress field fell so far below the HRR and the β=0 field that single parameter characterisation by J through the HRR field was not possible. Plasticity for these geometries (which feature negative biaxiality β_T as well as negative biaxiality β_S) extended through the ligament before gross yielding as illustrated by the plastic zone for (a/W=0.1) shown in Fig (5.10b).

5.4. Comparison Between the Full Field Solution and the Boundary Layer Formulation solution.

The stress at a distance $(2J/\sigma_0)$ ahead of the crack tip for axisymmetric central cracks with (a/W) ratios equal to 0.1,0.3 and 0.9 which all have (S/T) ratios close to +1 are compared to the stress field of the modified boundary layer formulation corresponding to the same value of (S/T)=+1 in Fig (5.15). The results show that for different values of $a\sigma_0/J$ corresponding to different levels of plasticity there is agreement between the full field solutions and the boundary layer formulation. Similarly the axial stress ahead of the crack tip for the axisymmetric circumferential crack with (a/W)=0.1, 0.3 and 0.9 are compared to the stress field for the boundary layer formulation

with the appropriate (S/T) ratio in Figs (5.16, 5.17 and 5.18). The results again show that the stress field for the full field solution are described very well by the modified boundary layer solution with the same (S/T) ratio. Fig (5.19) shows the axial stress σ at a distance $(2J/\sigma_o)$ ahead of the crack tip for axisymmetric circumferential cracks with (a/W) equal to 0.1, 0.3 and 0.9 compared to a plane strain T=0 boundary layer formulation. The results indicate that although the three geometries have different (S/T) ratios the stress fields are well described by modified boundary layer formulations, within the limit that the out of plane strain is less than the yielding strain.

5.5. Discussion:

Finite element calculations for the plane strain problems have established the effect of the first in-plane non-singular term (T) on stress induced fracture mechanisms, and established the T as a second parameter which enables the stress field to be characterised when single parameter characterisation becomes inadequate.

Modified boundary layer formulations for different ratios of (S/T) demonstrate that there is no significant effect due to the change of the S stress from compressive to tensile. The stress fields corresponding to different (S/T) ratios are similar to those obtained under plane strain conditions in which the (S/T) ratio is equal to Poisson's ratio (υ). This observation has been confirmed by comparing full field solutions of round bars with axisymmetric central cracks and the cracked bar with axisymmetric circumferential cracks with plane strain boundary layer formulations as shown in Fig (5.20). The results show that all the stresses field for both geometries are well described by the plane strain

boundary layer formulation field. Present results indicated that the out of plane, non-singular terms and the associated modest departure from plane strain conditions have a weak effect on the stress fields.

5.6. Conclusions

The results obtained in this chapter suggest that the elastic plastic stress states for the three dimensional configurations can also be characterised by J and T into full plasticity within the limit that the out of plane strain is about less than the yield strain. The results also suggest that it is no longer necessary to have different criteria for different configuration for modest departure from plane strain loading conditions. It also confirmed that J dominance is a special case of two parameter characterisation of the crack tip field such that the effect of the non-singular terms (T,S) on the non-linear asymptotic expansion of the crack tip field is negligible.

5.7. References

Hibbitt, Karlsson and Sorensen Inc, (1984), ABAQUS User Manual, Providance., Rhode Island.

Parks, D. M., (1974), Int. J. of Fracture., 10,487-496.

Li,F. Z.,Shih, C. F. Needleman, A., (1985), Engineering Fracture Mechanics, 21, 405-421.

Rice, J. R., (1974), J. Mech. Phys. Solids, 22,17.

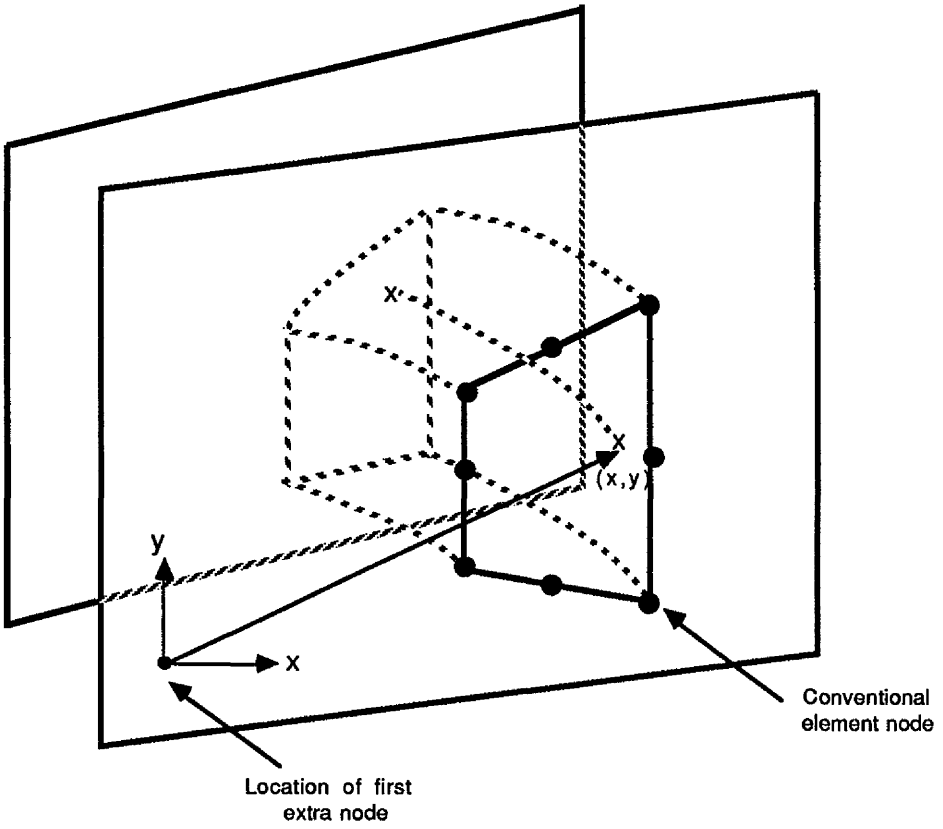

Length of line through the thickness at (x,y) is

$$t_o + \Delta u_z + \Delta\phi_x(y - Y_o) - \Delta\phi_y(x - X_o)$$

Fig (5.1) : Generalised plane strain model.

After the ABAQUS manual(1989)

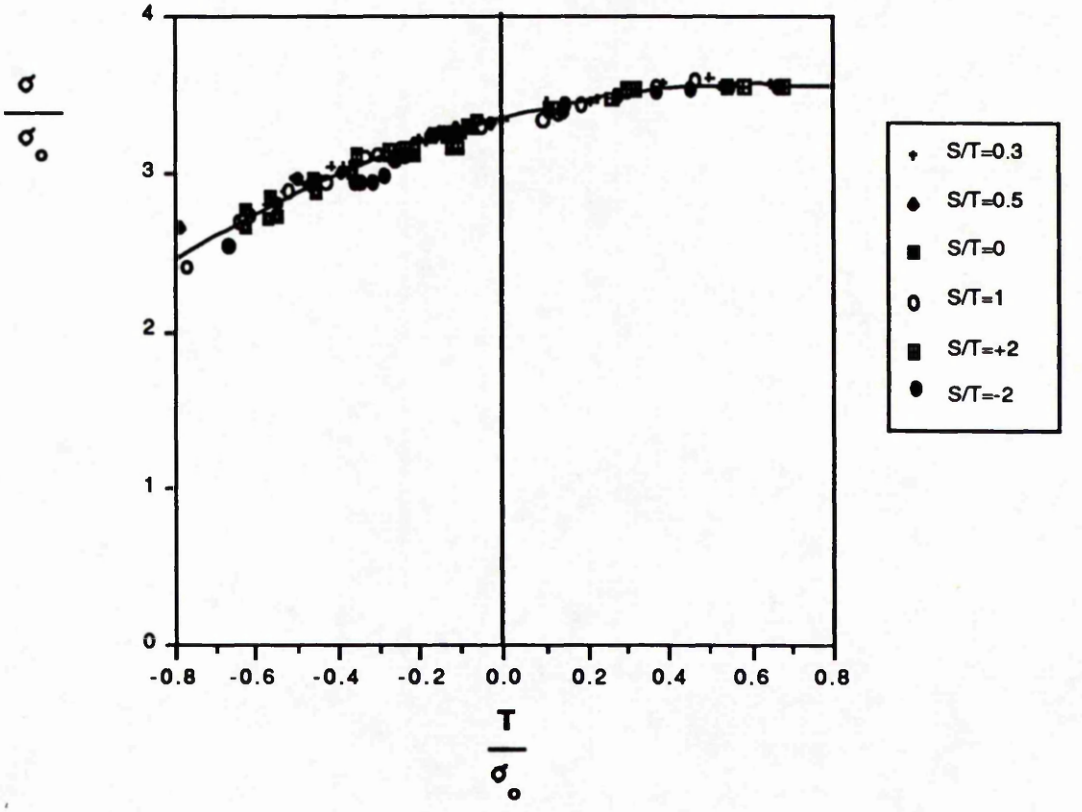

Fig (5.2) : The stress directly ahead of the crack at distance $2J/\sigma_o$ as a function of T/σ_o with different ratio of S/T in boundary layer formulations.

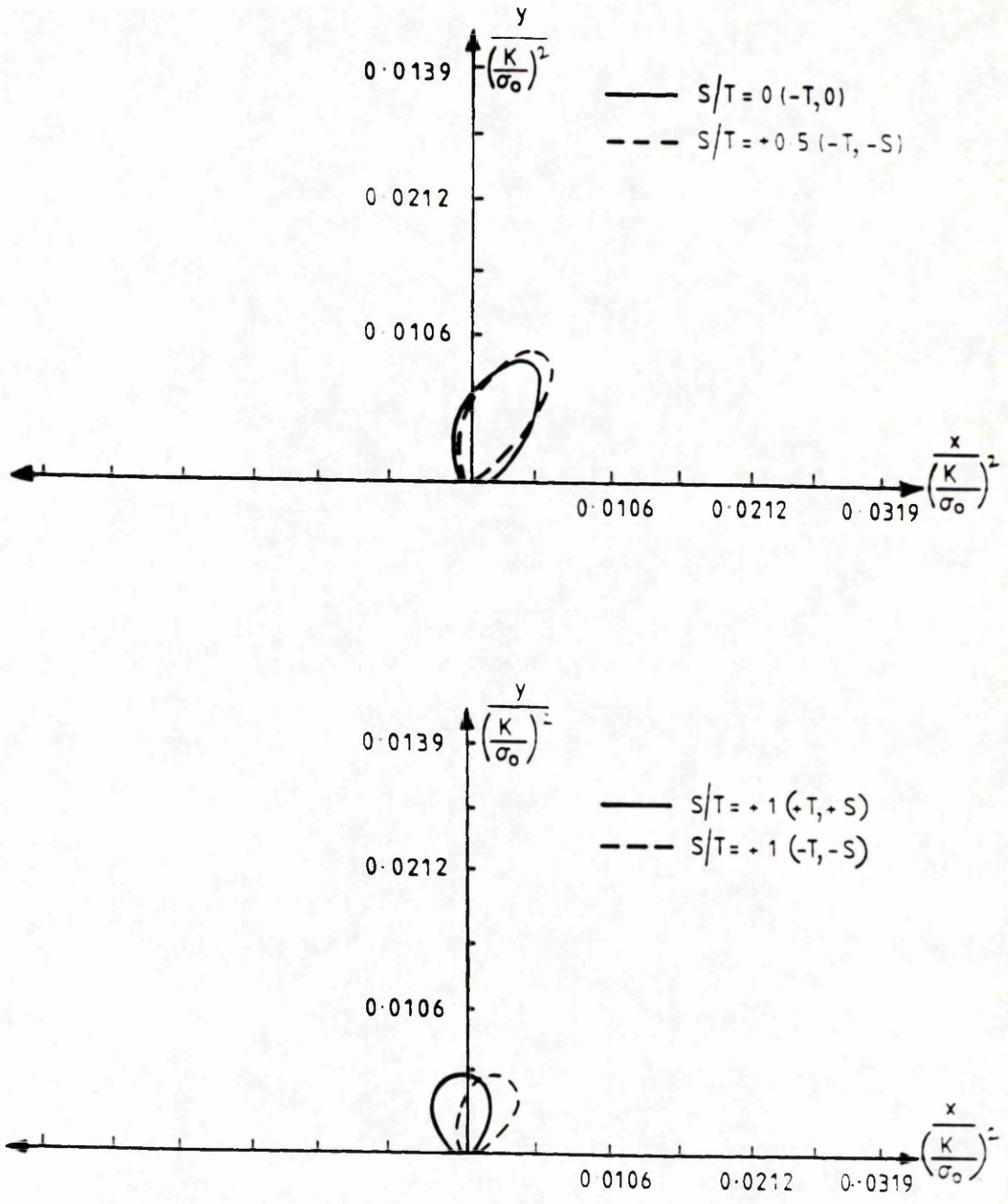

(a)

Fig (5.3) : The effect of the ratio S/T on the non-dimensionalised plastic zone

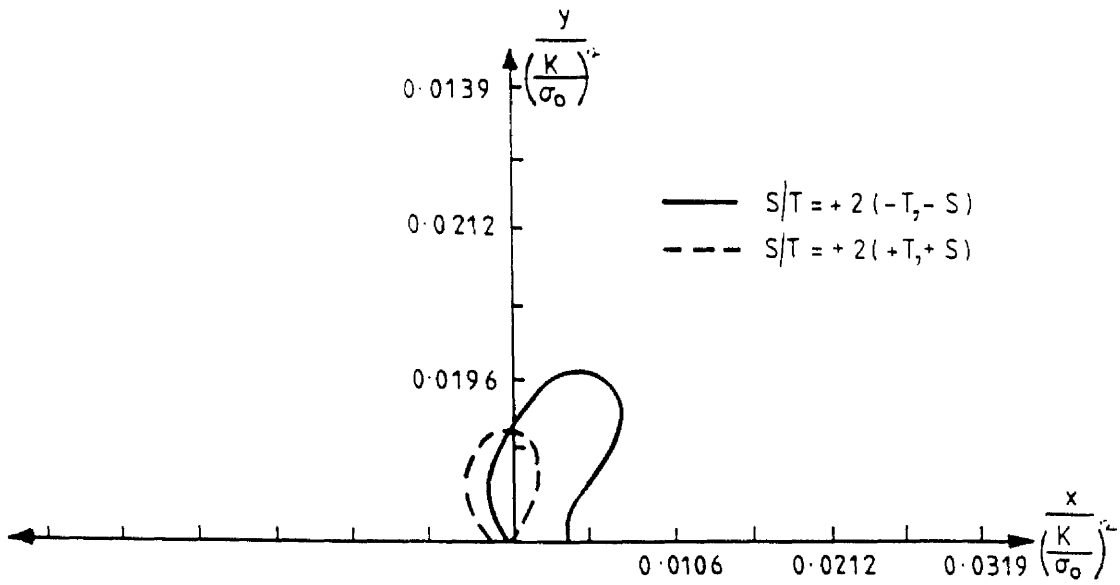
y
$\left(\frac{K}{\sigma_o}\right)^2$
0·0139
0·0212
0·0196
S/T = + 2 (- T, - S)
S/T = + 2 (+ T, + S)
x
$\left(\frac{K}{\sigma_o}\right)^2$
0·0106
0·0212
0·0319

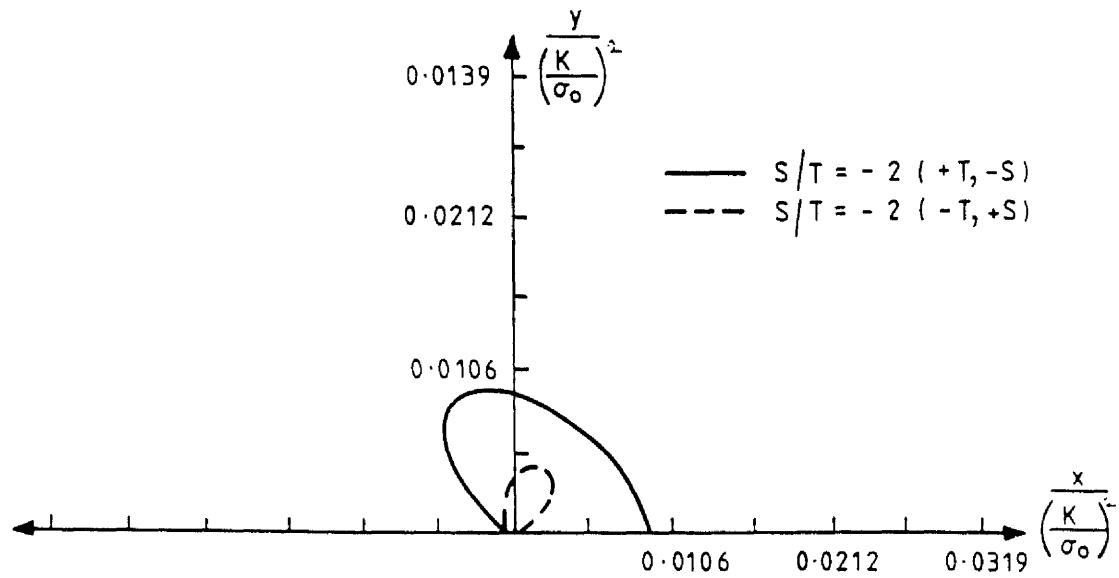
y
$\left(\frac{K}{\sigma_o}\right)^2$
0·0139
0·0212
0·0106
S/T = - 2 (+ T, - S)
S/T = - 2 (- T, + S)
x
$\left(\frac{K}{\sigma_o}\right)^2$
0·0106
0·0212
0·0319

(b)

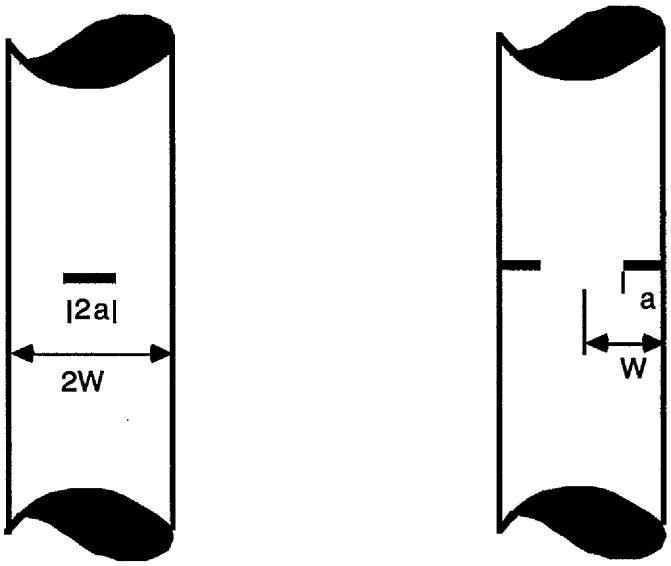

Fig (5.4) : The geometry of the axisymmetric round bar
(a) : The centre crack
(b) : The circumferential crack

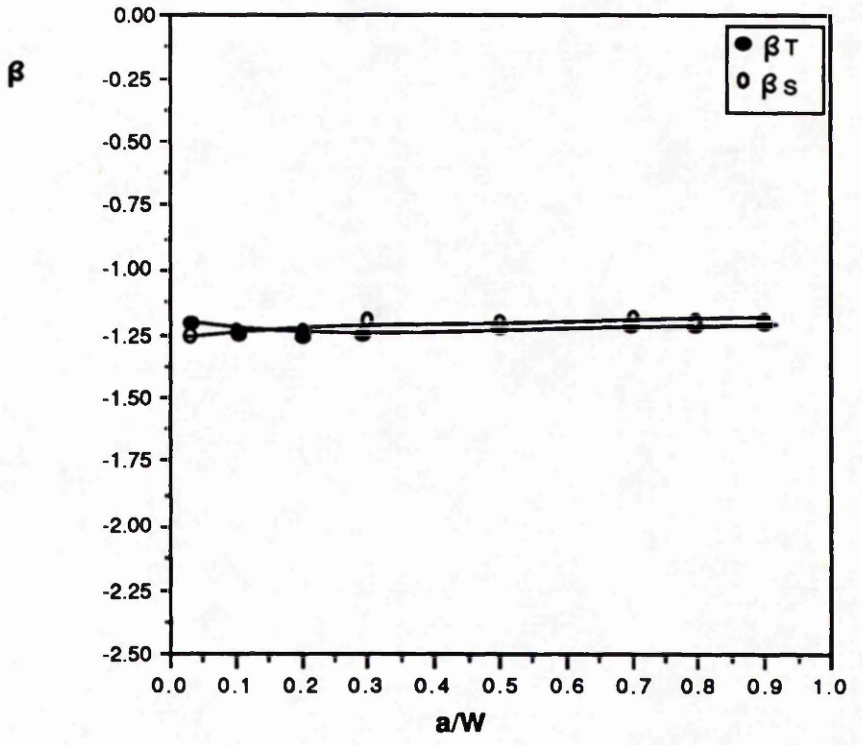

Fig (5.5) : The biaxiality parameter corresponding to the non-singular terms T and S for the penny shaped cracked in a round bar.

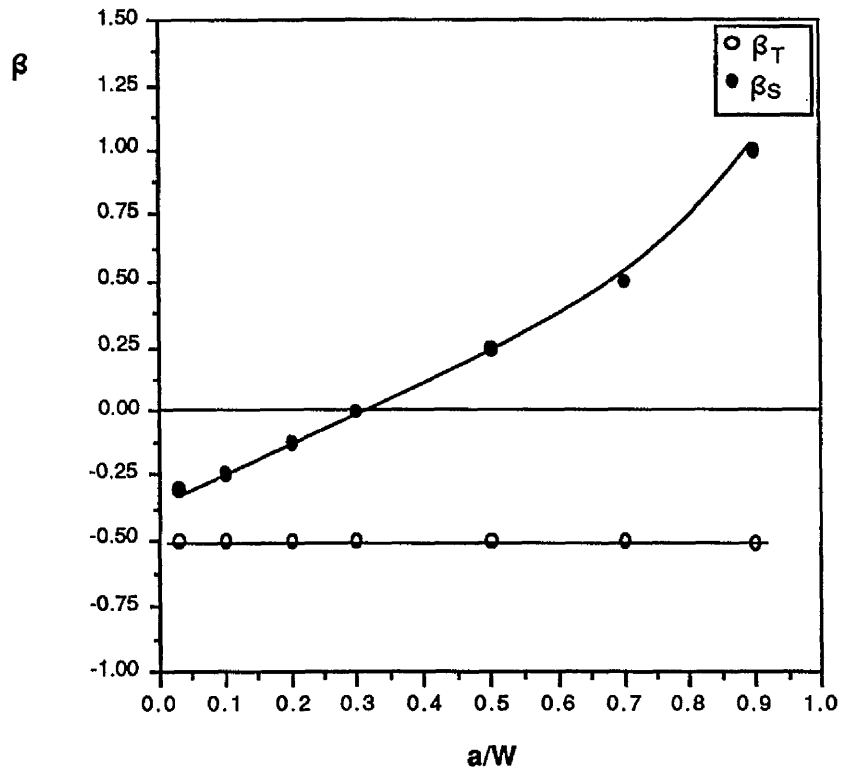

Fig (5.6) : The biaxialty parameter corresponding to the non-singular terms T and S for the circumferential crack in a round bar.

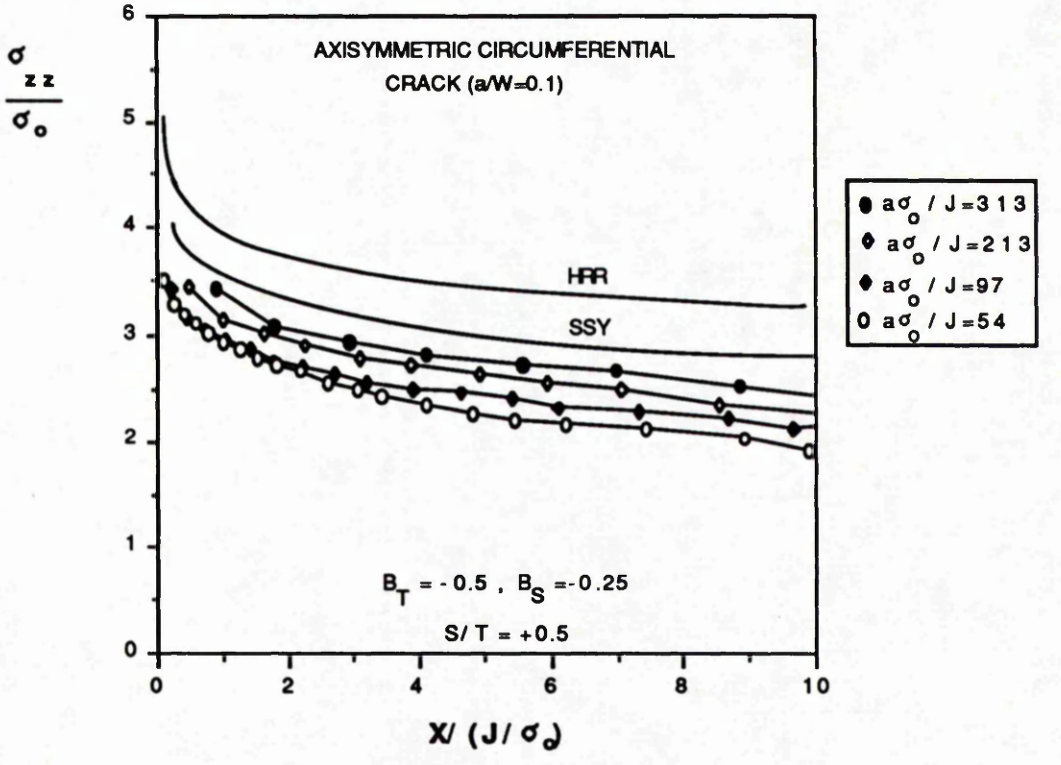

Fig (5.7) : The stress directly ahead of a circumferential crack with (S/T=+0.5).

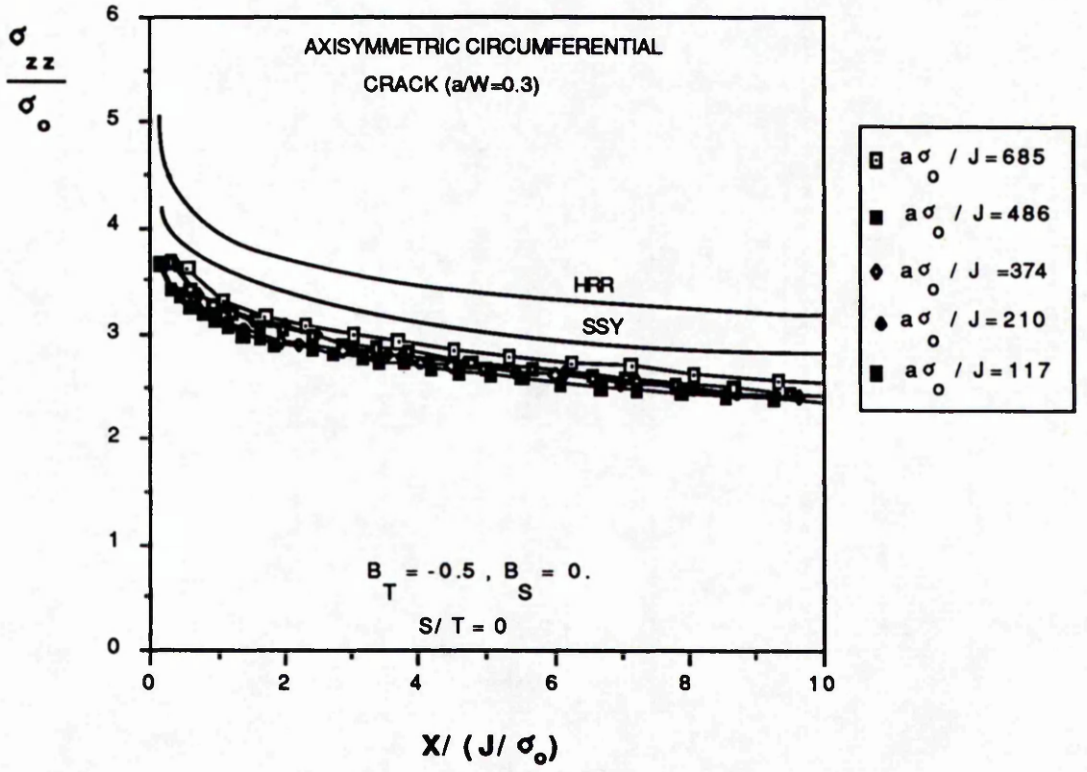

Fig (5.8) : The stress directly ahead of a circumferential crack with (S/T=0).

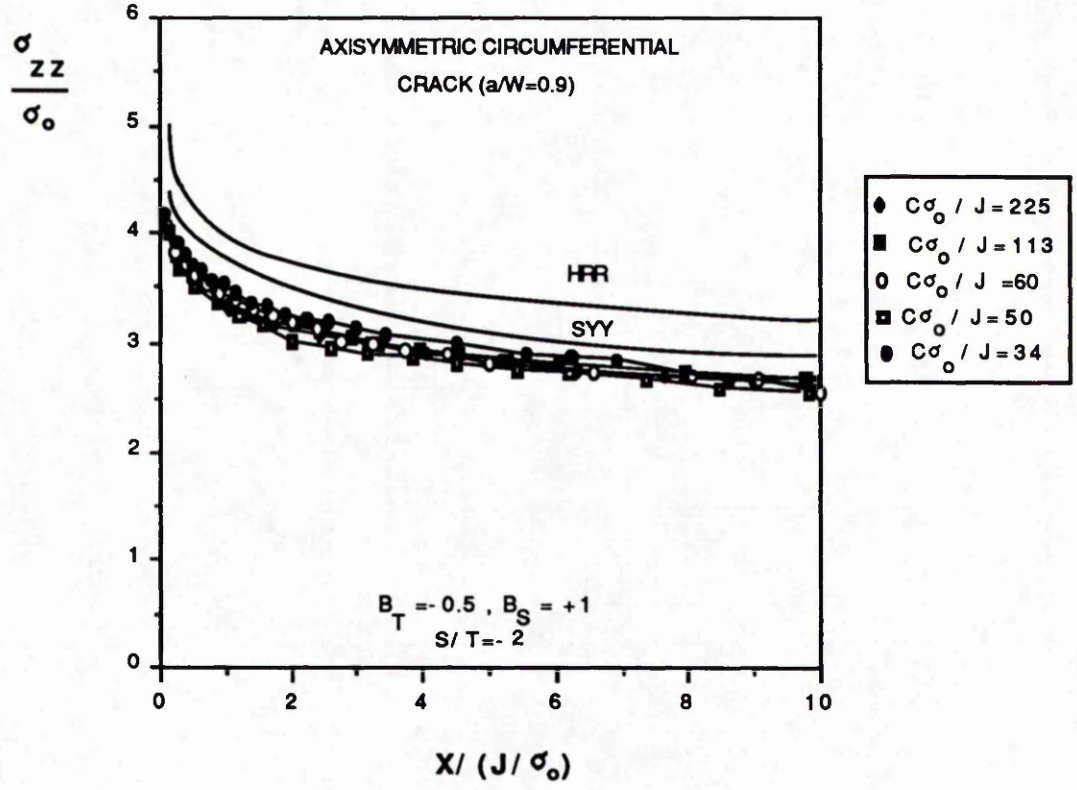

Fig (5.9) : The stress directly ahead of a circumferential crack with (S/T=-2).

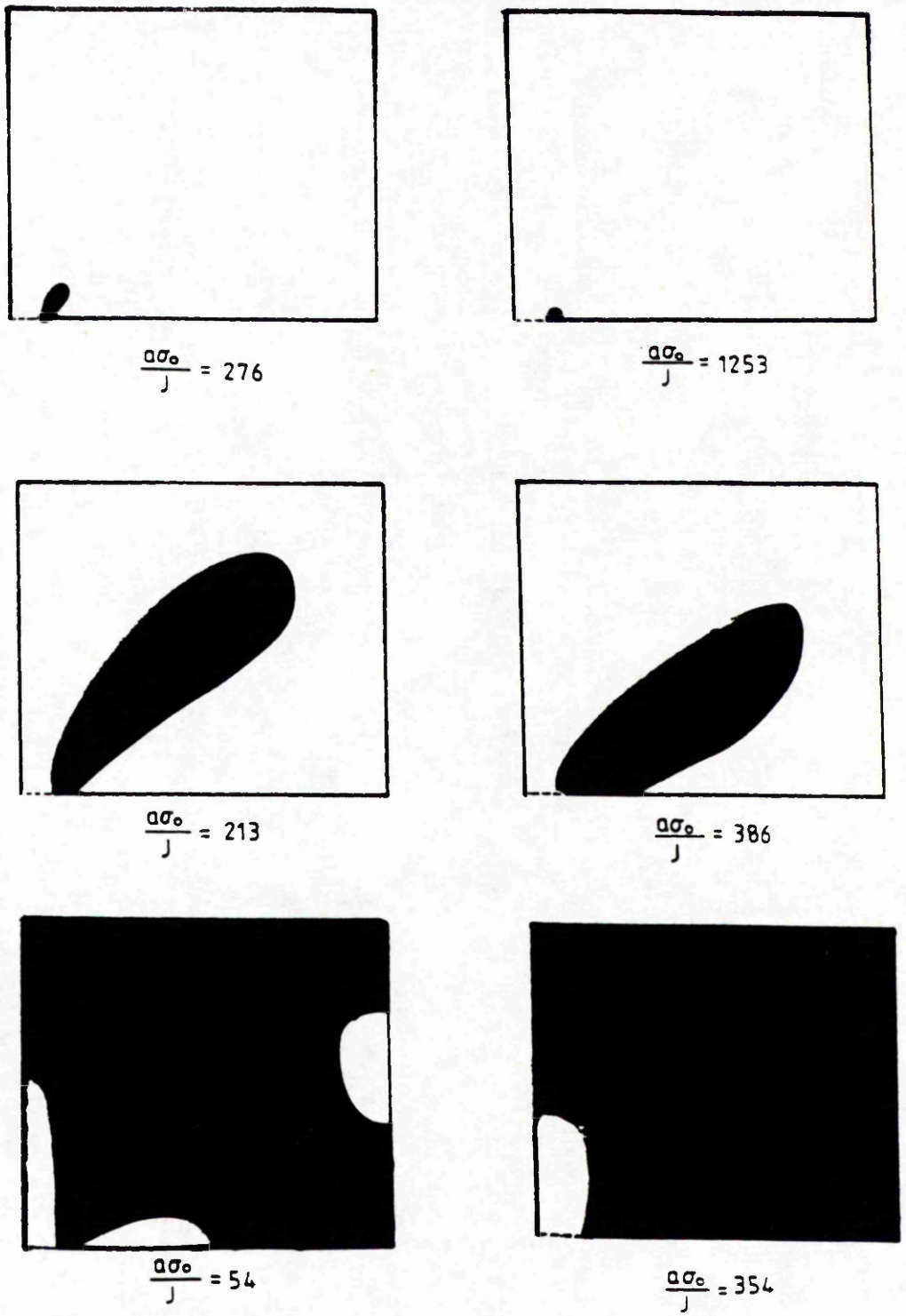

Fig (5.10) : Plastic zone for
(a) : Circumferential crack in an axisymmetric round bar (a/W=0.1), (S/T=+0.5)
(b) : Centre crack in an axisymmetric round bar (a/W=0.1), (S/T=+1)

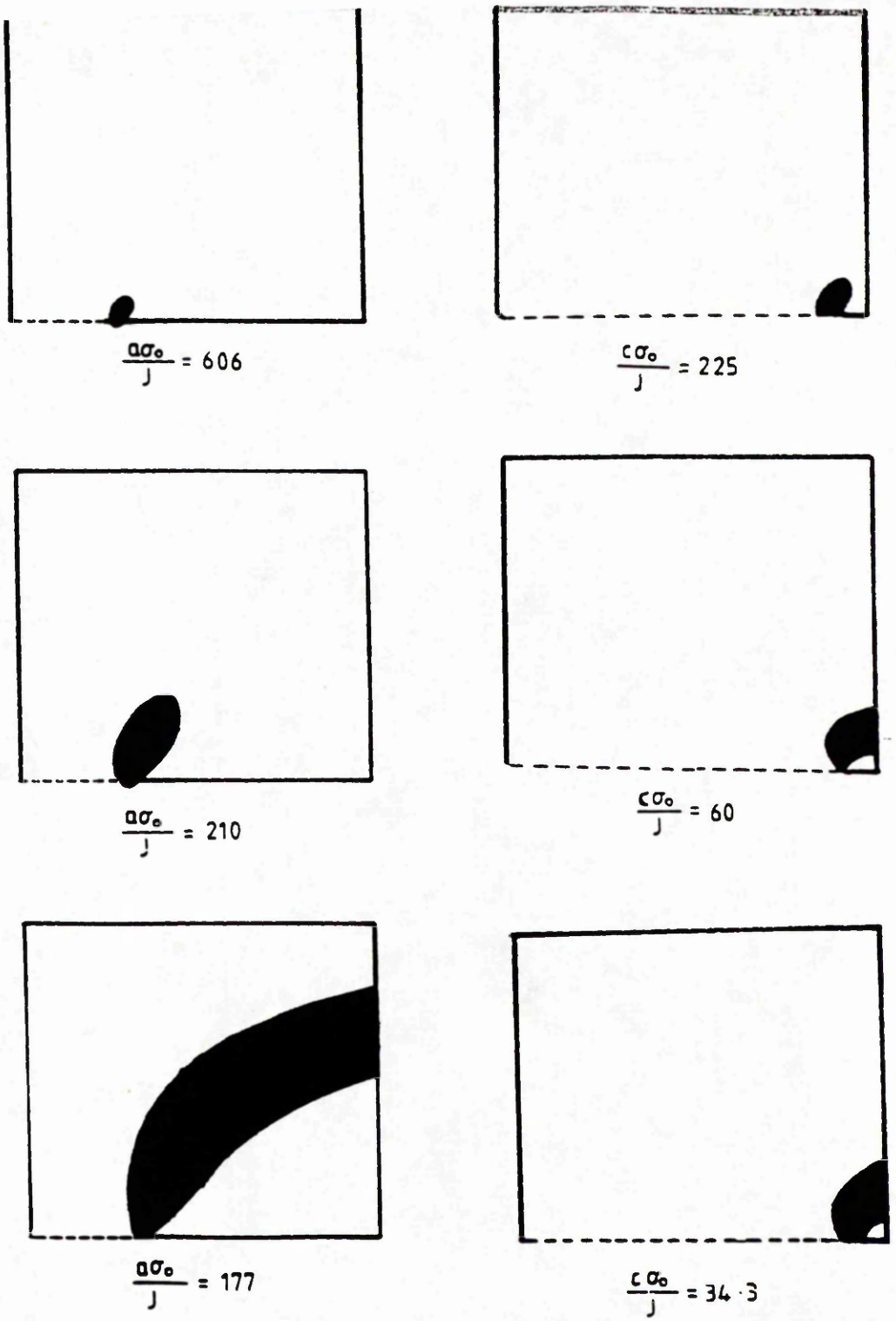

Fig (5.11) : Plastic zone for
(a) : Circumferential crack in an axisymmetric round bar (a/W=0.3) (S/T=0)
(b) : Cricumferential crack in an axisymmetric round bar (a/W=0.9) (S/T=-2)

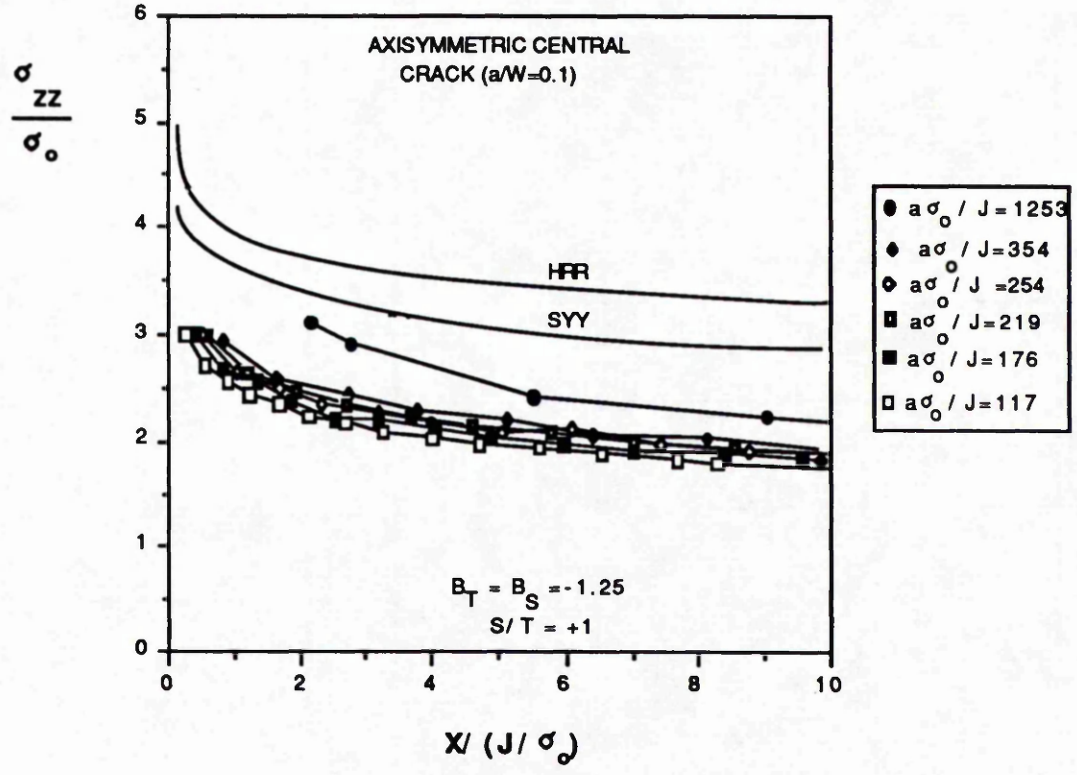

Fig (5.12) : The stress directly ahead of a penny shaped crack for (S/T=+1.0).

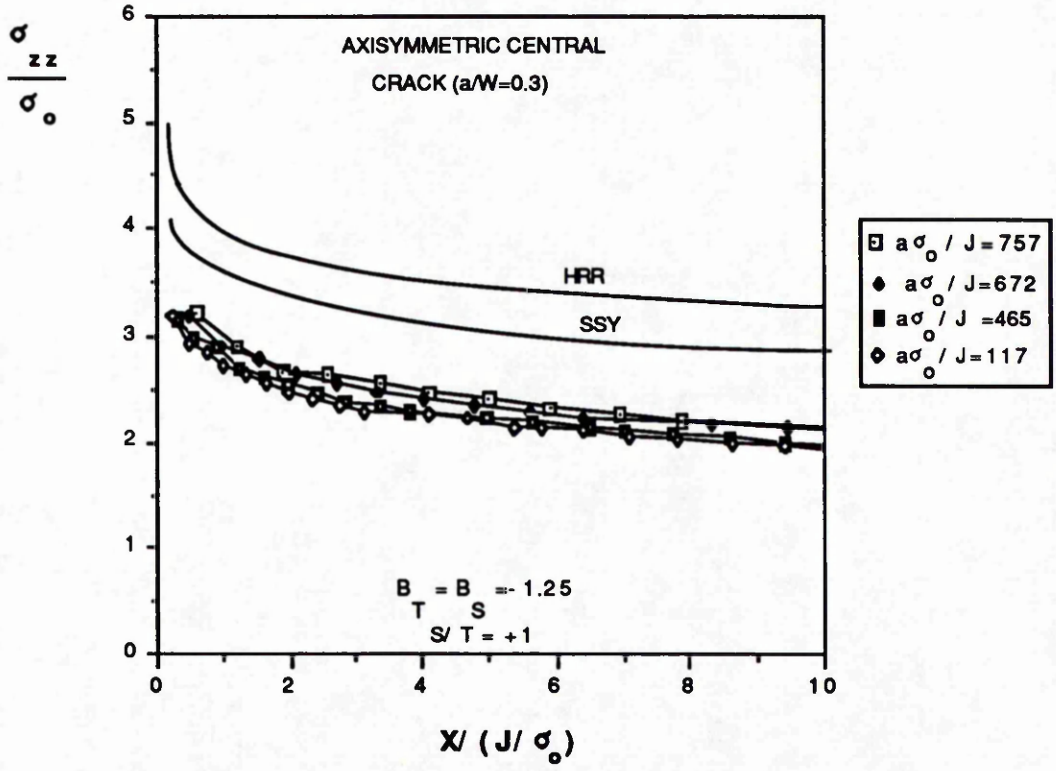

Fig (5.13) : The stress directly ahead of a penny shaped crack (S/T=+1.0)

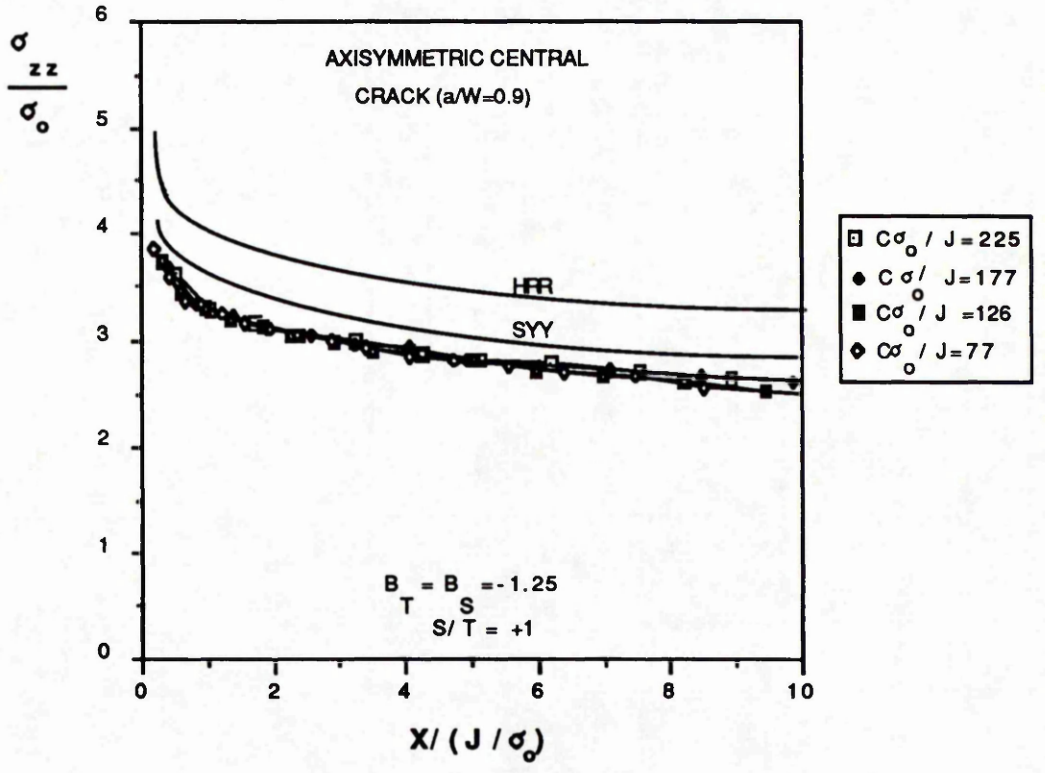

Fig (5.14) : The stress directly ahead of a penny shaped crack (S/T=+1.0).

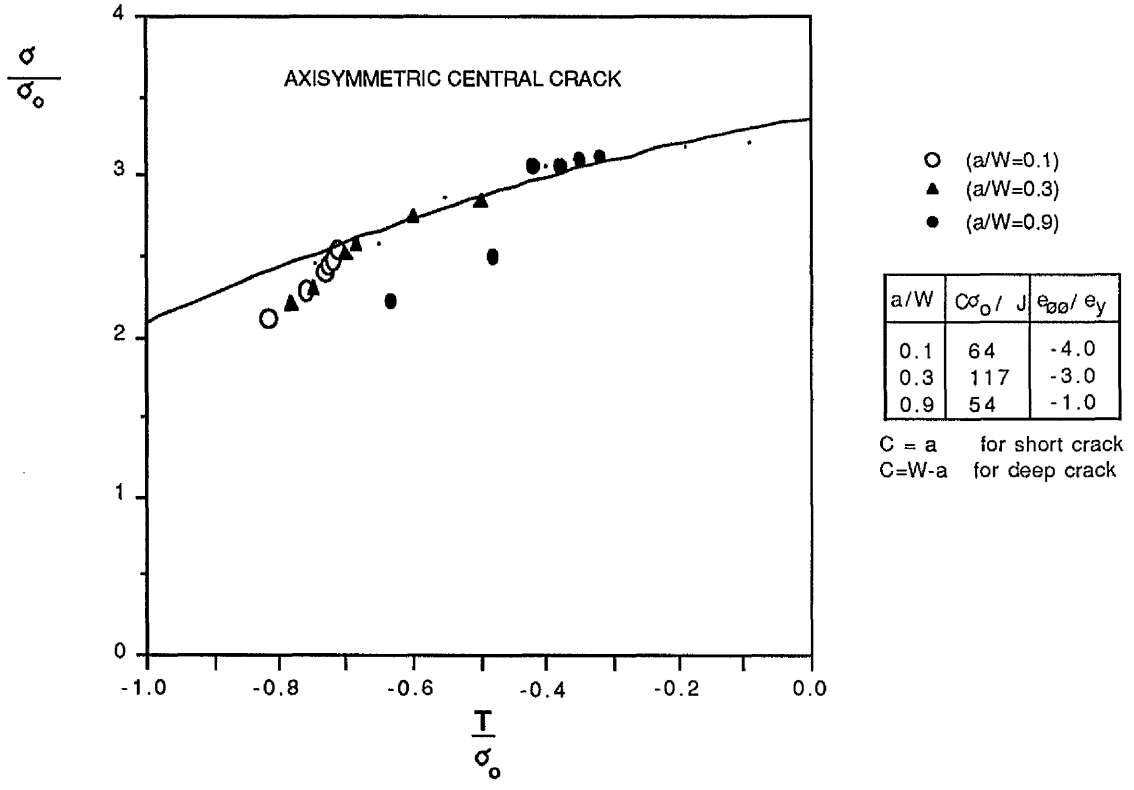

Fig (5.15) : The stress directly ahead of the crack at distance $2J/\sigma_o$ as a function of T/σ_o from the full field solutions compared with the plane strain boundary layer formulation.

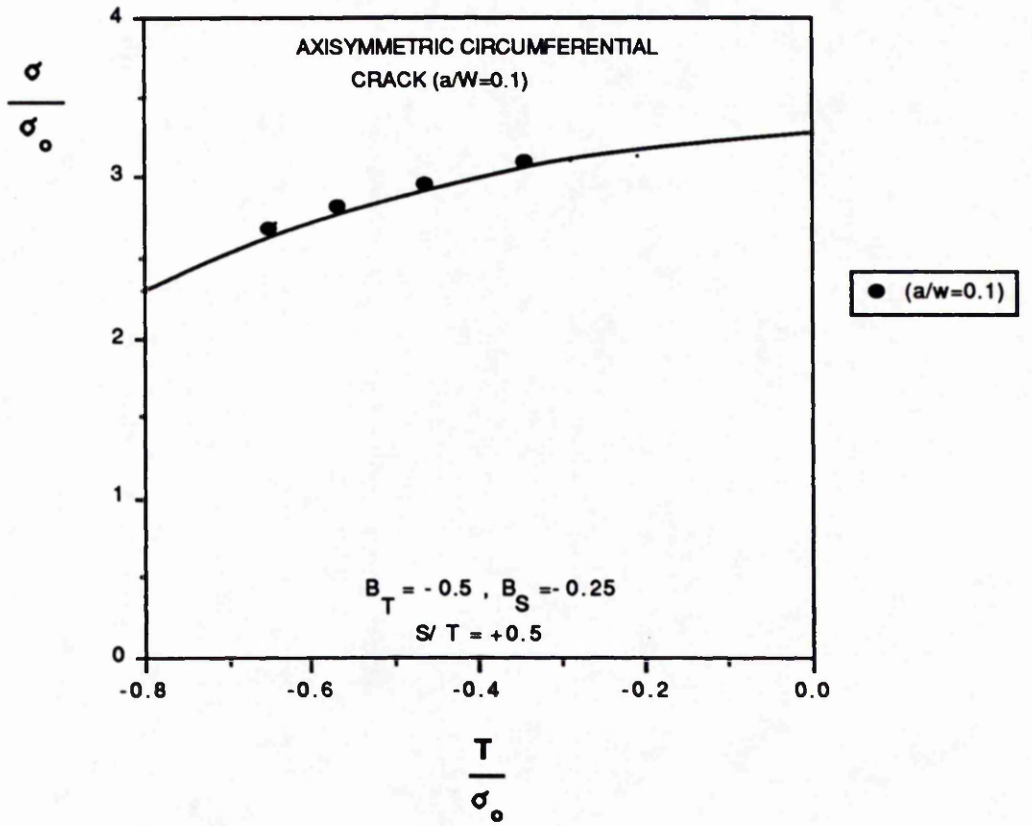

Fig (5.16) : The stress directly ahead of the crack at distance $2J/\sigma_o$ as a function of T/σ_o from the full field solution with S/T=0.5 compared with boundary layer formulation with S/T=0.5

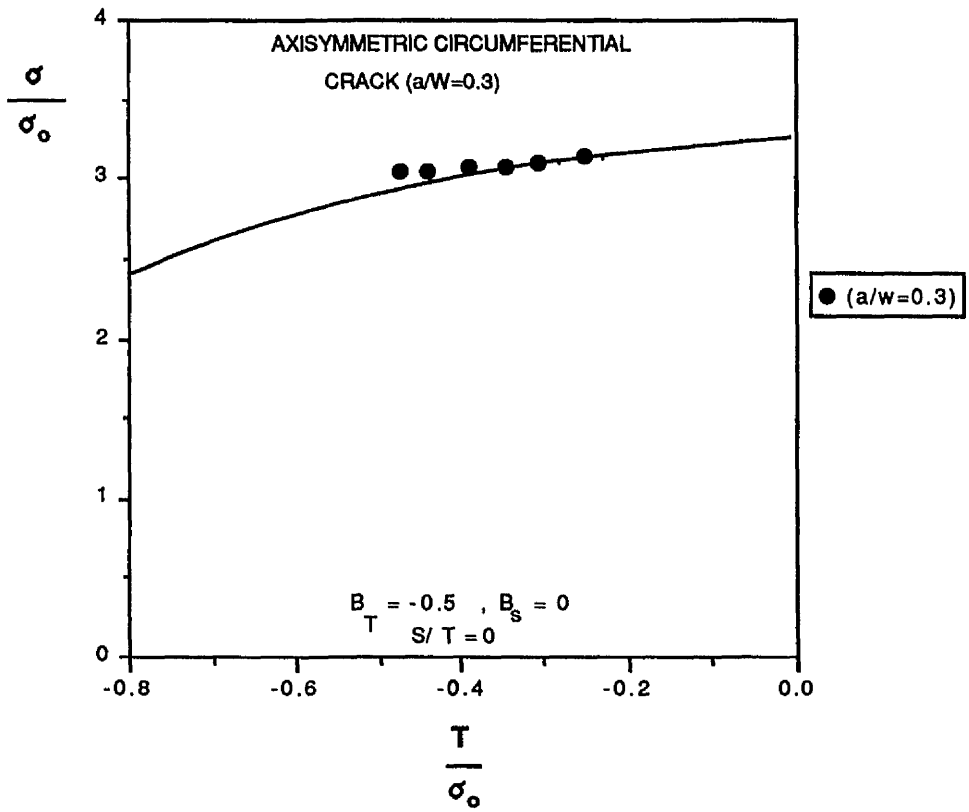

Fig (5.17) : The stress directly ahead of the crack at distance $2J/\sigma_o$ as a function of T/σ_o from the full field solution with S/T=0 compared with boundary layer formulation with S/T=0.

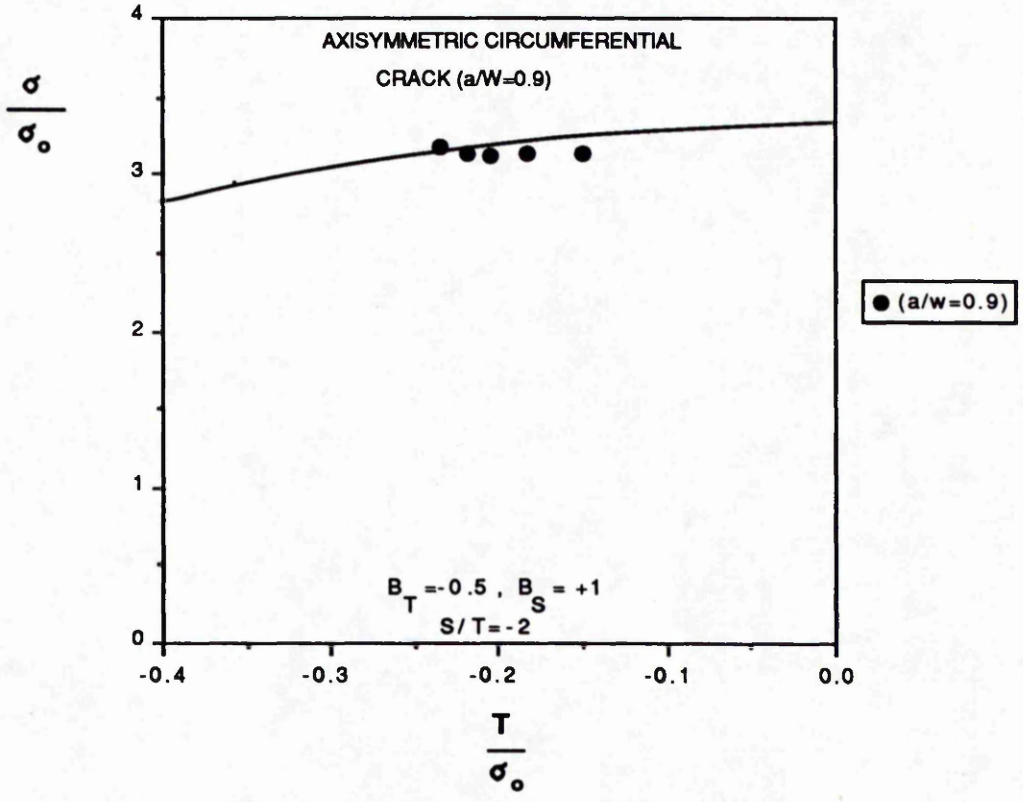

Fig (5.18) : The stress directly ahead of the crack at distance $2J/\sigma_o$ as a function of T/σ_o from the full field solution with S/T=-2 compared with the boundary layer formulation with S/T=-2

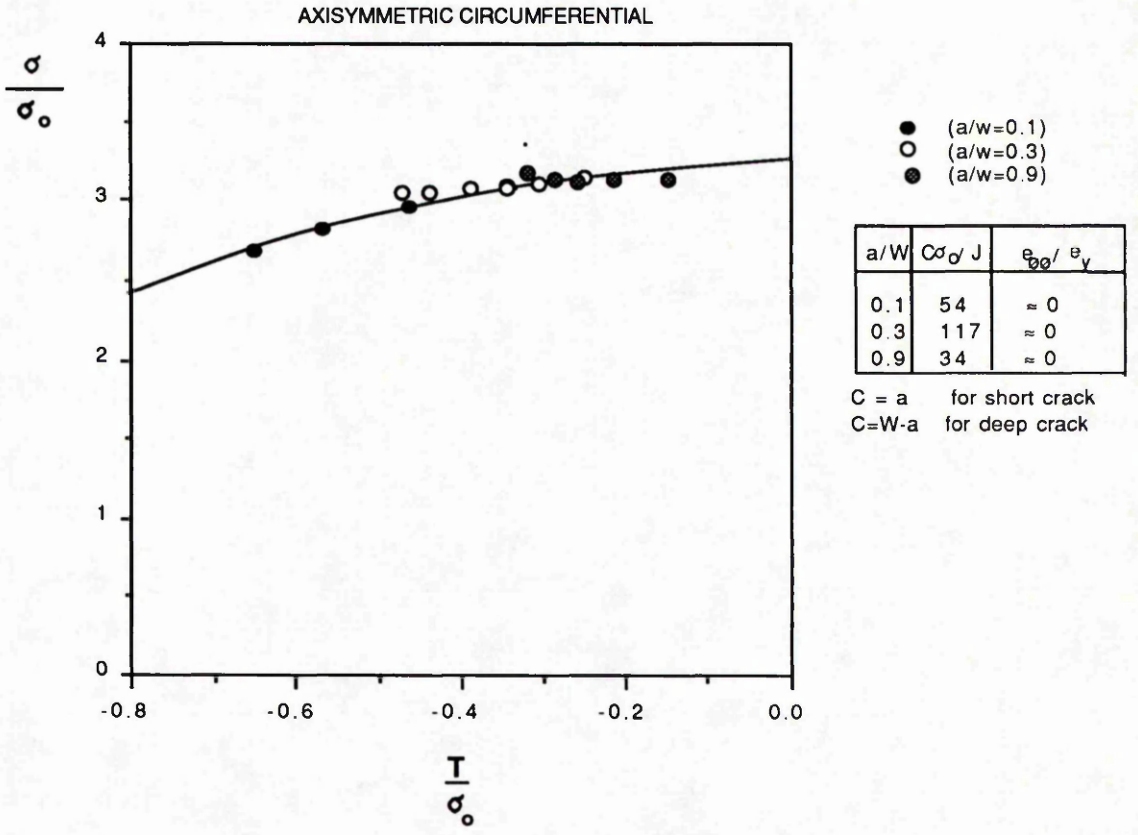

Fig (5.19) : The stress directly ahead of the crack at distance $2J/\sigma_o$ as a function of T/σ_o from the full field solutions compared with the plane strain boundary layer formulation.

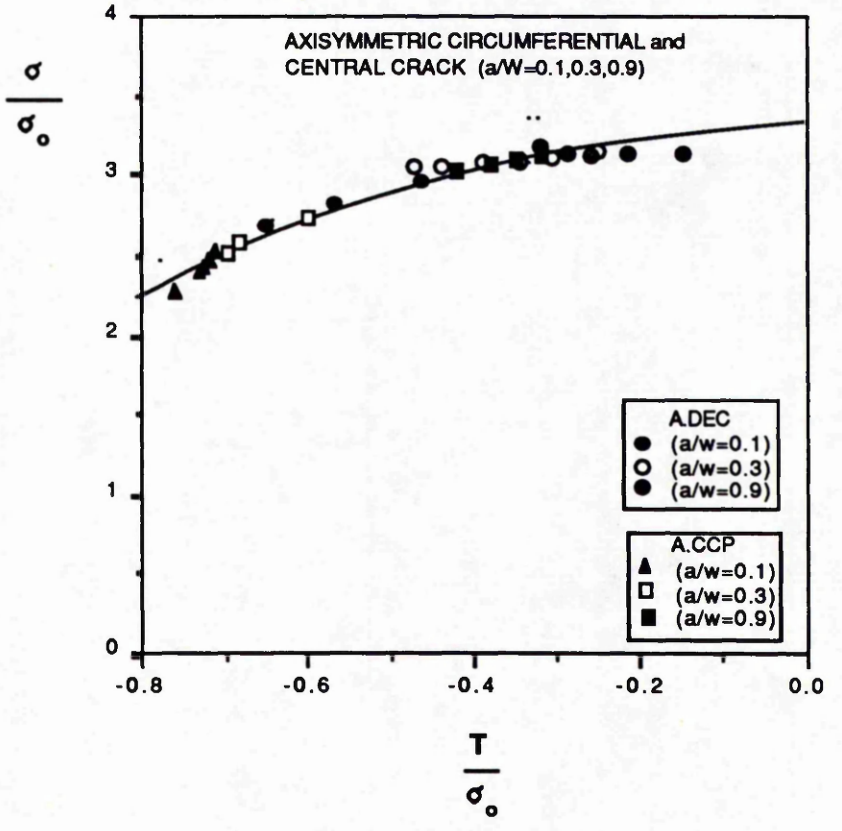

Fig (5.20) : The stress directly ahead of the crack at distance $2J/\sigma_o$ as a function of T/σ_o from the full field solutions compared with boundary layer formulation.

Chapter (6)

Elastic-Plastic Fracture Toughness Parameters (Experiments Test)

6.1. Introduction

Three point bend tests to measure elastic-plastic fracture toughness indicate that there is a significant effect of crack depth on fracture toughness parameters such as δ_c or J_c, Sumpter (1986), Aboutorabi (1985), Sorem et al (1989) and Betegón (1991).

Sumpter (1987) presented fracture toughness data for two HY80 weld metals in terms of J_C. The results show the application of J_C as a fracture analysis parameter in a form analogous to that developed for the critical crack tip opening displacement. The results illustrate that the crack depth has significant effect on the fracture toughness parameter. For example, for a manual weld, at room temperature, the maximum value of the fracture toughness J_C of a short crack (a/W=0.15) was approximately fifty times higher than the minimum value of the fracture toughness J_C of a deep crack (a/W=0.5).

Experimental work by Aboutorabi (1985) to investigate the effect of degree of constraint on the fracture toughness parameter over a wide temperature range confirmed this observation. The geometries selected in that work were a deep double edge cracked bar in tension (DECT) and single edge crack in tension (SECT). The slip line field for these two geometries is significantly different. The DEC geometry develops contained plasticity in the ligament with the full constraint of Prandtl slip line field. For the SECT configuration the slip line field consists essentially of two straight lines inclined at 45 degrees to the crack plane.

At room temperature the failure of these geometries was associated with a ductile tearing fracture mechanism due to void coalescence with the blunting crack tip. The fracture toughness value J_C for SECT was higher than for the DEC geometries at all temperatures. At the lowest temperatures (-196C$^{\circ}$) fracture initiation and propagation occured by cleavage leading to immediate failure.

Recently Sorem et al (1989) presented a laboratory test and numerical analysis for a bend bar with a/W =0.15. The tests were conducted on an A36 steel using a square cross section three point bend specimen in order to examine the effect of the crack depth on the critical fracture toughness (as represented by CTOD) through the lower shelf and lower transition regions. The experimental results were compared with previous deep crack results presented by Sorem et al (1988). Sorem et al (1989) produced a three dimensional finite element calculation for the test specimens. The results show that the influence of the crack depth on the fracture toughness parameter, depends on the extent of the plasticity. For example at the lower-shelf region the size of the plastic zone was extremely small with respect to the specimen dimensions and the radius of the plastic zone did not exceed 1/50 of the crack depth or the remaining uncracked ligament, allowing the fracture toughness to be characterised by a single parameter, independent of the specimen size, geometry configuration, or crack depth. In the transition region there was more extensive plasticity, more crack tip blunting, and a larger plastic zone developed in the short crack specimens than the deep one. The plastic zone for the short crack specimens extended to the free surface, while for deep crack specimens plasticity was confined to the uncracked ligament. This study again confirmed a relationship between the crack depth and

the elastic-plastic fracture toughness for laboratory test specimens.

At the lower shelf for both shallow and deep cracks, failure was controlled by cleavage with limited crack tip plasticity. At the upper transition region crack initiation and propagation was controlled by ductile tearing mechanisms and the fracture toughness of the short crack was higher than the fracture toughness of the deep one. The extent of plasticity for short and deep cracks was markedly different. For the short crack specimens, plasticity spread to the free surface while plasticity remains confined to the uncracked ligament for the deep crack. In this region at identical fracture toughness values (CTOD), the crack tip stress field is different between deep and shallow cracks. This demonstrated the inability of single parameter fracture mechanics to characterise the stress field.

This is consistent with the finite element calculations presented by Al-Ani (1988) and Al-Ani and Hancock (1991). In their finite element analysis of single edge cracked bar with a/W ratios between 0.03 to 0.5 in bending and 0.1 to 0.3 in tension, Al-Ani and Hancock (1991) pointed out that the characteristics of the HRR field are lost for short cracks as the plastic zone extends toward the cracked surface. The loss of J dominance is related to the increase in the near tip-strains and a reduction of the stress triaxiality, as the deformation disrupts small scale yielding fields similar to the HRR field. For the deeply cracked geometries the results show that there is a unique relationship between small and large scale yielding, while for short cracks the results show that there is a gradua loss of J dominance. J dominance was lost before $a\sigma_0/J=200$ for both tension and bending and the stresses for short cracks were less severe than those for deep ones.

The present work extends the work of Al-Ani (1988) by explaining

the geometry effect in terms of the T stress discussed by Bilby et al (1986) and more recently by Betegón and Hancock(1991)

In the present work, and in that discussed in chapter (3 and 4) there is a remarkable correlation between the T stress and the loss of J dominance. In geometries which have a negative T stress, plasticity spreads to the free surface and leads to a loss of J dominance, while in geometries with positive T stresses plasticity remains confined to the uncracked ligament allowing J dominance to be maintained up to the criteria given by McMeeking and Parks (1979) and Shih and German (1981).

More recently experimental data on bend and tension specimens presented by Sumpter and Hancock (1990) for HY80 weld, confirms the observation that there is a significant increase in the fracture toughness as the crack depth decreases as illustrated in Fig (6.1). The results confirm the finite element calculations of Al-Ani and Hancock (1991) that the loss of constraint in the short crack specimen starts before break back of the plastic zone for both tension and bending specimens. Both the experimental results of Sumpter and Hancock (1990) and the finite element calculations of Al-Ani (1988) and Al-Ani and Hancock (1991) show that deeply notched bend specimen produce a conservative estimate of structural failure conditions. Following this work an experimental combined Jc plus T stress approach is now introduced. This has the ability to remove this conservatism. For a more accurate prediction of the structural failure condition the following steps were suggested by Sumpter and Hancock (1990). Firstly, produce an elastic finite element analyses for the defect size of interest to obtain the biaxiality parameter β, hence the T stress as a function to the applied stress. Secondly a range of material tests must be performed to generate Jc as a function of the T stress. Finally by

matching the applied J in the structural to the Jc from the laboratory specimens at a given value of T, one can predict structural failure.

For three point specimens with a wide range of a/W ratios, varying from 0.044 to 0.48, Betegón (1990) produced a combined CTOD-T stress locus and Jc-T locus at room temperature Figs (6.2 and 6.3). The results indicated that geometries with negative T stress lose constraint and have higher fracture toughnesses than those with less negative or positive T-stress. The results also show that there is a remarkable increase in the fracture toughness associated with the change of the T-stress from positive to negative. It is also important to note that geometries with positive T stress maintain the same value of fracture toughness independent of T.

In the work presented in this section, an experimental investigation was carried out on a carbon-manganese structural grade 50D steel to investigate the effect of the crack depth on the fracture toughness and to produce a Jc-T stress locus for this material for a range of temperatures between room temperature (+23C) and liquid nitrogen temperature (-196C).

6.2. Materials

Three point bend specimens with a range of a/W ratios between 0.1 and 0.5 were machined from a 25mm thick plate, of a carbon manganese structural steel specified as BS4360 grade 50D, normalised at 910C. Table (6.1) gives the chemical analysis and mechanical properties of the steel. The yield stress as a function of the temperature for a similar steel is shown in Fig (6.4) after Bennet and Sinclair (1966).

6.3. Test Procedure

6.3.1. Fatigue Pre-cracking

Fatigue pre-cracking of all the specimens was performed in a high frequency fatigue testing machine under constant amplitude three point bending at a frequency of approximately 20Hz. The fatigue crack was initiated at the root of a 5mm deep V notch, machined on the surface of the specimen and the crack was grown half way through the specimen. To produce a short crack specimen, the deep crack specimens were re-machined to the required size. For example the specimen dimensions for a short crack with (a/W=0.1) are the ligament (W-a=25mm), thickness (B=25mm) and crack length=2.77mm. In all the specimen the ligament and thickness were maintained at 25mm and the crack length was varied. Care was taken to produce an aligned fatigue crack. Prior to the final test, each specimen was examined to satisfy the straightness of the crack .

6.3.2. Fracture Toughness Tests

Experimental tests were carried out on a 250 KN Instron TT-K servo-hydraulic testing machine at constant displacement rate, under displacement control. The crack mouth opening displacement (CMOD) was measured by using a clip-gauge placed between two 3mm thick knife edges attached the specimen Fig (6.5). Both the load and the crack mouth opening displacement were recorded. The low temperature tests (-196C) were carried while the specimen was immersed in liquid Nitrogen using a special tank designed to contain the three point bend specimens. Liquid Nitrogen was pumped into the

tank through a pipe from a centrifugal pump attached to a liquid Nitrogen container Fig (6.6). At temperatures of (-50C, -80C-100C and -120C), the liquid Nitrogen was pumped continuously through a small brass tanks fitted onto both side of the specimen until the required temperature was achieved Fig (6.7). At room temperature multiple specimens were tested in order to obtained an accurate initiation fracture toughness value Ji

In all the tests the specimens's temperature was measured using a Copper-Constantan thermocouple attached to the specimen using silicon sealant. Care was taken to ensure that the inside of the specimen achieved the required temperature as shown in Fig (6.8)

6.4. Interpretation of the Data

The experimental value of the fracture toughness value is presented in terms of the initiation value of J denoted Ji. In all the tests, the value of the fracture toughness J was calculated using a procedure due to Sumpter and Turner (1980). In this method J is split into elastic and plastic component Je and Jp.

$$J = Je + Jp \tag{3}$$

The elastic component of J was calculated from the stress intensity factor K using the formula.

$$J_e = \frac{K_c(1-\upsilon^2)}{E} \tag{4}$$

E is Young modulus and υ is Poisson's ratio. The critical value of the stress intensity factor K_c was calculated using

$$K_c = \frac{P_i \lambda}{B\sqrt{W}} \qquad (6)$$

where P_i is the load at initiation, B is the specimen thickness, W is the specimen width, and λ is the stress intensity factor coefficient. For a three-point bend specimen which has a span (S) =4W, λ is given by Sorem (1989) as :

$$\lambda = \frac{6\left(\frac{a}{W}\right)^{1/2}\left(1.99 - \frac{a}{W}\left(1 - \frac{a}{W}\right)\right)\left(2.15 - 3.93\left(\frac{a}{W}\right) + 2.7\left(\frac{a}{W}\right)^2\right)}{\left(1+ 2\frac{a}{W}\right)\left(1- \frac{a}{W}\right)^{3/2}} \qquad (7)$$

The plastic component of J was calculated using the relation.

$$J_p = \frac{\eta_p P_i V_p}{B\,(W-a)} \frac{W}{a_t + r(W-a)} \qquad (8)$$

η_p is a function of the crack depth varying between 1.13 at a/W=0.1 to 0.2 at a/W≥0.28, P_i is the load at initiation, V_p is the crack mouth opening displacement measured from the load-CMOD trace, r is a rotational constant varying linearly between 0.35 at a/W=0.1 to 0.45 at a/W≥0.3 and a_t is the the crack depth plus the depth of the knife edge.

6.5. Calculation of the T -Stress

In the present experimental work the T-stress was calculated from the elastic component of the J-integral even when extensive plasticity was involved. As discussed in the previous chapter, the elastic T-stress has been defined through the biaxiality parameter β using the following form.

$$T = \frac{K\beta}{\sqrt{\pi\ a}} \qquad (9)$$

The biaxiality parameter β is calculated using elastic finite element methods in the present work and by Sham (1989). The stress intensity factor K was calculated using the experimental applied force in equation (6) together with the specimen dimensions.

6.6. Results and Discussion :

The experimental data are shown in Figs (6.9 and 6.10), in which the fracture toughness for both deep and the shallow crack are plotted as a function of the temperature. For both the deep and the shallow crack, the fracture toughness is characterised in terms of the CTOD or Jc.

At room temperature ($23C^{o}$) the results indicated that the initiation of ductile tearing for the short crack occured at a Jc value approximately 1.5 times larger than the initiation value for the deep one and the value of the CTOD was approximately twice that of the deep crack. Figs (6.11 and 6.12) show the fracture toughness CTOD and Jc plotted as a function of the ratio a/W.

At room temperature ductile fracture initiated by tearing of associated with micro-void coalescence ahead of the blunting tip. At -50C and -80C fracture initiated by ductile tearing for both the deep and shallow cracks and the fracture toughness of the short crack was greater than that of the deep crack. The results are consistent with experimental investigations of Sumpter (1986), Aboutorabi (1985), Matsoukas et al (1986), Ebrahini (1988) , and Sorem et al (1989). At -100C^{o} fracture initiation and propagation for the deep crack occured by a ductile initiation leading to a final cleavege failure. This behaviour could be explained in terms of the critical combination of the strain and stress state required to initiate failure as discussed by Mackenzie, Hancock and Brown (1977). If the level of the local tensile stress exceeds the critical cleavage stress value over a microstructurally significant distance, fracture occurs by cleavage as discussed by Ritchie, Knott and Rice (1977), if not fracture initiation and crack propagation will occur by a ductile tearing mechanism. At -100C^{o}, the short crack exhibited ductile fracture initiation and reached the ductile criterion before the critical cleavage stress was achieved. The fracture toughness value was significantly higher than that for the deep crack which failed by cleavage

At -120C^{o} although failure of both the deep and shallow cracks fracture occured by cleavage, the fracture toughness of the short crack was still higher than the fracture toughness of the deep one. At temperatures below -120C^{o} (the lower -shelf region) for both deep and shallow crack fracture occured by cleavage leading to catastrophic failure when the plastic zone size requirement of A.S.T.M-399 were satisfied in the relation to the ligament Although the failures occured by cleavage and the plastic zone size requirements for valid LEFM

were satisfied, the fracture toughness of the short crack was slightly higher than the deep one.

The geometry dependence of fracture toughness is expressed in the form of a J_i-T locus in Fig (6.13) and as a CTOD-T locus in Fig (6.14). The figures show the toughness as a function of temperature. As the toughness and associated plasticity decrease with temperature it was intended to determine the conditions for single and two parameters characterisation. In Fig (6.13) the ligament size requirement for J dominance in bending is plotted, using a temperature dependence yield stress σ_o. Single parameter characterisation loses its validity at temperature above -80C as the ligament is not large enough. Below this temperature there is still a geometry dependent toughness which can only arise from the crack length requirement not being met. At -120C° the toughness of short crack is still greater than that of deep crack. At this temperature ($a\sigma_o/J$) for deep crack is approximately 200 whereas it is only 22 for the short crack. The finite element calculations presented in this work suggest ($a\sigma_o/J \leq 200$) for single parameter characterisation and J dominance. Thus at -120C° the deep crack is expected to produce a valid J dominant result whereas the shallow crack does not. This explaines the geometry dependence at -120C°

Geometry independence is only recovered within the limits of experimental error at -196C. At this temperature ($a\sigma_o/J$) for the deep crack is 1300 and for the shallow crack ($a\sigma_o/J$) is 230. This basically confirms the finite element prediction that J dominance required ($a\sigma_o/J \geq 200$). Single parameter characterisation thus only achieved at -196C° whereas two parameter characterisation extends the application of fracture mechanics to at least -80C and possibly higher.

6.7. Conclusions

The experiments presented in this section show how the geometry dependence of fracture toughness can be rationalised by two parameter characterisation. The experiments confirm the finite element results that a negative T stress is associated with enhanced fracture toughness due to a loss of crack tip constraint. The Ji-T approach has two major advantages over other predictive models. Firstly the Jc-T approach has the potential to remove the conservatism of fracture toughness which arises when the traditional deep bend crack geometries which produce lower bound fracture toughness value. The structural failure condition can be estimated by matching the applied J in the structure to the Jc from laboratory specimen tests at a given value of T, which in turn can be calculated by elastic finite element methods.

The experiments finally show that single parameter characterisation is subject to severe geometric requirements on the crack length. The data supports the finite element prediction that single parameter characterisation by J as only attained at crack lengths greater than $(200J/\sigma_o)$

6.8. References:

Aboutorabi, A.A., (1985), Ph.D Thesis, Mech. Eng. Dept., University of Glasgow.

Al-Ani, A.M., (1988), M.Sc. Thesis, Mech. Eng. Dept., University of Glasgow.

Al-Ani A. M. and Hancock, J. W.,(1991) J. Mech Phys Slds, 39, 23.

Bennet, P. E. and Sinclair, G. M., (1966), J. Basic. Eng, Trans, ASME Series D, 88,518-.

Betegón, C., and Hancock J., W.,(1991) J. Appl. Mech. in press

Betegón, C.,(1990) Ph.D Thesis (Caracterizacion Biparametrica De Los Campos Tensionales En La Mecanica De La Fractura Elastoplastica Department of Engineering Construction, University of Oviedo.

Bilby, B. A. ,Cardew, G. E., Goldthorpe, M. R. and Howard,I. C. (1986) "Size Effects in Fracture. I. Mech. Eng. London. 37.

Ebrahimi, F. (1988), ASTM STP 945, American Society for testing and Material, 555.

Mackenzie, A. C., Hancock, J. W., and Brown, D. K., (1977)., Eng. Frtacture. Mech., 9,167.

Matsoukas, G.,Cotterel, B. and Mai, Y. M., (1986), J. Mech. Phys. Slds.,34,499-510

McMeeking ,R. M. and Parks, D. M.,(1979), ASTM. STP 668, 175.

Ritchie, R. O., Knott, J. F., and Rice, J. R., (1973), J. Mech. Phys. Slds.,21,395

Sham, T.-L. (1989), The Determination of the Elastic T-Term using Higher Order Weight Functions. Mech Eng. Dept. Troy, New York 12180. ,U.S.A

Shih, C. F., and German, M. G. (1981), Int. J. of Fracture.,17, 27

Sorem, W. A.,Dodds. R. H. and Roife, S. T., (1988) " An Analytical Comparison of Short and Deep crack CTOD Fracture

Specimen of A36 steel" to Appear in ASTM STP for the 21st National Symposium of Fracture Mechanics.

Sorem, W. A.,Dodds. R. H. and Roife, S. T., (1989)., Effect of Crack Depth on Elastic-Plastic Fracture Toughness in bending Bar Specimen., A Report on a Reserch Project

Sumpter, J. D. G., (1986), Design Against Fracture in Welds Structures, ARE,Dumfermline, Scotland, 20 May, 16

Sumpter, J. D. G., (1987), Fatigue and Fracture of Engineering Material and Structures., 10,479.

Sumpter, J. D. G., and Hancock, J. W., (1990)," Shallow Crack Toughness of HY80 welds. An Analysis Based on T-Stress. to be Published

Sumpter, J. D. G., and Turner, J. W., (1976), Int. J. of Fracture., 12, 861.

Chemical Composition (Wt%)

C	Si	Mn	P	S	Cr	Mo	Cu	Nb
0.17	0.29	1.30	0.010	0.008	0.09	0.01	0.11	0.045

Mechanical Properties

Yield Stress MPa	Ultimate Stress MPa	Elongation %	Reduction of Area %AV
360	558	26	56

Table (6.1)

Chemical composition and mechanical properties of BS4360 grade 50D steel

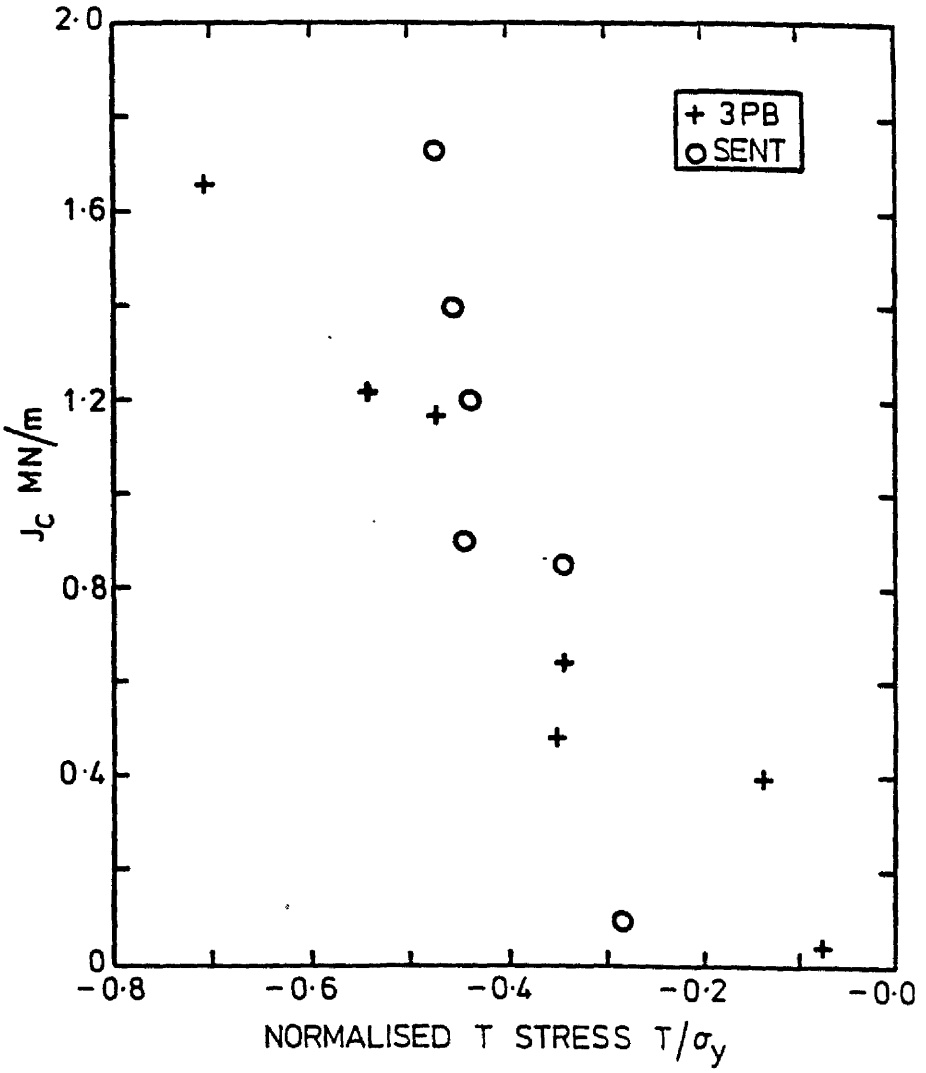

Fig (6.1) : Jc as a function of normalised T-stress

After Sumpter and Hancock (1990)

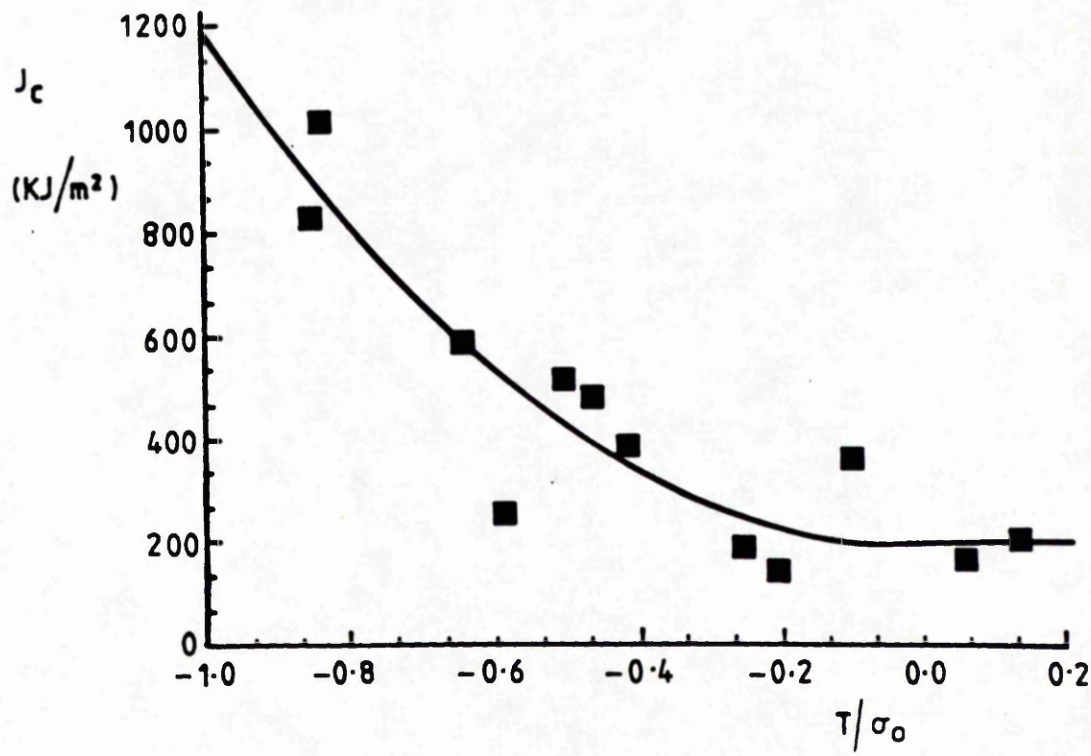

Fig (6.2) : Jc as a function of normalised T-stress

After Betegon (1990)

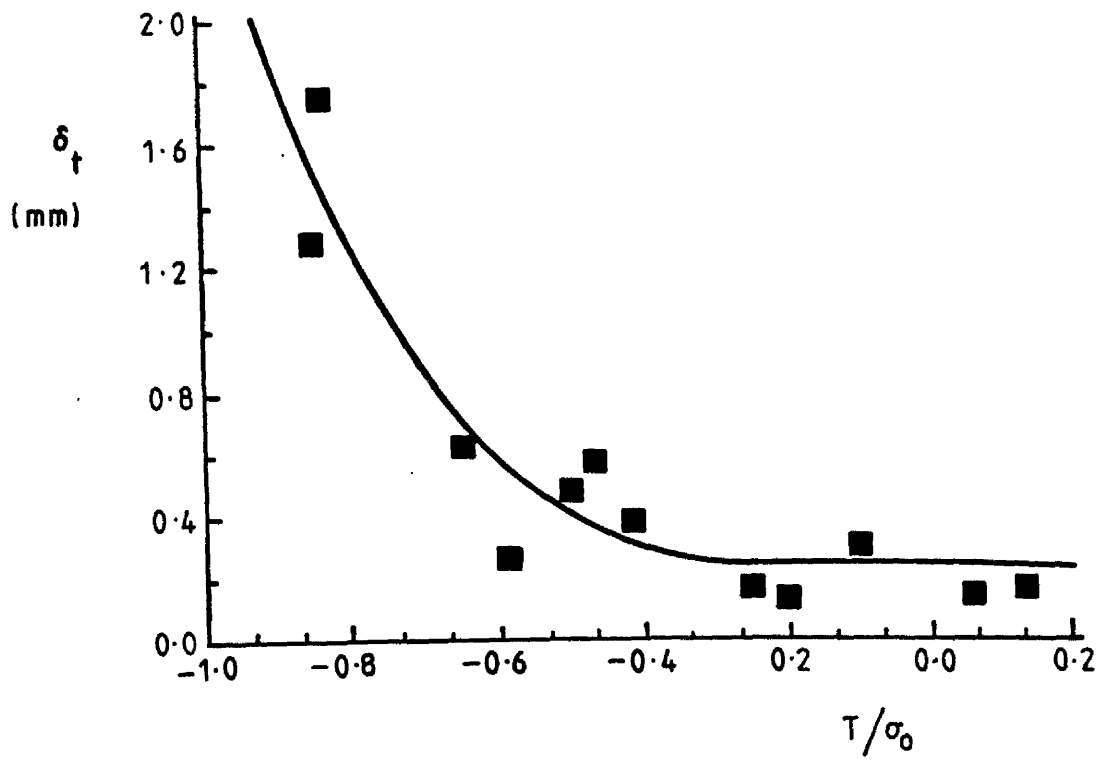

Fig (6.3) : CTOD as a function of normalised T-stress

After Betegon (1990)

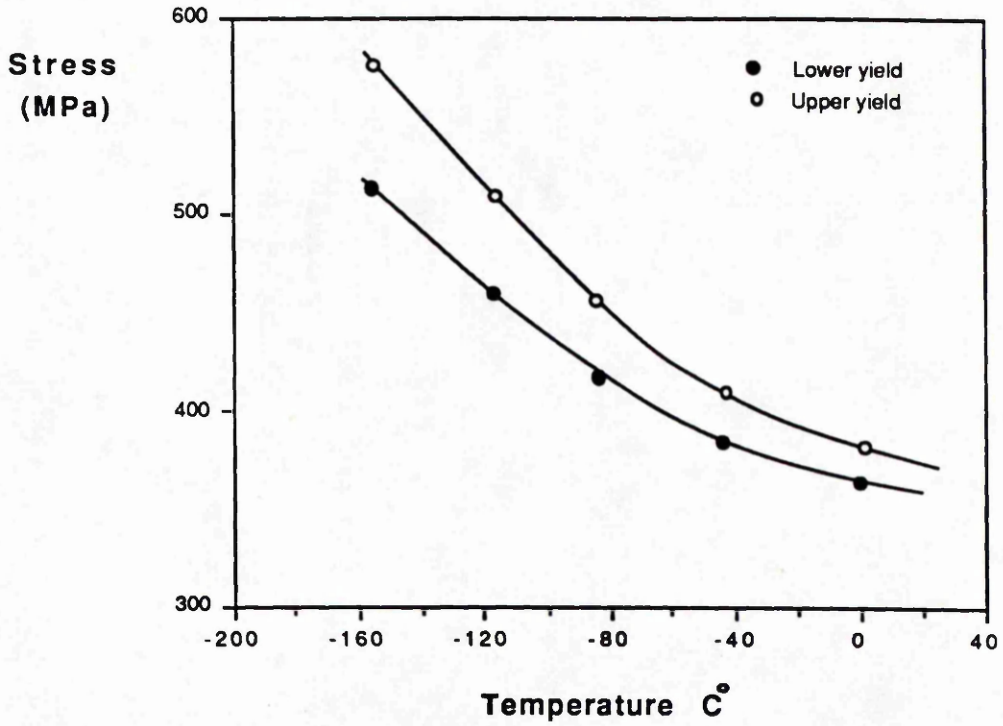

Fig (6.4) : Variation of upper and lower yield stress with temperature

After Bennett, P.E. and Sinclair (1966)

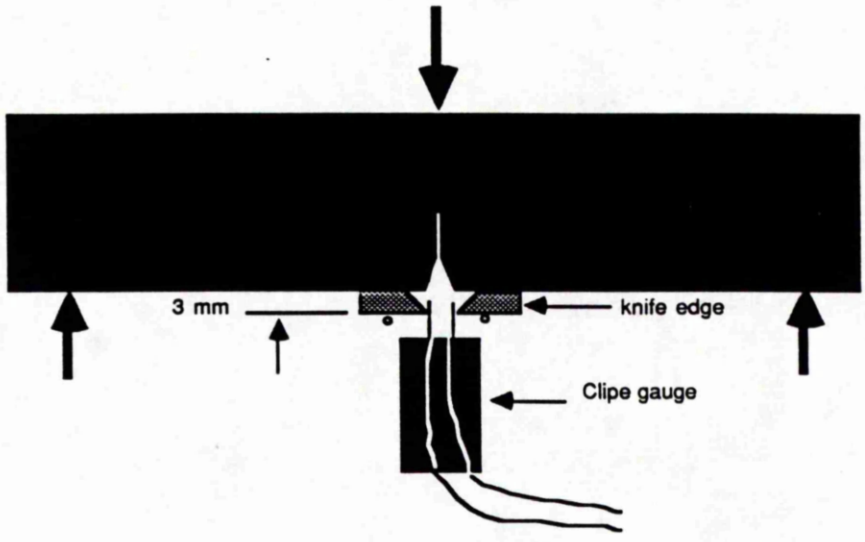

Fig (6.5) : Three point bend specimen with clipe gauge placed betweem two knife edge

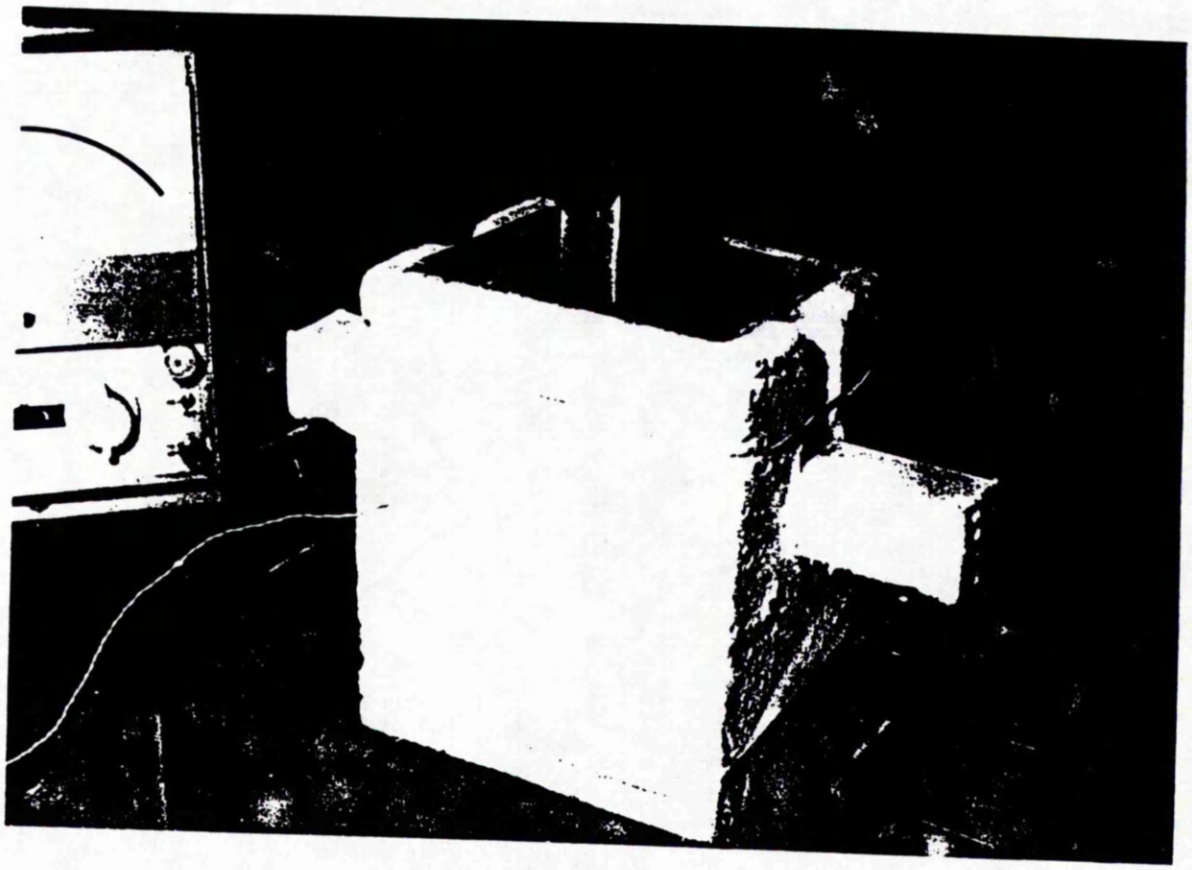

Fig (6.6) : The exprimental setup for the -196°C test

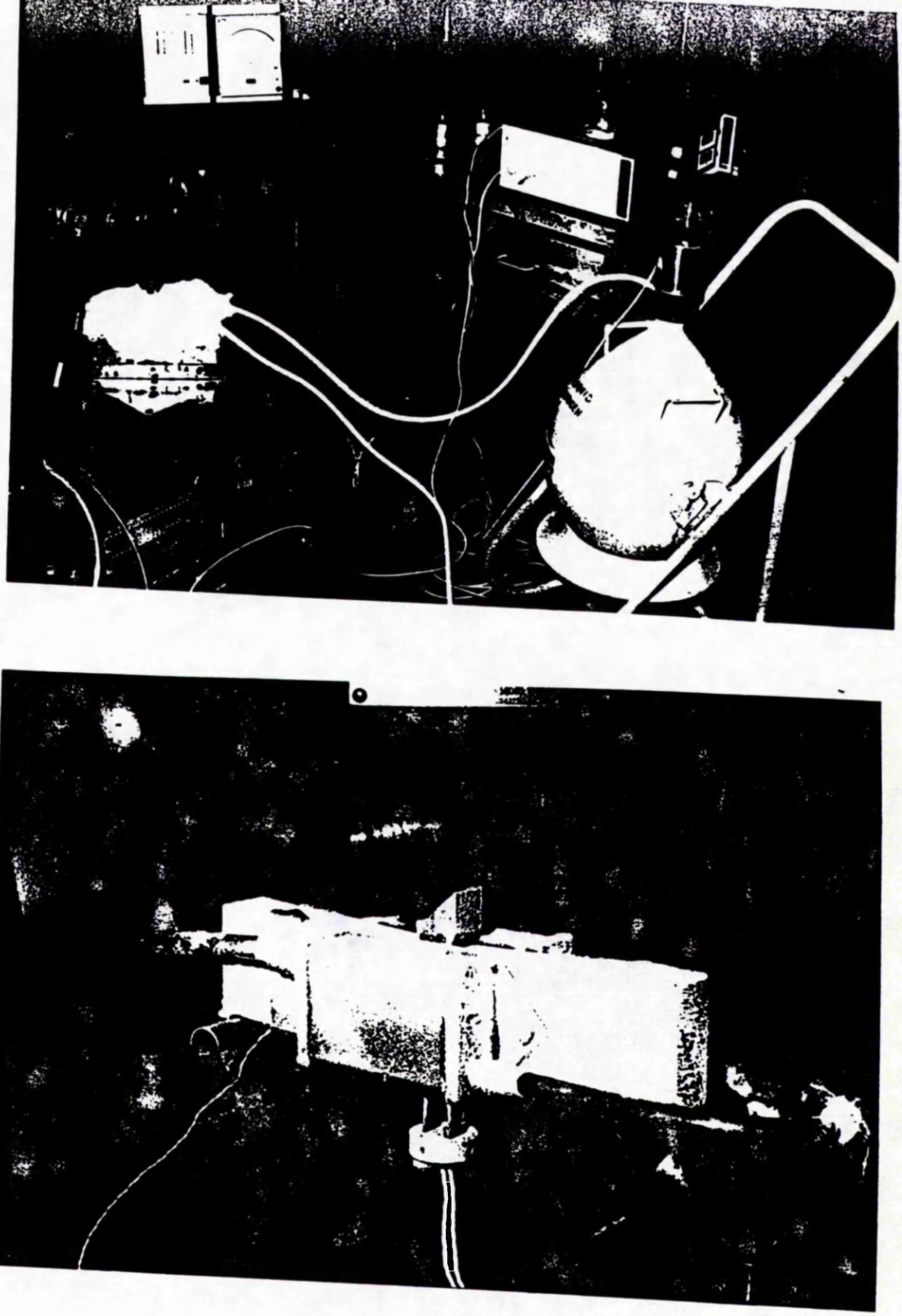

Fig (6.7) : The exprimental setup for the -120$\overset{\circ}{C}$ test

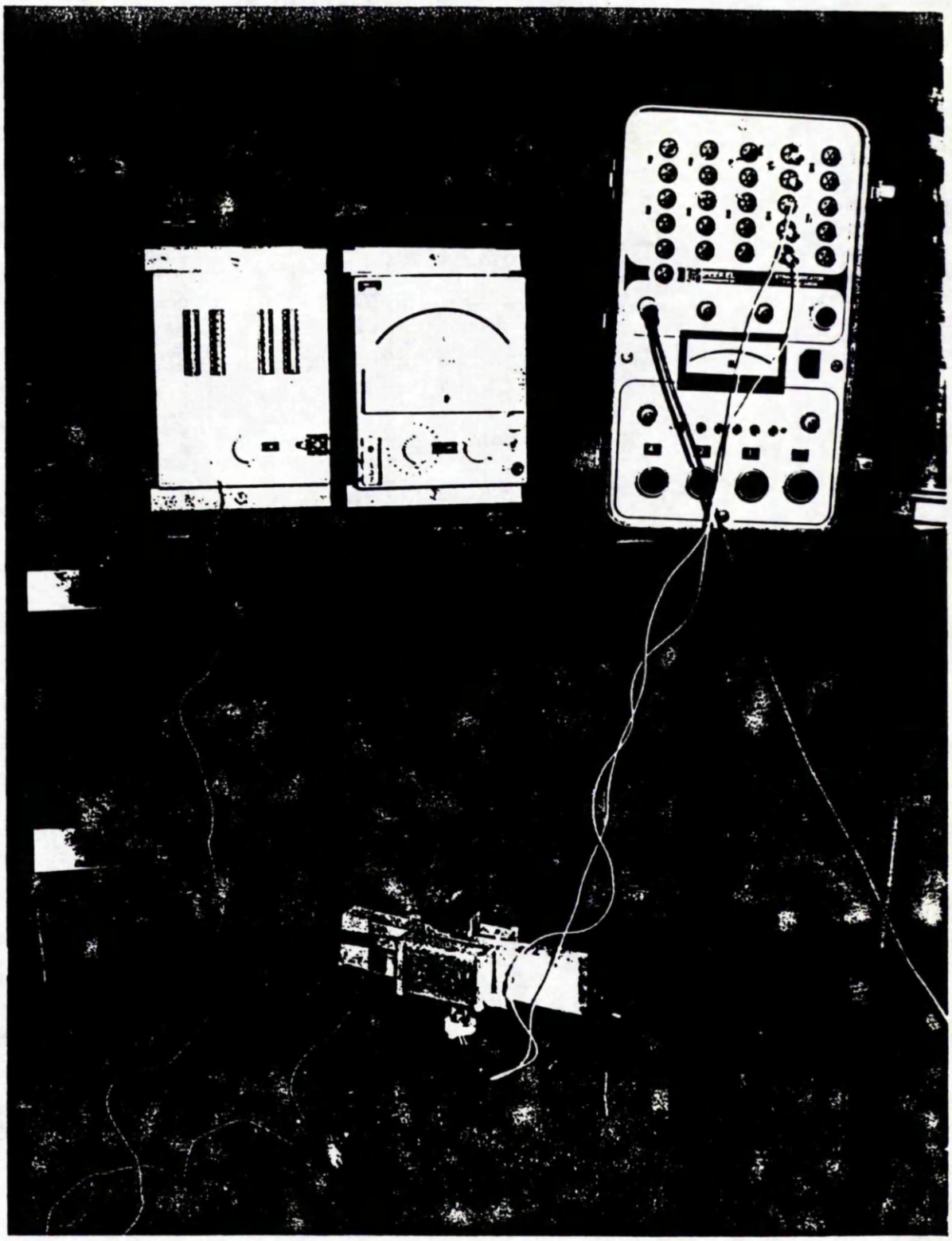

Fig (6.8) : The Connection of the thermocouple to the specimen

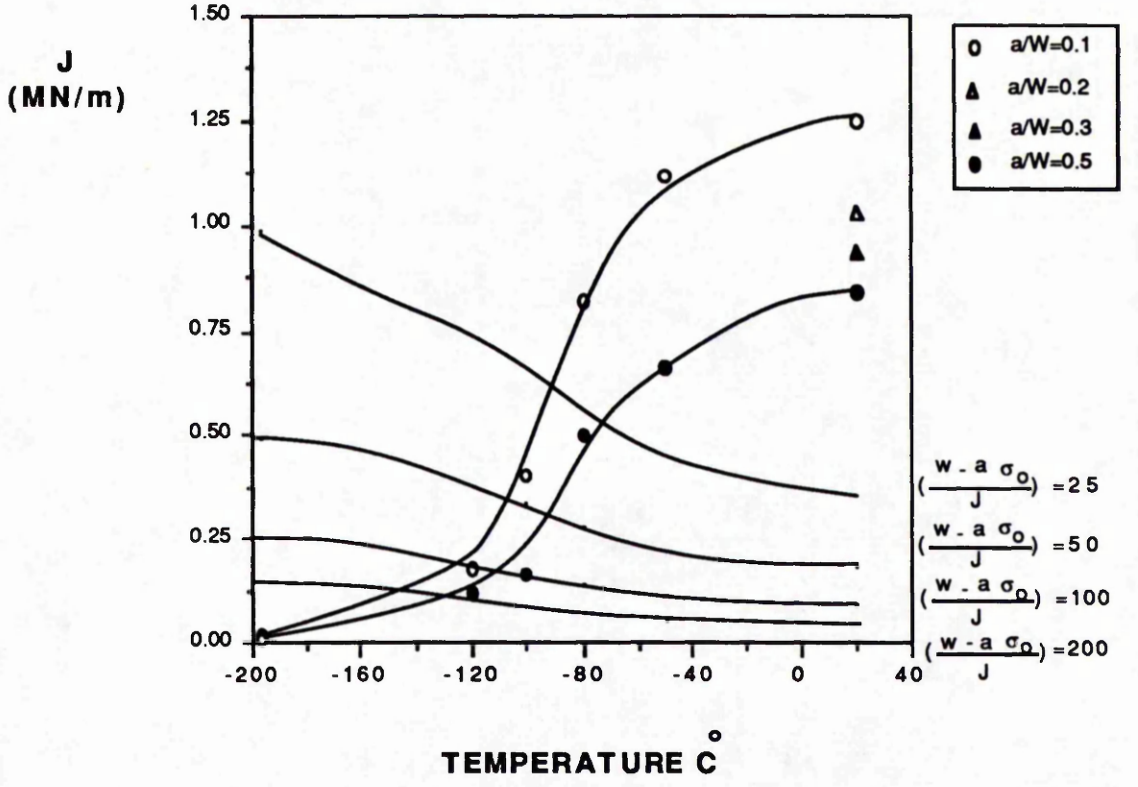

Fig (6.9) : Variation of initiation J as a function of the temperature

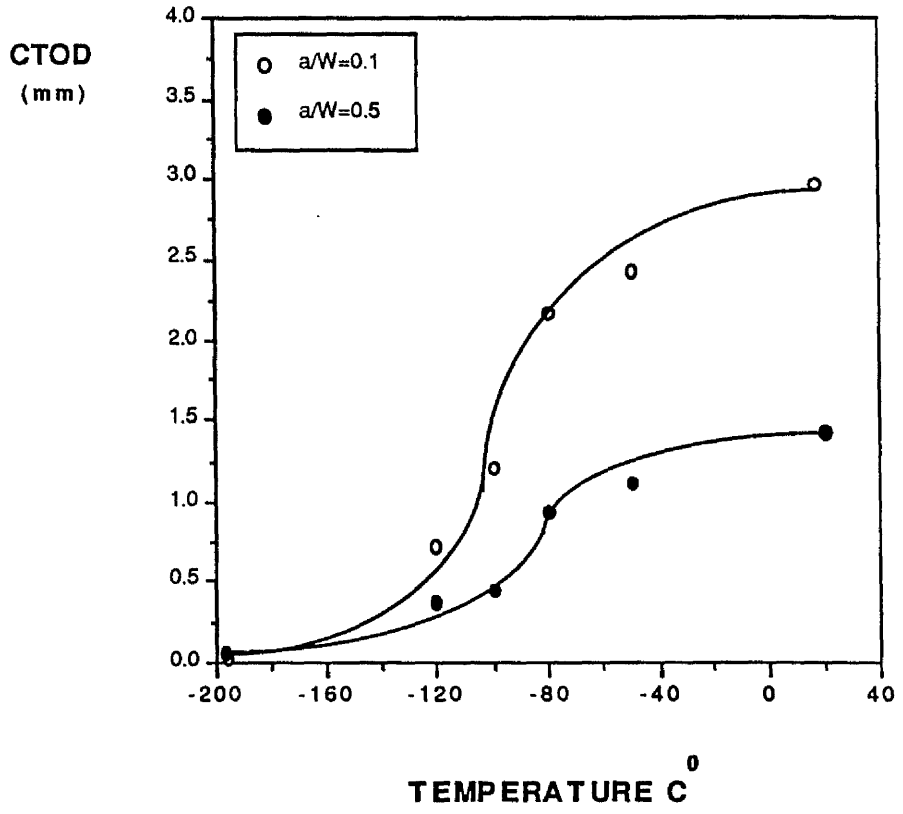

Fig (6.10) : Variation of the crack tip opening displacement (CTOD) as a function of the temperature

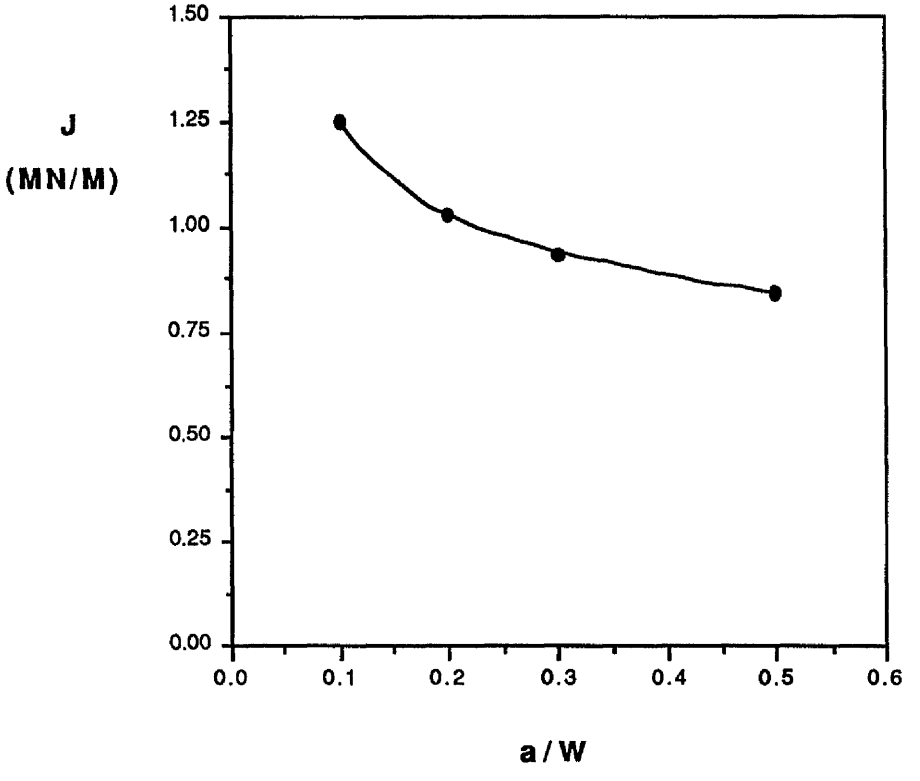

Fig (6.11) : The initiation value of J as a function of a/W ratio at room temperature.

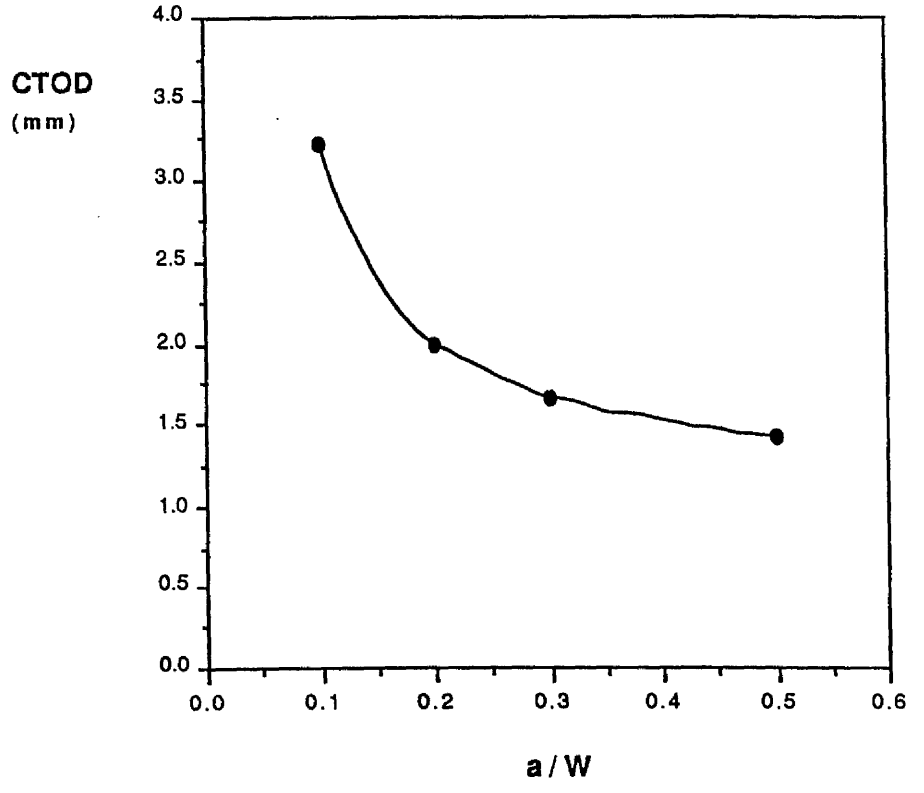

Fig (6.12) : The crack tip opening displacement (CTOD) as a function of a/W ratio at room temperature

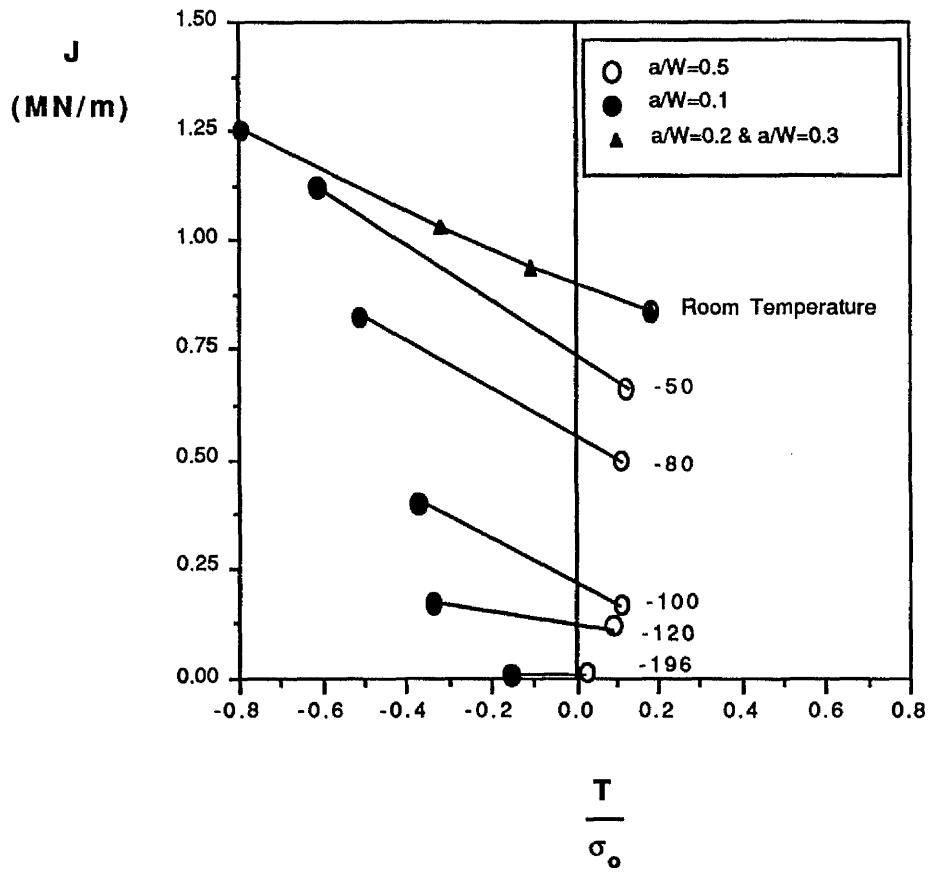

Fig (6.13) : The initiation value of J as a function the T-stress

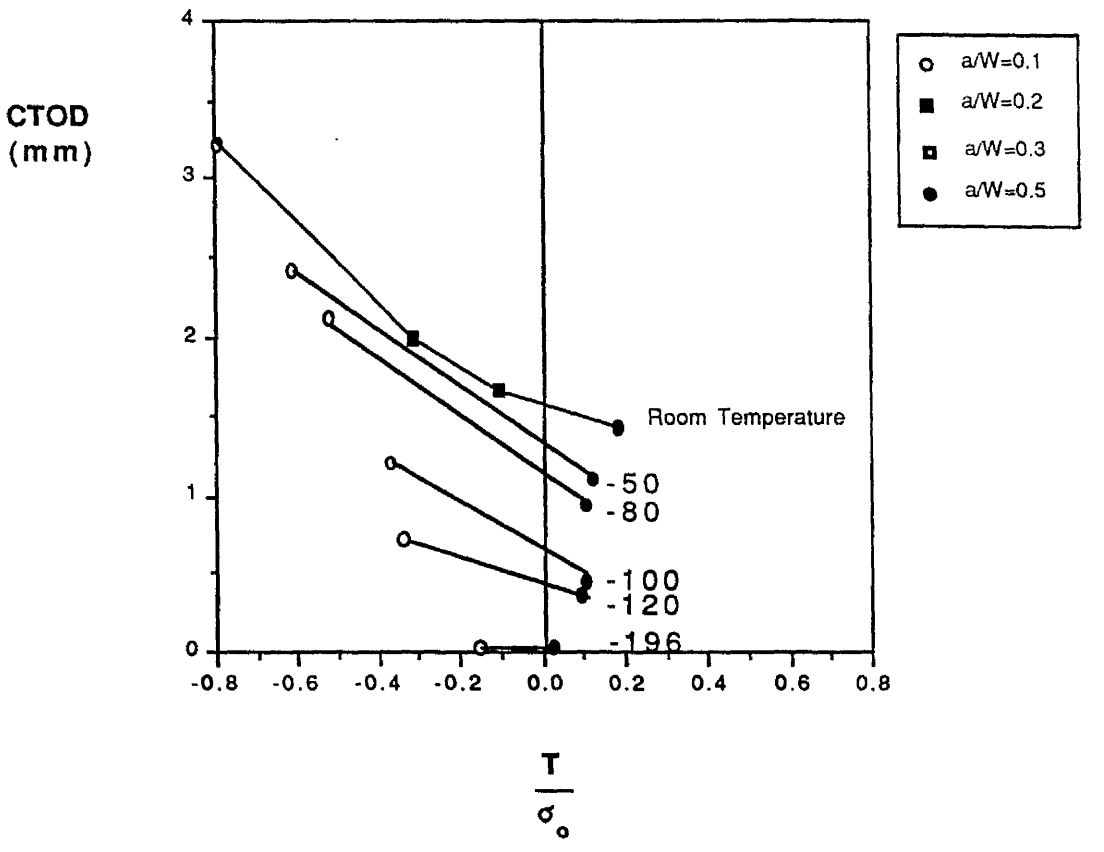

Fig (6.14) : The crack opening displacement (CTOD) as a function of T-stress

Chapter (7)

Elastic Analysis of T and S Stresses in Circumferentially Cracked Pipes

7.1. Introduction.

Circumferential cracks in pressure vessels and pipe-work are common types of defects. A realistic assessment of these defects is therefore important for structural integrity. Finite element studies by a number of investigators have demonstrated that at some stage of deformation, fracture toughness parameters such as K and J or δ become inadequate in characterising the failure of such structures. Results of the finite element studies by Larsson and Carlsson (1973), Betegón and Hancock (1991), Al-Ani and Hancock (1991) and Du and Hancock (1990) have shown that the inclusion of the non-singular term (T-stress) as a second parameter to be used with K or J extends the characterisation of the stress field. The present section is concerned with the estimation of the non-singular terms (T-stress and S stress) for circumferential cracks in pipes. Two models were considered, a continuum model and shell analysis combined with a line spring representation of the crack. The shell- line spring analysis was first introduced in (1972) by Rice and Levy who estimated the stress intensity factors in plates containing part-through surface cracks subjected to tension and bending. They pointed out that the line spring analysis is an efficient and accurate computational method. The method allows three dimensional crack problems to be effectively reduced to a 2-dimensions which are more economical in computing time. Recent studies by Parks (1981), Huang and Hancock (1987) and

Du and Hancock(1990) have confirmed this by comparing results of shell line-spring model with results of alternative numerical methods.

7.2. The Line Spring-Model

The line spring analysis was first introduced by Rice and Levy (1972) to estimate the stress intensity factors for a plates and shells containing part-through surface cracks subject to tension and bending. As an introduction, it is appropriate to review the basic concept of the line-spring model. Fig (7.1a) shows the cross section of a part-through surface crack of total length $2c$ and of varying depth a(x) in a plate or shell of thickness t. As illustrated in Fig (7.1b), the plate or shell is idealised as a two-dimensional continuum subjected to a membrane force N^{∞} and bending moment per unit length M^{∞}, while the part-through surface crack is idealised as a one dimensional discontinuity of length $2c$. The force and the bending moment transmitted by each section (x) of uncracked ligament [t-a(x)] are denoted N(x) and M(x) per unit length. Similarly the discontinuity in normal displacement of the plate's mid-surface and relative rotation are denoted by $\delta(x)$ and $\theta(x)$, respectively. In the linear elastic case the response of the crack to the local loads N(x) and M(x) can be expressed in the form.

$$\begin{bmatrix} \delta(x) \\ \theta(x) \end{bmatrix} = \begin{bmatrix} C_{11}(x) & C_{12}(x) \\ C_{21}(x) & C_{22}(x) \end{bmatrix} \begin{bmatrix} N(x) \\ M(x) \end{bmatrix} \qquad (1)$$

Here the matrix [C] is a local elastic compliance which can be regarded as the response of a generalised spring. Rice and Levy

(1972) matched this compliance with that of a long plane strain single edge cracked bar of crack depth a and width (t) as shown in Fig (7.1c).

7.3. T stress Analysis

7.3.1. Continuum model

For the continuum model, methods of calculating the T stress under plane strain conditions are reviewed in detail in chapter (2). In the present section stress σ_{xx} behind the crack was used to calculated the T stress and the out of plane stress σ_{zz} was used to calculated the S stress. The magnitude of T was identified through the biaxiality parameter β_T introduced by Leevers and Radon (1983)

The out of plane non-singular term,S stress, which is expressed in terms of a biaxiality parameter denoted as β_S.

$$\beta_S = \frac{S\sqrt{\pi a}}{K} \qquad (2)$$

The S stress is defined as the limit of the out plane stress σ_{zz} as r approaches zero on the crack flanks.

$$S = \lim_{r \to 0} \sigma_{zz} \qquad (\varnothing = \pm \pi) \qquad (3)$$

Therefore

$$\beta_S = \lim_{r \to 0} \frac{\sigma_{zz}\sqrt{\pi a}}{K} \qquad (4)$$

7.3.2. Line Spring Model

Following Levers and Radon (1983) the T stress is defined through a non-dimensional biaxiality parameter β.

$$\beta_T = \frac{T\sqrt{\pi a}}{K} \tag{5}$$

Here K is the mode I stress intensity factor. The stress intensity factor K may also be expressed in a non-dimensional form, such as :

$$K = \lambda \sigma \sqrt{\pi a} \tag{6}$$

This allows T to be written in the form

$$T = \lambda \beta_T \sigma \tag{7}$$

T may then be non-dimensionalised as a stress concentration factor (T/σ).

$$\frac{T}{\sigma} = \beta_T \lambda \tag{8}$$

In the elastic line spring analysis each section of the crack is regarded as a edge cracked bar subject to tension and bending. In linear elasticity the tension and bending components may be treated separately and then superimposed. Thus the T stress due to the tension component can be written as :

$$T = \lambda_T \beta_T \sigma \tag{9}$$

Where the subscript T denotes the appropriate factors for an edge cracked bar subjected to a tensile stress σ. The nominal tensile force at each section of the crack is given from the finite element analysis in the form of a force gradient denoted S_{11} :

$$s_{11} = \frac{\partial F}{\partial x} \tag{10}$$

from which :

$$\sigma = \frac{1}{t}\frac{\partial F}{\partial x} = \frac{S_{11}}{t} \tag{11}$$

For the tension component T can then written as :

$$T = \beta_T \lambda_T \frac{S_{11}}{t} \tag{12}$$

Turning now to the bending component, the stress intensity factor is usually non-dimensionalised in the form :

$$K = \lambda_B \frac{6M}{B t^2}\sqrt{\pi a} \tag{13}$$

where the subscript B denotes bending. It is convenient to define a nominal bending stress :

$$\sigma_B = \frac{6M}{B t^2} \tag{14}$$

This allows the T stress due to the bending component to be written as :

$$\frac{T}{\sigma_B} = \beta_B \lambda_B \tag{15}$$

Again finite element output for the line spring gives the moment at each section in the form of a moment gradient denoted S_{22} :

$$S_{22} = \frac{\partial M}{\partial x} \tag{16}$$

From which :

$$T = \beta_B \lambda_B \frac{6}{t^2} S_{22} \tag{17}$$

Finally the combined loading case is considered by adding the tensile and bending components :

$$T = \beta_T \lambda_T \left(\frac{S_{11}}{t}\right) + \beta_B \lambda_B \left(\frac{6}{t^2}\right) S_{22} \tag{18}$$

To simplify this calculation values of $\beta_T \lambda_T$ and $\beta_B \lambda_B$ are given in Figs (7.2 a) and (7.2 b) as a function of (a/W) from the data of Sham (1989).

7.4. Numerical Methods.

7.4.1. Continuum Model

Pipes containing circumferential cracks with (a/t) ratios varying from 0.1 to 0.9 have been modelled with continuum elements as shown in Fig (7.3). The models were meshed using 8-noded biquadratic

axisymmetric elements. Symmetry allows a quarter of the model to be modelled. The material response was linear elastic with Youngs modulus (211 GPa) and Poisson's ratio 0.3. Uniform displacement was applied on the remote boundary of the model to create a uniform tensile loading.

7.4.2. Line Spring Model

Cylinders with an axisymmetric circumferential crack with (a/t) ratios between 0.1 and 0.9, and subjected to uniform tension were analysed by the shell line-spring method. These models were meshed with 8-noded shell elements and corresponding 3-noded (symmetry plane) line spring elements type provided by the finite element code ABAQUS (1984). Due to symmetry only quarter of the model was modelled as shown in Fig (7.4). The crack depth (a) is defined by the (* SURFACE FLAW) option provided by ABAQUS, by giving a constant depth to the node set located on the crack line, as well as identifying which surface of shell was cracked. The material was elastic with the same material properties used in the continuum model.

7.5. Calculations of the S Stress

Let U_r represent the displacement in the r direction for any node located at the crack section, and R be the radius of the cylinder. Therefore the strain in the third direction is equal to :.

$$e_z = \frac{u_x}{R} \qquad (19)$$

$$e_z = \frac{1}{E}(S - \upsilon T) \tag{20}$$

Therefore :

$$S = \frac{E u_x}{R} + \upsilon T \tag{21}$$

The amplitude of the S stress is defined through a biaxiality parameter β_S :

$$\beta_S = \left(\frac{E u_x}{R} + \upsilon T\right) \frac{\sqrt{\pi a}}{K} \tag{22}$$

T is the first non-singular term the (T-stress) given by equation (18) and K is the stress intensity factor.

7.6. Results and Discussion.

Fig (7.5) shows the biaxiality parameter β_T corresponding to the first in plane non-singular term T plotted as a function of the ratio a/t. The results show that all geometries exhibit a negative biaxiality β_T. Results for the biaxiality parameter β_S corresponding to the second non-singular term S-stress are plotted as a function of the a/t ratio and are shown in Fig (7.6). These results indicate that all the geometries show negative biaxiality β_S

Fig (7.7) shows the biaxiality parameter β_T of the continuum model, plotted against a/t and compared with biaxiality parameter values calculated using the shell-line spring model. The comparison shows that there is a good agreement between the results of the two

methods. Results of the biaxiality parameter β_s are also compared with those obtained from the shell-line spring model. Results corresponding to both models are similar and again there is very good agreement as shown in Fig (7.8).

7.7. Conclusions.

Good agreement has been found between the results of the continuum model and shell-line spring models of axisymmetric cracked pipes. The agreement confirms the observation that the line spring method is an accurate and efficient computational method and provides an inexpensive evolution of the non-singular terms T and S with acceptable accuracy.

7.8. References:

Al-Ani, A.M. and Hancock, J.W., (1991), J Dominance of Short Cracks in Bending and Tension J. of Mech. Phys. Solids., 39, 23.

Betegón, C., and Hancock J., W.,(1991) J. Appl. Mech. in press

Du, Z. Z. and Hancock J.W. ,(1990) J. Appl. Mech. in press

Hibbitt, Karlsson and Sorensen Inc, (1984), ABAQUS User Manual, Providance., Rhode Island.

Huang, X. and Hancock, J. W., (1987) , Eng. Frac. Mech, 25,35.

Larsson, S. G. and Carlsson, A. J., (1973), J. Mech. Phys. Solids, 21,263.

Leevers, P. S. and Radon, J. C., (1983)., Int. J. Fracture.,19,13.
Parks, D. M., (1981) Int. J. of pressure Vessel Technology., 13,246.

Rice, J. R., and Levy, N. J., (1972)., J. Appl.Mech., 39,185-195.

Sham, T. L., (1989), The Determination of the Elastic T-Term using Higher Order Weight Functions. Department of Mechanical Engineering. Tory, New York 12180, U.S.A.

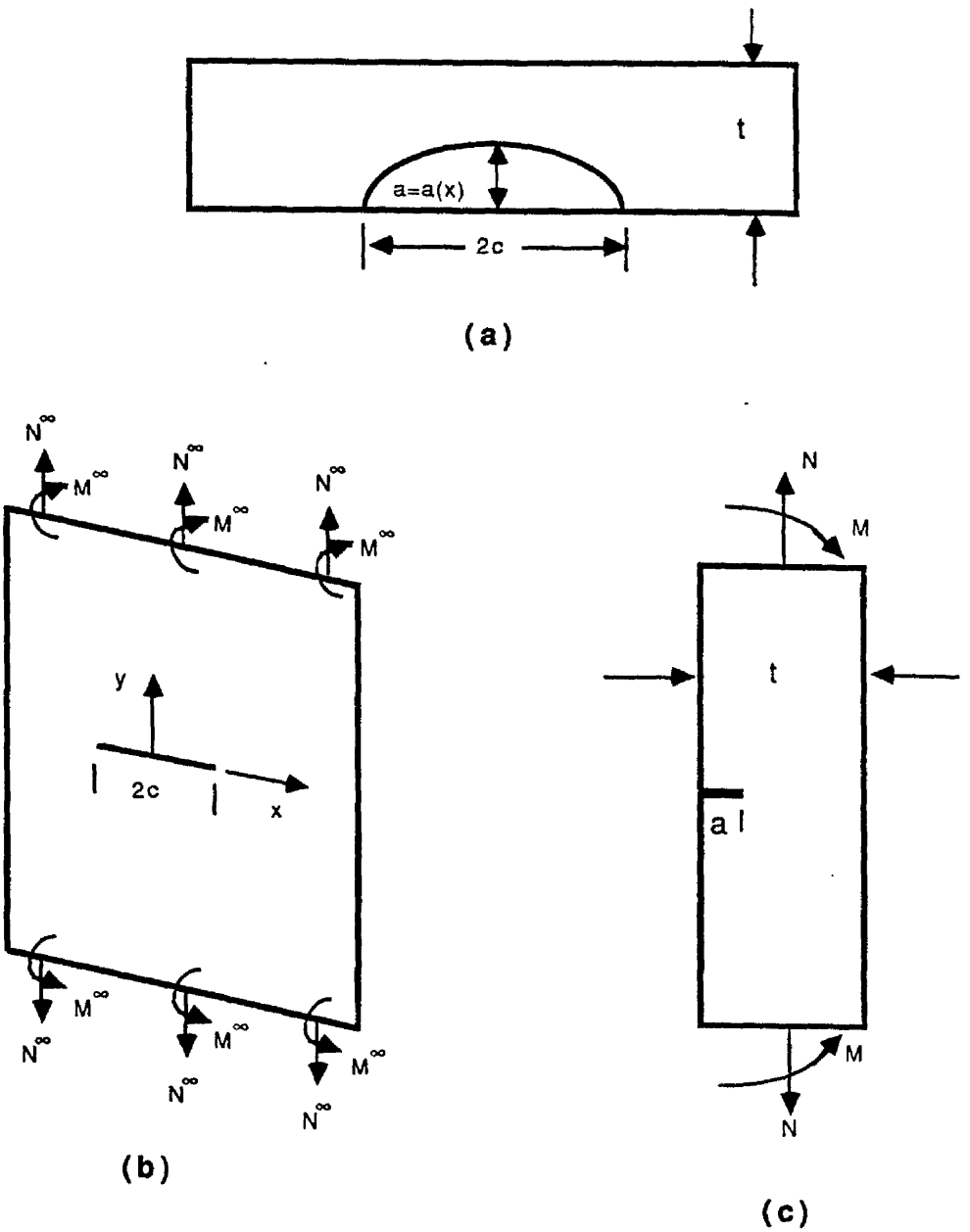

Fig (7.1) : Schematic illustration of the essential components of the line spring model

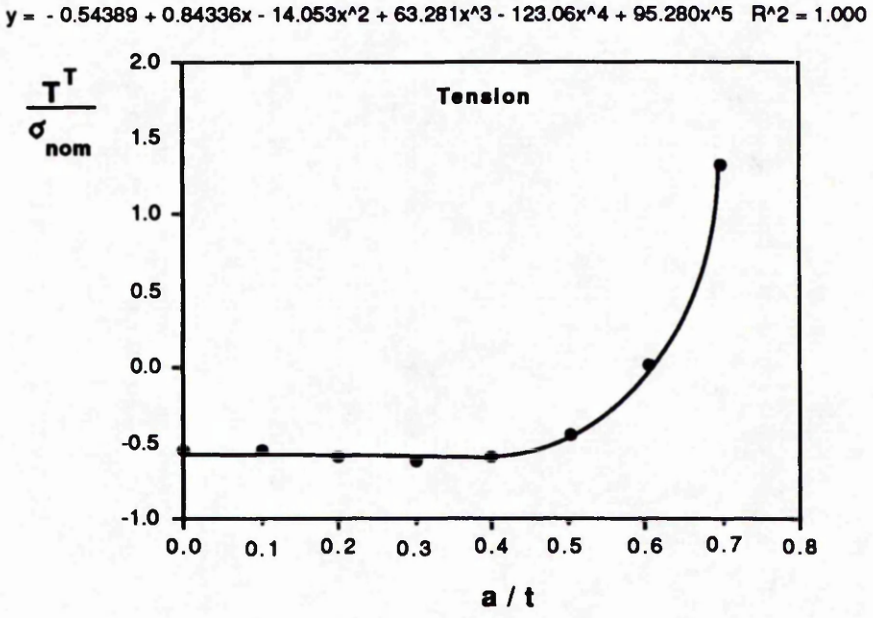

(a)

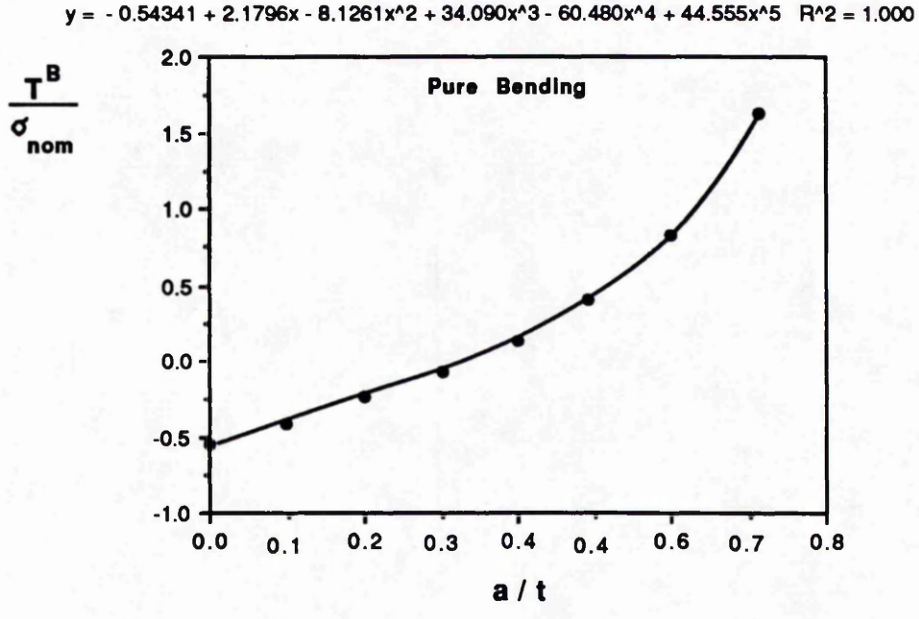

(b)

Fig (7.2) : Normalised T stress as a function a/t for
(a) : Single edge cracked bar in tension.
(b) : Single edge cracked bar in bending.

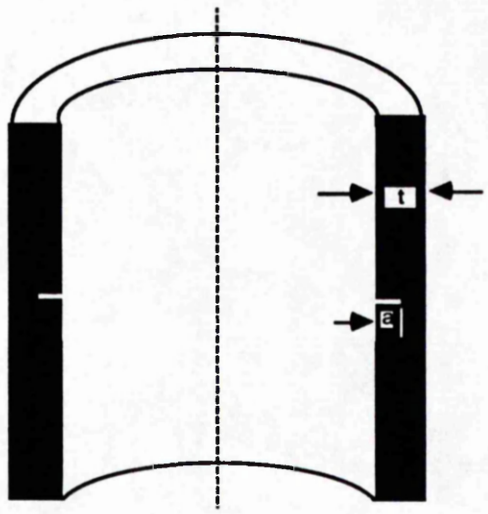

(a)

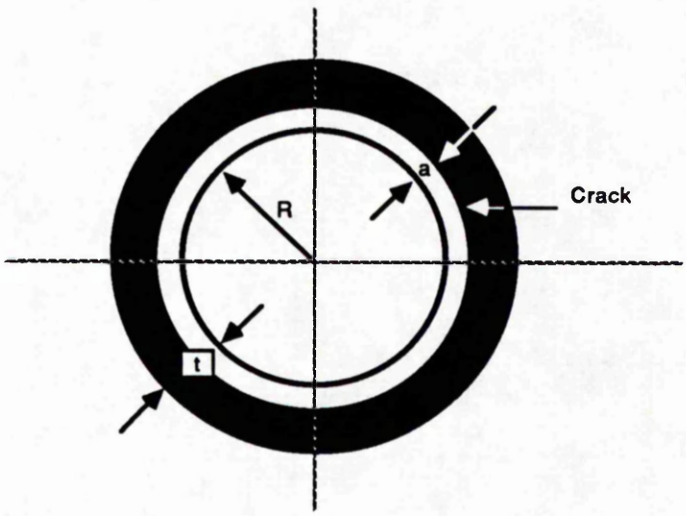

(b)

Fig (7.3) : Schematic illustration of pipe with internal circumferential crack

(a) : Continuum model

(b) : Shell-Line spring model

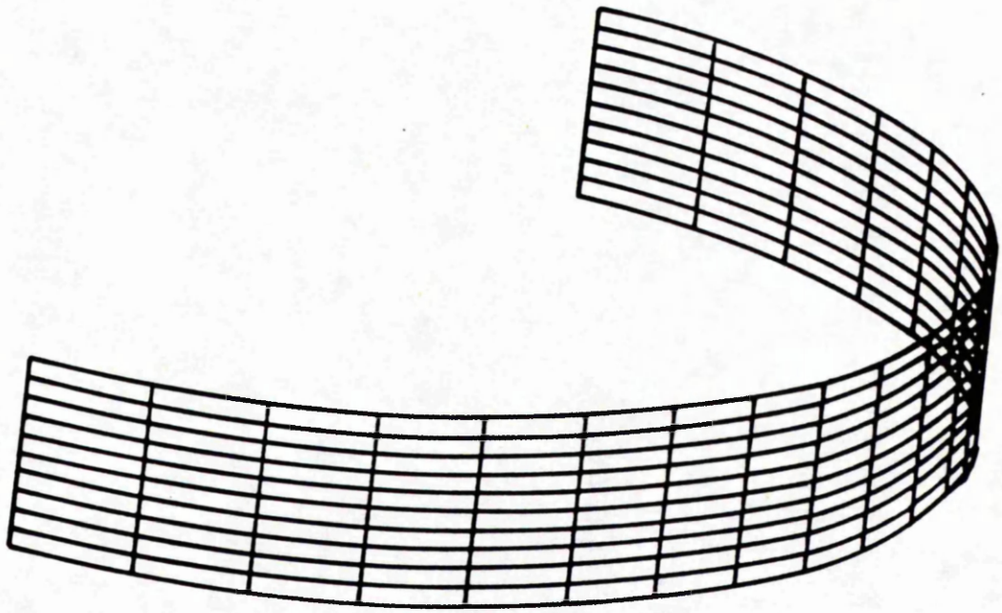

Fig (7.4) : Finite element mesh of the shell model.

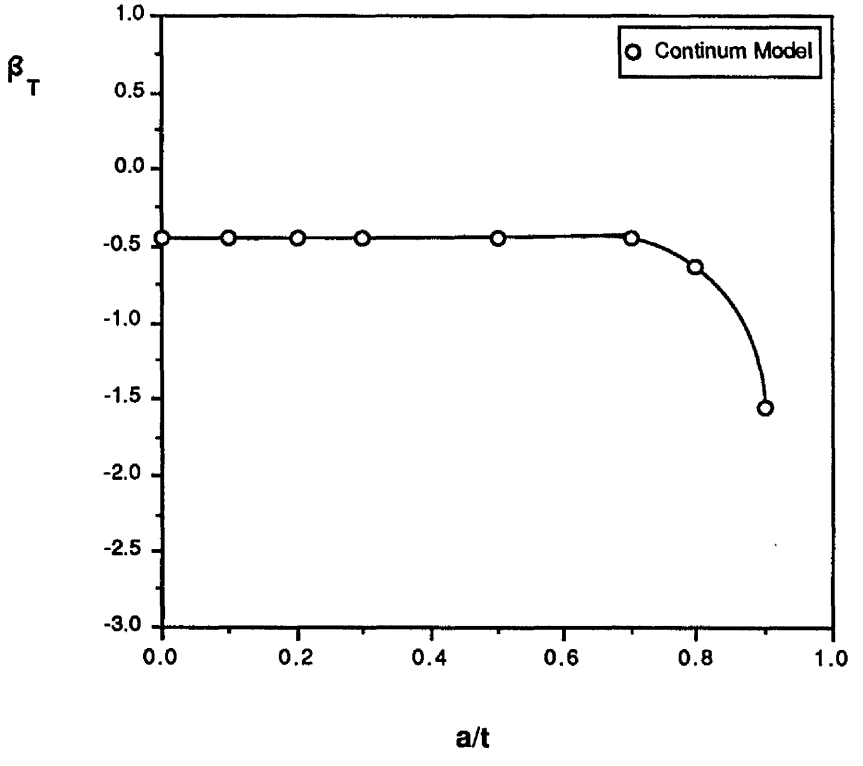

Fig (7.5) : Biaxialty parameter β_T as a function of a/t

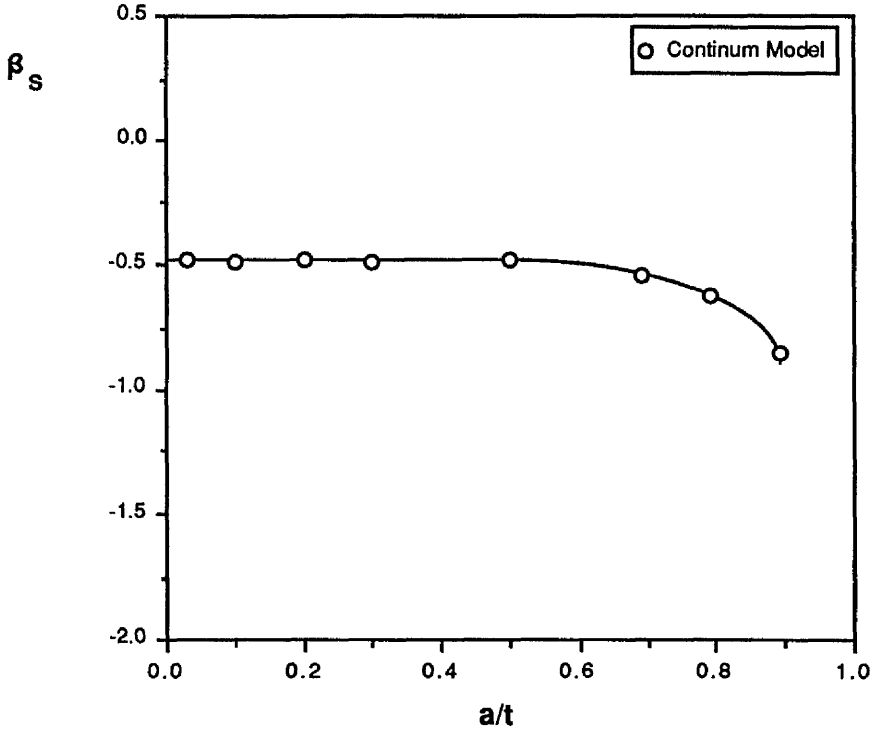

Fig (7.6) : Biaxialty parameter β_s as a function of a/t

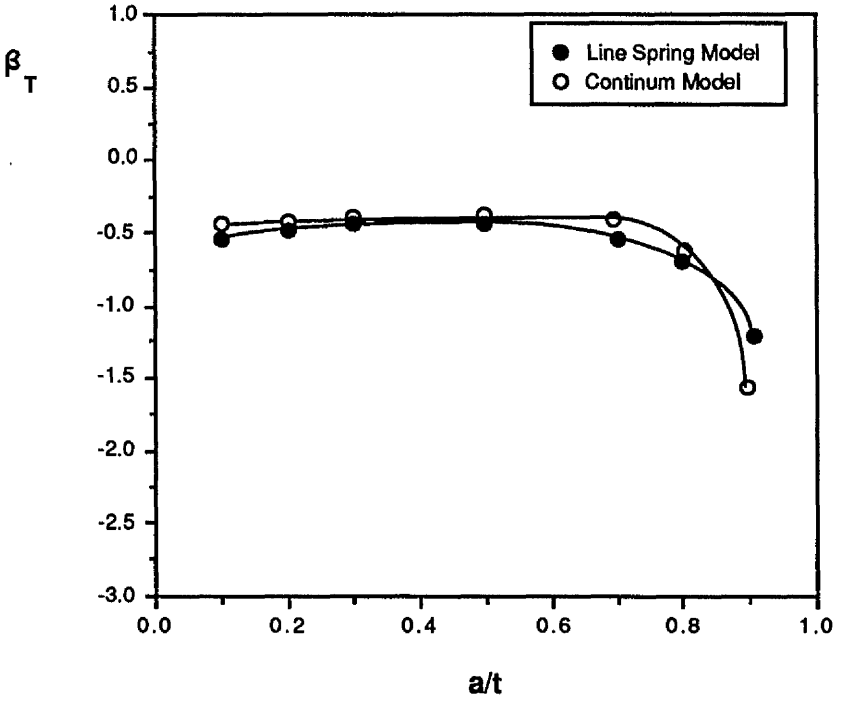

Fig (7.7) : Comparison of biaxialty barameter β_T obtaind from shell-line spring model and finite element contiuum model

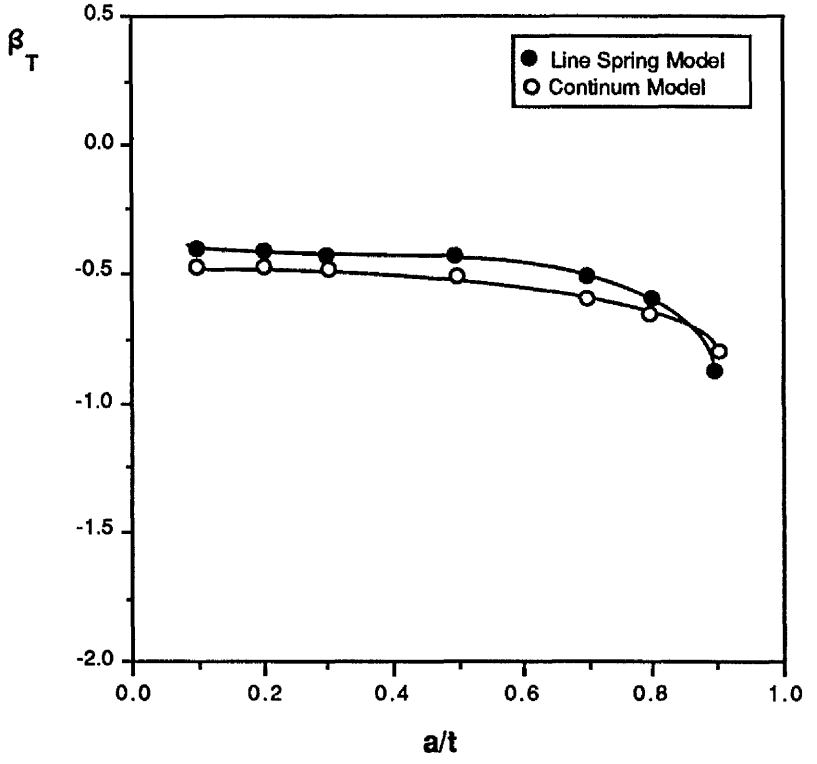

Fig (7.8) : Comparison of biaxialty parameter β_T obtaind from shell-line spring model and finite element contiuum model.

Chapter (8)

T Stress Analysis of Internal Longitudinal and Circumferential Semi-elliptical Cracks in an Internally Pressurised Cylinder

8.1. Introduction.

The T stress for longitudinal and circumferential semi-elliptical surface cracks located on the inner surface of a pressurised cylinder has been calculated using a finite element technique. The analysis is based on the line-spring model introduced by Rice and Levy (1972), which has been extended to calculate T, and thus infer the crack tip constraint

8.2. Geometry and Finite Element Model.

Two cylinders have been considered. The first one has a radius to wall thickness ratio t/R=0.1.The second has t/R=0.01. The stress intensity factors of both circumferential and longitudinal cracks in pipes of this size have been considered by Raju and Newman(1982) using brick elements and by Delale and Erdogan(1982) using line springs. This problem thus provides a further convenient benchmark for the numerical techniques. Following the benchmark problem, the problem of main interest has been considered. This comprises of an internally pressurised cylinder with a radius to wall thickness t/R=0.01. Both cylinders had length to radius ratio L/R=3 and contained an internal longitudinal or circumferential surface cracks with a depth (a/t)=0.2 and aspect ratio (a/c=0.2). In all cases symmetry

allowed the problems to be represented by a symmetric quarter as shown in Figs (8.1a,b). The models were meshed with eight noded isoparametric shell elements provided by the finite element code ABAQUS (1984). The model comprised 300 shell elements which were refined around the crack. The crack itself was represented by five 3 noded line spring elements. The models were restrained from a rigid body motion by pinning one node remote from the crack. This produced no problems with the (t/R= 0.1) cylinder, but led to local mesh distortions for (t/R=0.01), however being remote from the crack this appeared to have little effect on the stress intensity factors or the calculated T stresses.

8.3. Material and Loading

The material response was linear elastic with Young modulus (211 GPa) and Poisson's ratio 0.3. For both cracks the loading consisted of a uniform internal pressure applied to all of the shell elements, with a uniformly distributed force applied to the remote end of the cylinder corresponding to closed end conditions. As a variation on the problem uniform internal pressure was applied to all of the shell elements, and the line-spring elements (the exposed crack face) with uniformly distributed stresses applied to the remote end of the cylinder corresponding to closed end conditions.

8.4. Results.

Figs (8.2 through to 8.5) show the stress intensity factors for cylinders with (t/R=0.1 and 0.01), for both longitudinal and

circumferential cracks. The results are given in terms of the angle (ø) along the surface crack, such that the deepest point of the crack is located at $\pi/2$ and the free surface at $\phi = 0$. The mode I stress intensity factors K were normalised by

$$\frac{PR}{t}\sqrt{\frac{\pi a}{Q}} \qquad (1)$$

where P is the applied pressure, R is the inner radius of the cylinder, t is the wall thickness and Q is the shape factor for an elliptical crack which is a square of the complete elliptic integral of the second kind.

Figs (8.6 through to 8.9) show the values of the normalised T-stress as a function of the parametric angle (ø)). For both the longitudinal and the circumferential surface cracks T was normalised by (PR/t) which is the nominal hoop stress ($\sigma_{øø}$) for a thin walled cylinder. Finally Figs (8.10 through 8.13) show the biaxiality parameter β as a function of the non-dimensionalised angle (ø) along the crack face for both cylinders with (t/R=0.1 and 0.01), with longitudinal and circumferential cracks.

8.5. Discussion.

The cylinder with (t/R) =0.1 containing a longitudinal crack with (a/t)=0.2 and (a/C=0.2) was chosen as a benchmark problem for comparison with the detailed three dimensional finite element solution of Raju and Newman (1982) and the line spring analysis of Delale and Erdogan (1982). A comparison of the stress intensity factors is given

on Fig (8.14). The present results agree well with both solutions for the deepest section of the crack. However the results diverge from the solution of Raju and Newman (1982) as the free surface is approached, as it has been widely recognised that the physics of the line-spring breaks down close to the surface. In the present context, the benchmark suggests that reliable results may be expected from T stress calculations in the deepest section of the crack, but that some caution should be exercised over results close to the free surface

The central result of the T stress calculations is that T is negative around the perimeter of the crack. The significance of this result lies in the recent work of Hancock and co-workers (Betegón and Hancock 1991, Al-Ani and Hancock 1991, Du and Hancock 1991, Sumpter and Hancock 1991) who have shown that compressive T stresses associated with a loss of crack tip constraint and an enhanced fracture toughness above that expected from a valid J_{Ic} test.

8.6. References.

Al-Ani A and Hancock J.W (1991). J. Mech. Phys. Solids 39, 23.

Betegón and Hancock J.W.(1991) J.Appl Mech. in press

Du Z.Z. and Hancock J.W.(1991) , J. Mech. Phys. Solids in press.

Delale, F., and Erdogan, F.,(1982) J. Appl. Mech., 49,97.

Hibbitt, Karlsson and Sorensen, Inc., (1984), ABAQUS Users Manual, Providence., Rhode Island.

Leevers, P.S., and Radon, J. C. (1983), Int. J. Fracture, 30,301.

Raju I. S.and Newman, Jr, J. C. (1982), J. of. Pressure Vessel Technology 4, 293.

Rice, J.R., and Levy, N. J., (1972), J. Appl. Mech., 39,185-195.

Sham, T. L., (1989), The Determination of the Elastic T-Term using Higher Order Weight Functions. Department of Mechanical Engineering. Troy, New York 12180-3590,U.S.A.

Sumpter J and Hancock J.W.(1991) Int J Pressure Vessel Tech in press.

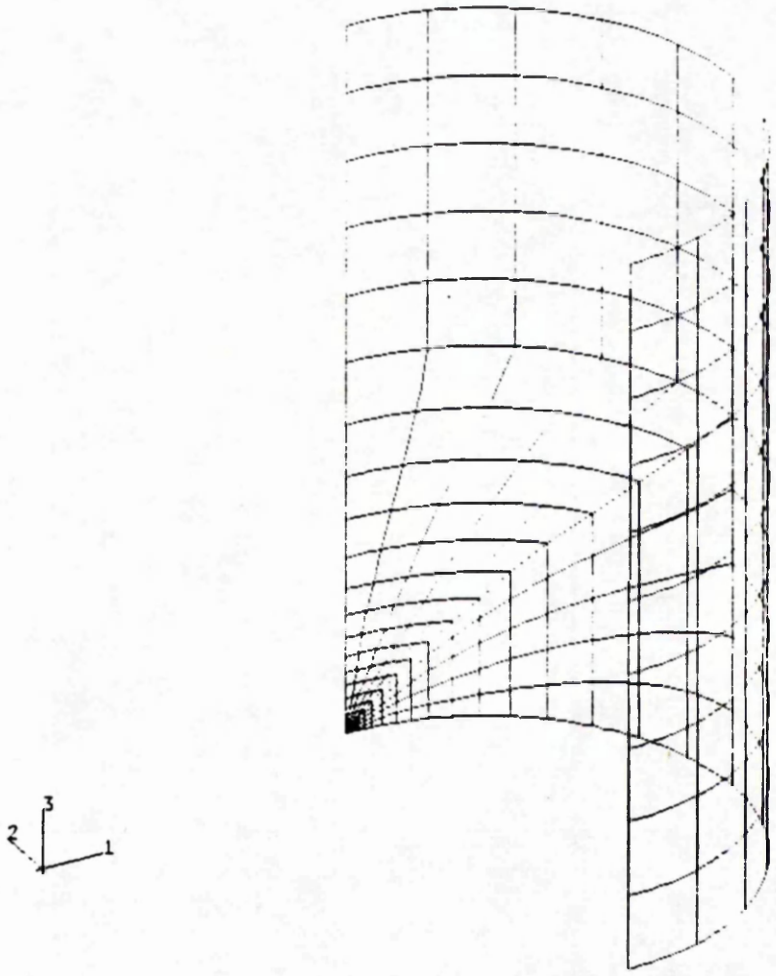

(a) : Undeformed mesh.

Fig (8.1) : Finite element model for a semi-elliptical crack in an internally pressurised cylinder

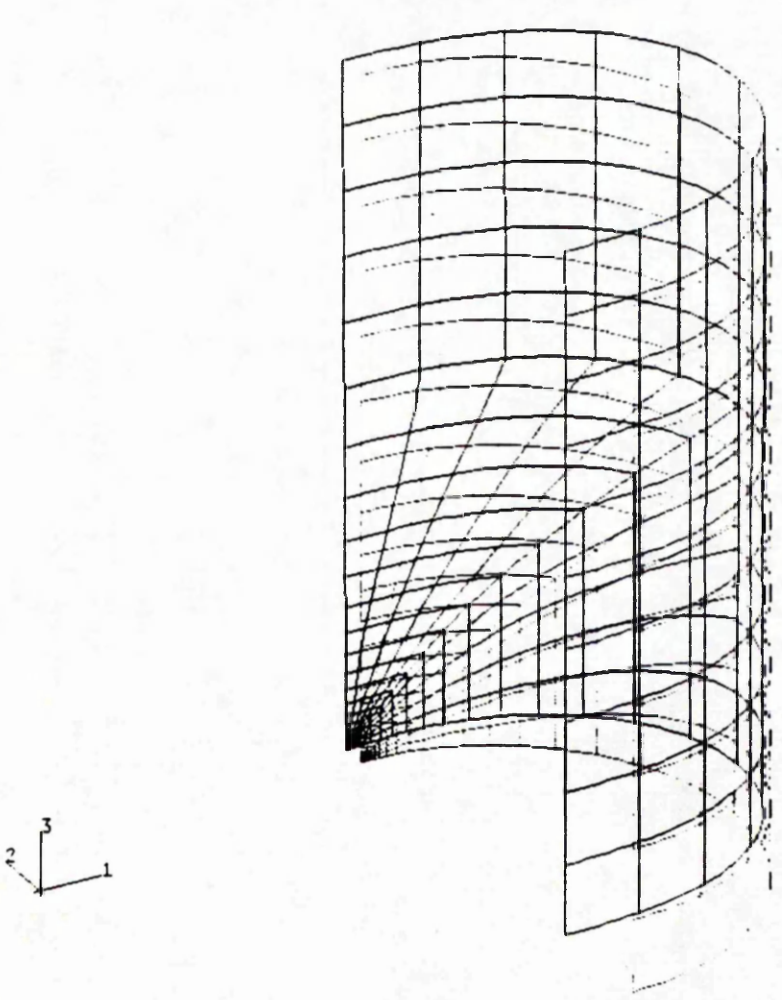

(b) : The deformed mesh.

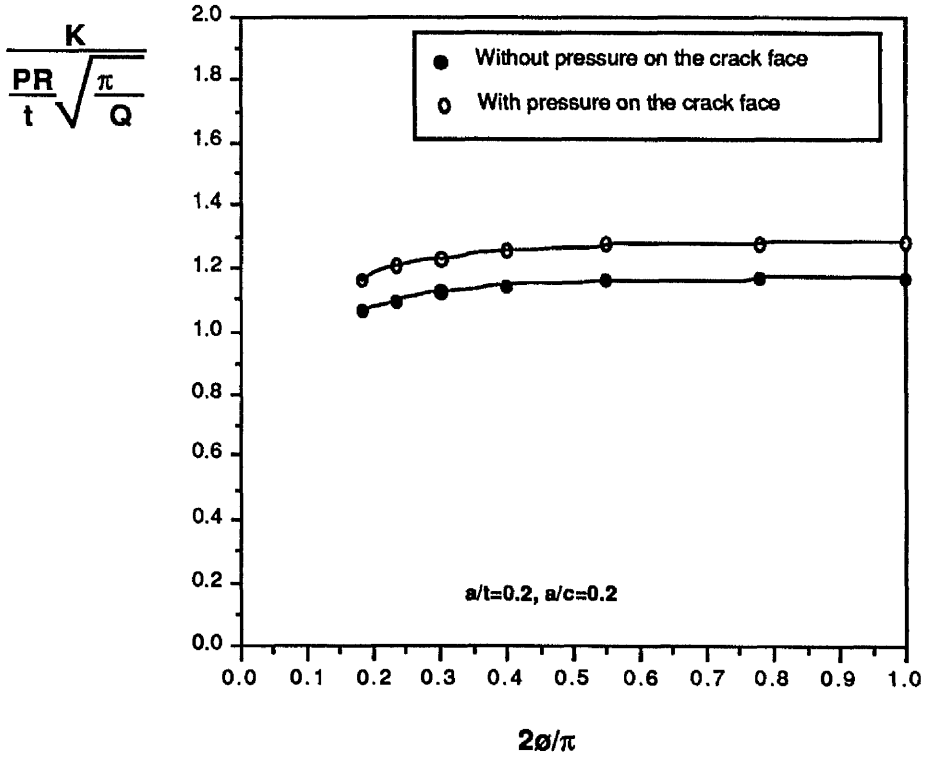

Fig (8.2) : Internal longitudinal crack in an internally pressurised cylinder with (t/R=0.1)

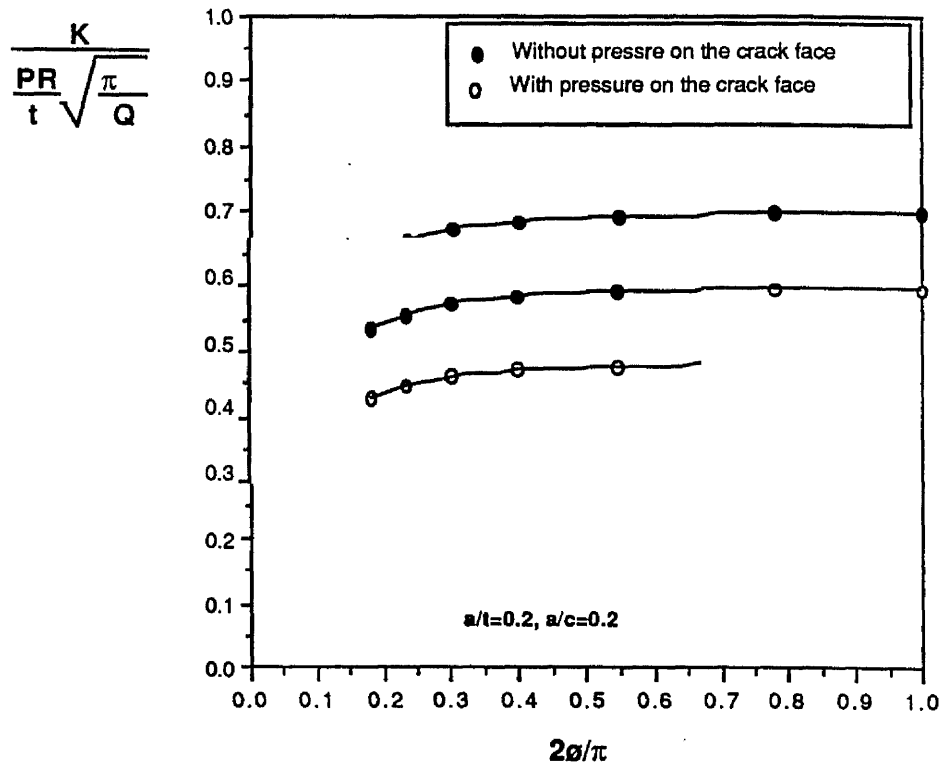

Fig (8.3) : Internal circumferential crack in an internally pressurised cylinder with (t/R=0.1)

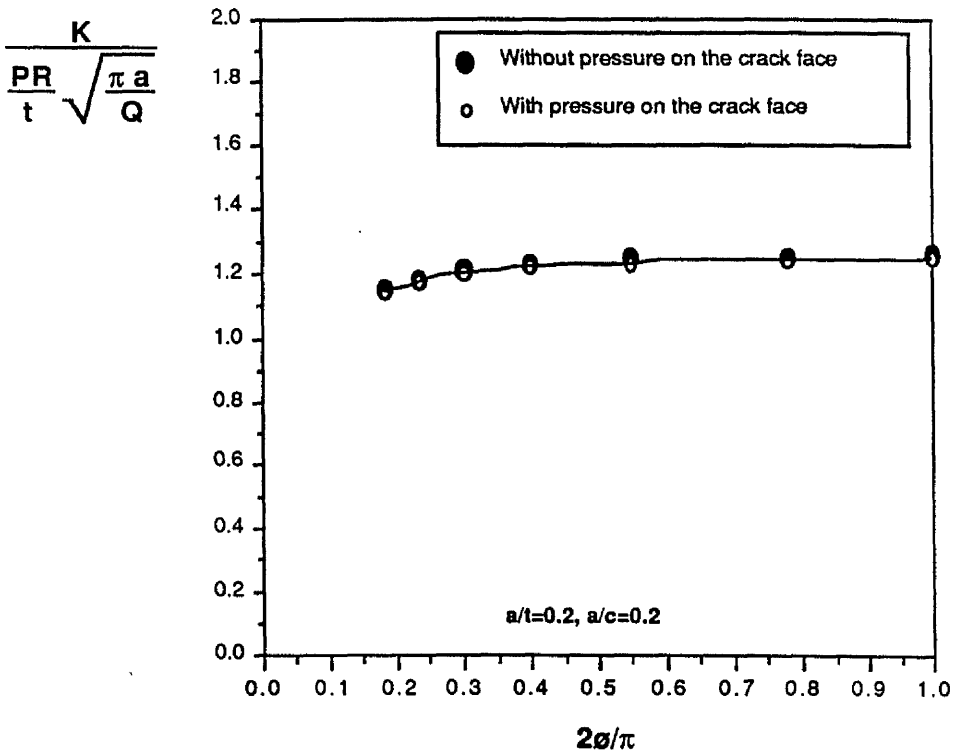

Fig (8.4) : Internal longitudinal crack in an internally pressurised cylinders with (t/R=0.01)

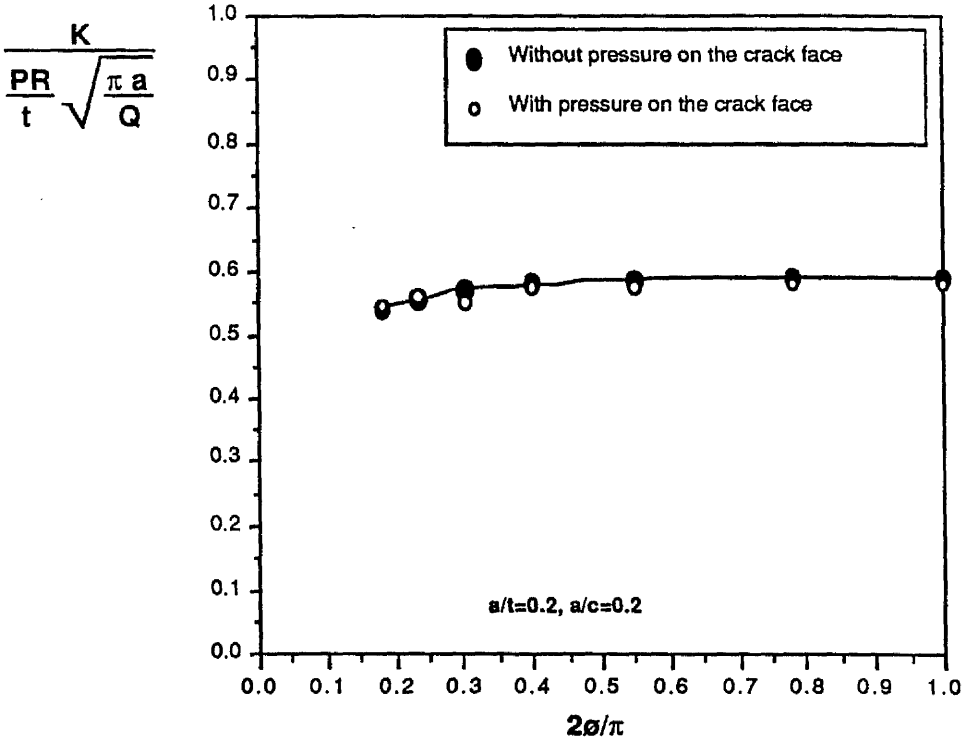

Fig (8.5) : Internal circumferential crack in an internally pressurised cylinder with (a/t=0.01)

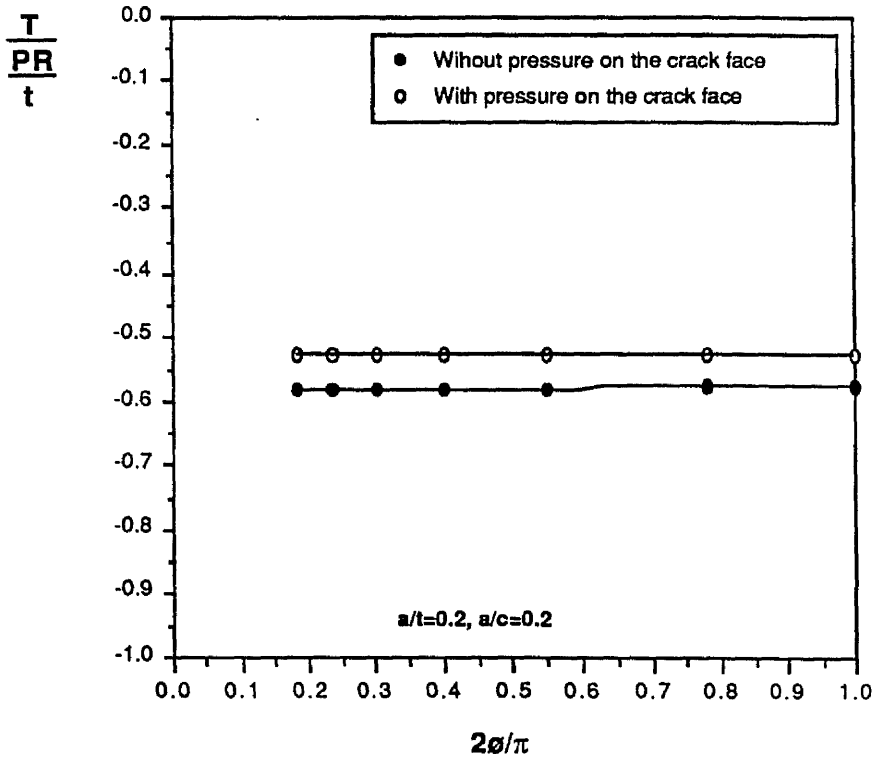

Fig (8.6) : Internal longitudinal crack in an internally pressurised cylinder with (at/R=0.1)

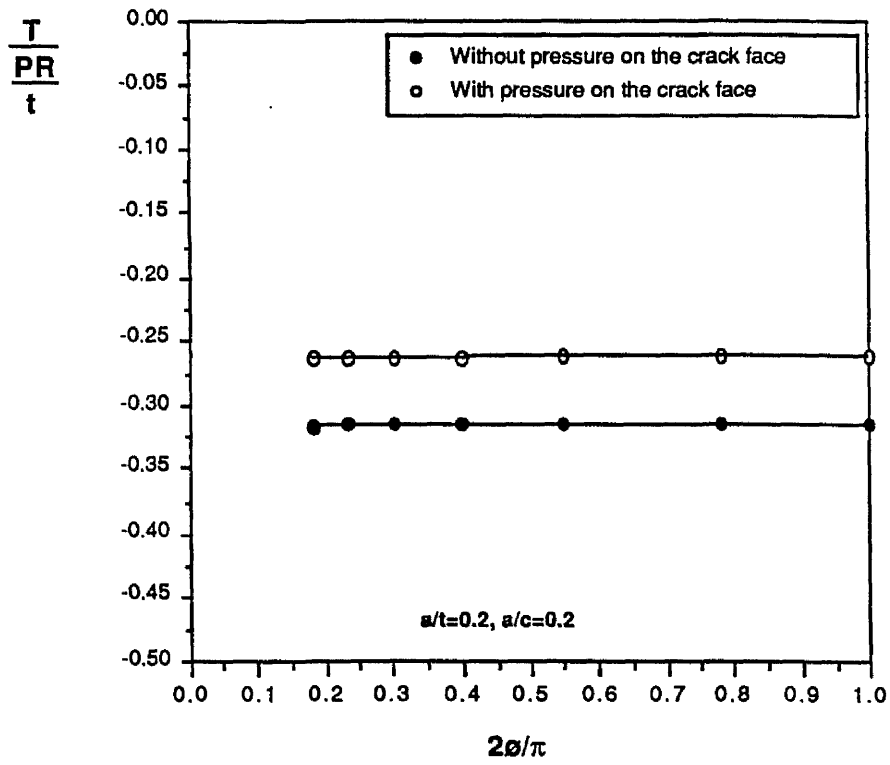

Fig (8.7) : Internal circumferential crack in an internally pressurised cylinder with (t/R=0.1)

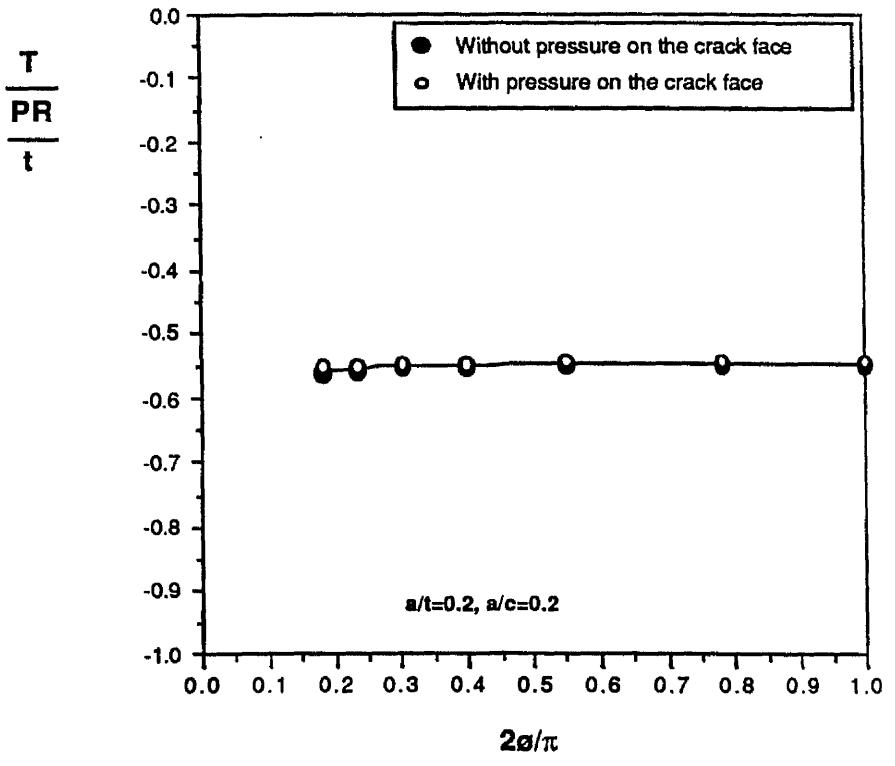

Fig (8.8) : Internal longitudinal crack in an internally pressurised cylinder with (t/R=0.01)

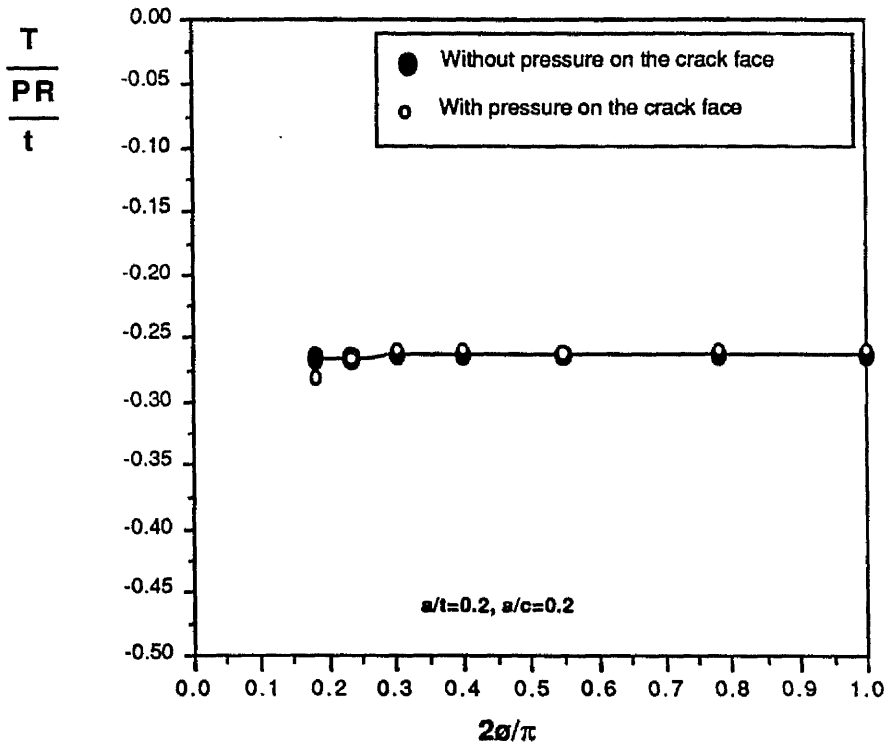

Fig (8.9) : Internal circumferential crack in an internally pressurised cylinder with (a/t=0.01)

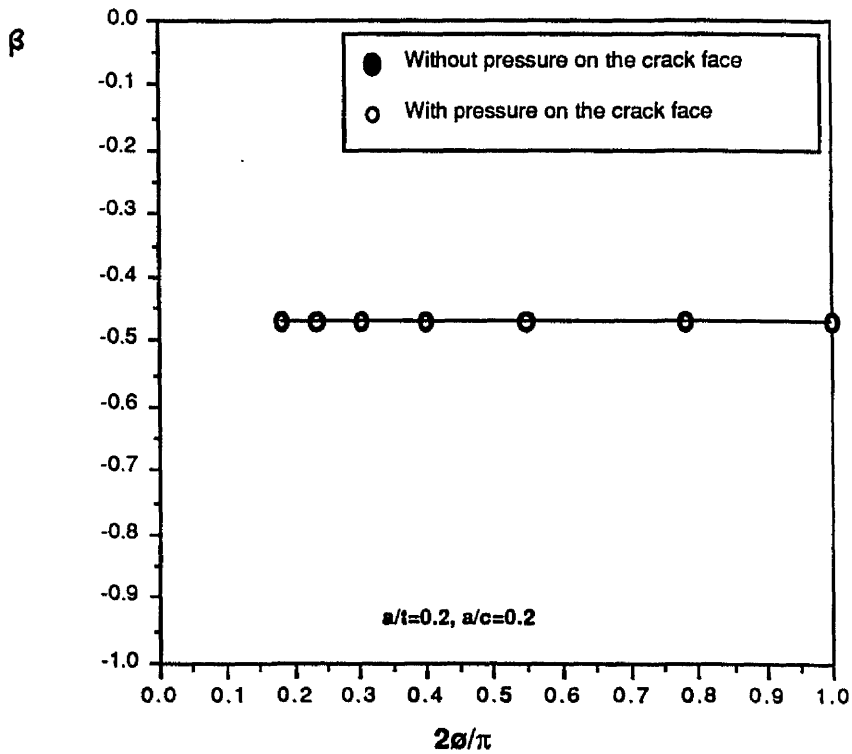

Fig (10) : Internally longitudinal crack in an internally pressurised cylinder with (t/R=0.1)

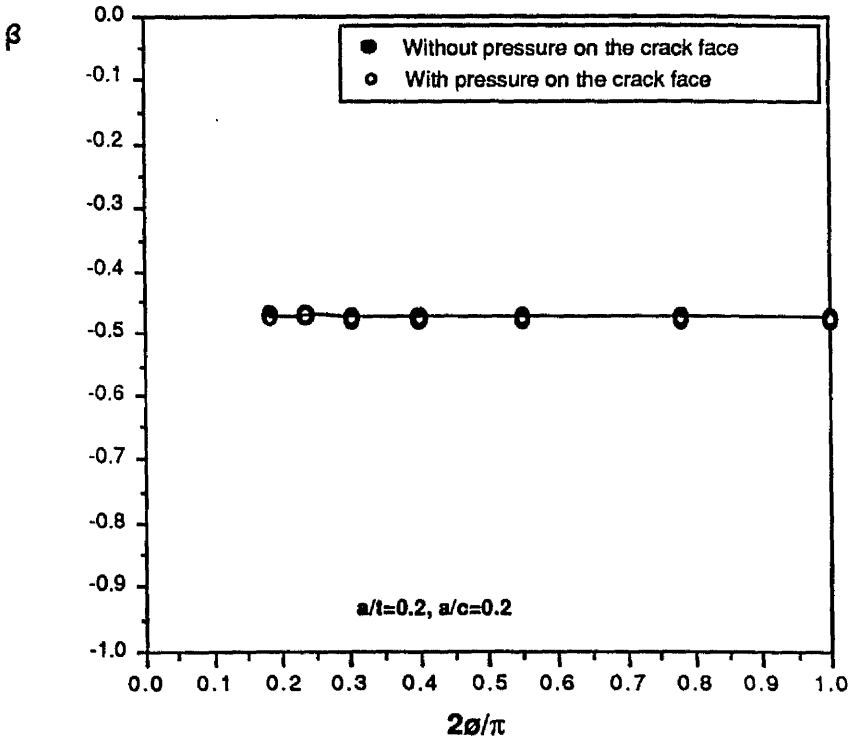

Fig (8.11) : Internal circumferential crack in an internally pressurised cylinder with (a/t=0.01)

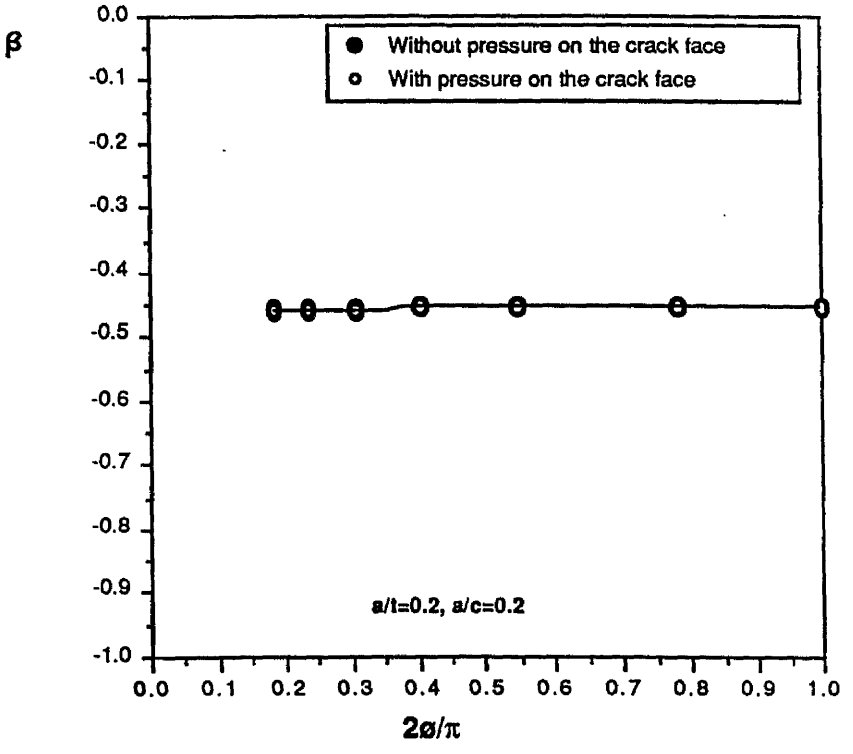

Fig (8.12) : Internal longitudinal crack in an internally pressurised cylinder with (a/t=0.01)

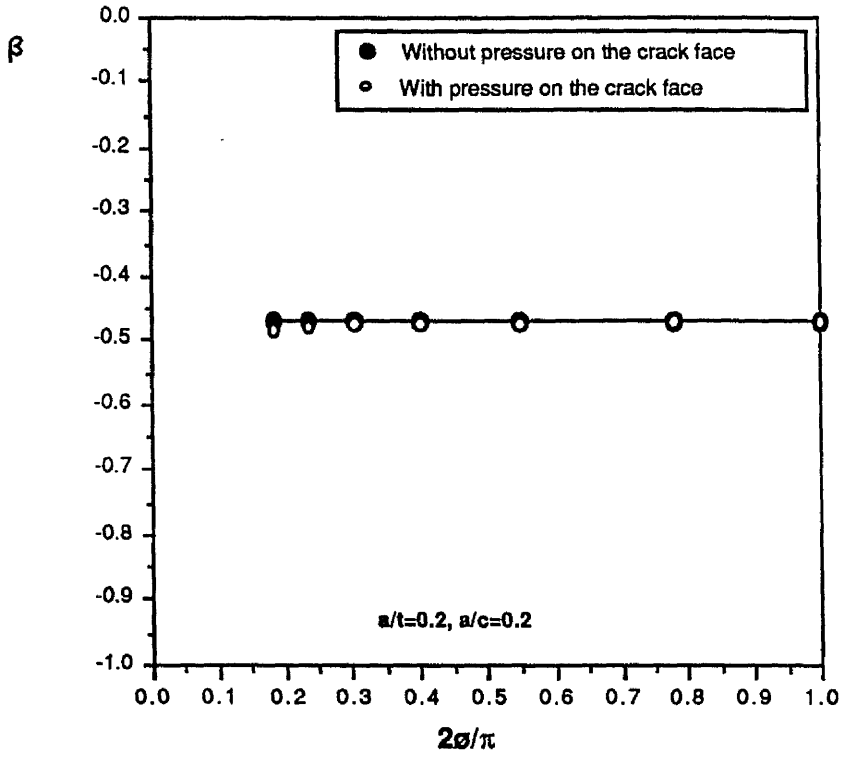

Fig (8.13) : Internal circumferential crack in an internally pressurised cylinder with (a/t=0.01)

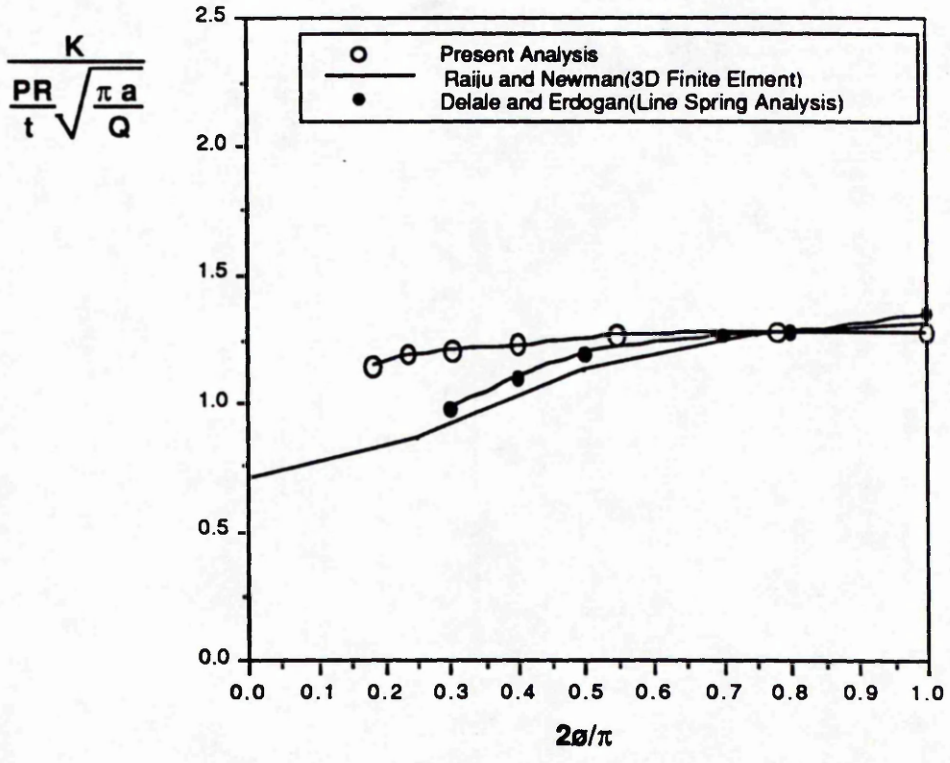

Fig (8.14) : Comparison of stress-intensity factors for internal surface crack in an internally pressurised cylinder (t/R=0.1; a/c=0.2; a/t=0.2)

Final Conclusions

The basis of classical elastic -plastic fracture mechanics is an analysis by Hutchinson(1968), Rice and Rosengren (1968) of the leading term in the non-linear asymptotic expansion of the stress field ahead of a crack tip. Here the deformation is characterised by a single parameter such as the crack tip opening displacement, δ, or the J integral. The basis of the one parameter approach to fracture using J or δ is that the stress field must be uniquely characterised by J or δ for different crack geometries. However the validity of the HRR field is subject to size requirements. The present work, and that of Al-Ani (1988), has shown that shallow cracked bars in bending and tension do not exhibit fields which can be characterised by J or δ at significant levels of plasticity. For extensive levels of plasticity the loss of single parameter characterisation or J dominance is associated with the lack of uniqueness of the fully plastic flow fields. Specifically it has been shown that for short cracks plasticity breaks back to the cracked surface, whereas deeply cracked geometries plasticity is limited to the ligament. However the present work has shown that J dominance is not lost abruptly, but evolves from the small scale yielding field, through the effect of the non-singular elastic T stress.

The T stress has been calculated as a function of (a/W) for edge cracked bars in tension and bending. The calculations used direct stress and displacement methods, which were benchmarked against published solutions. The central result was that edge cracked bars with (a/W) ratios of less than 0.35 in bending and 0.55 in tension exhibit negative T stresses, while geometries with deeper cracks exhibited positive T stresses. A remarkable correlation has been demonstrated

between the form of the fully plastic flow field and the T stress. Geometries with negative T stresses exhibit flow fields in which plasticity breaks back to the cracked surface developing unconstrained flow fields at the crack tip. Geometries with positive T stresses develop constrained flow fields which are confined to the ligament.

In order to examine the development of fully plastic plane strain flow fields from small scale yielding, modified boundary layer formulations have been used within the framework of small deformation plasticity. Interest was centered at distances of the order of $2J/\sigma_0$ which corresponds to a distance of one or two crack tip openings from the blunting tip, and represents the closest distance at which small strain theory can be applied. The loss of single parameter characterisation was associated with negative T stresses and the introduction of significant higher order terms in the non-linear expansion. A comparison between the modified boundary layer formulations and the full field solutions was achieved by identifying T with the elastic component of J as determined by virtual crack extension. The success of this correlation indicates the potential for a two parameter characterisation of elastic-plastic crack tip fields as discussed by Betegón and Hancock(1991). The issue of J dominance is thus resolved as corresponding to conditions in which the higher order terms in the non-linear asymptotic expansion are negligible in comparison to the leading HRR term, and corresponds to conditions under which the T stress is tensile.

In the plane strain studies it was only necessary to consider the in plane non-singular stress, T, as the out of plane non-singular term, (S), is coupled to the in plane non-singular stress by the plane strain condition and the stress strain relation. However for three

dimensional defects such as cracks in cracks in round bars, and semi-elliptical cracks in plates, plane strain conditions do not apply, and it has therefore been necessary to determine the role of S. Both full field solutions and modified boundary layer formulations were considered. Modified boundary layer formulations of crack tip deformation were investigated under conditions of generalised plane strain. Result of the boundary layer formulations in which K, T and S were applied at the outer boundaries indicated that S had a weak effect on the crack tip fields within the limit that the out of plane strain is less than the yield strain. Two types of full field solution were examined: circumferential cracks in a round bar and central penny shaped cracks in a round bar. The non-singular stresses S and T were determined for these geometries as a function of (a/W). Subsequently, full field analyses of these geometries matched the modified boundary layer formulations, and confirmed that the out of plane non-singular stress has little effect on the stress field ahead of the tip. This suggested that J and T can be used to characterise crack tip deformation in three dimensional cracked geometries showing modest departures from plane strain, without the need to supplement them with an additional parameter such as S.

In order to complement the theoretical analyses an experimental; program was carried out on a carbon-manganese steel described as 50D under BS 4360. The tests were carried out on three point bend bars with a/W ratios of 0.1, 0.2, 0.3 and 0.5 under a range of temperatures from -196C to 23C. The data were expressed in the form of a J-T locus. The experiments supported the idea that single parameter characterisation by J was lost before J reached $a\sigma_o/200$. Out with the J dominance requirements the boundary layer formulations predict that failure should occur at a constant, geometry independent value of J for for tensile T stresses. While the toughness

should increase as the T stress became more compressive. These concepts were supported by the experiments in which the fracture toughness as measured by J or δ increased with decreasing crack length for $a/w < 0.3$, corresponding to negative and thus compressive T stresses.

To provide a workable fracture design approach based on the Jc-T locus, a method for calculating the T stress and hence the crack tip constraint associated with semi-elliptical defects has been developed. To avoid the difficulties associated with full three dimensional solutions a technique based on the line spring method, was extended to calculate T. The technique has been benchmarked against published K solutions for semi-elliptical defects. Further benchmarking has been applied to axisymmetric cracks in cylinders for which K and T have been determined by both continuum and line-spring methods.

In conclusion, the work presented makes a contribution to the characterisation of three dimensional defects and attempts to extend the limited range of applicability single parameter elastic-plastic fracture mechanics by the introduction of two parameter characterisation.

9.1. References

Al-Ani A. M. (1988), MSc Thesis. Mech. Eng. Dept., Glasgow Unviersity.

Betegón, C., and Hancock J., W.,(1991), J. Appl. Mech. in press

Hutchinson, J. W, (1968), J. Mech. Phys. Solids, 16, 13.

Rice, J. R. and Rosengren, G. F. ,(1968), J. Mech. Phys. Solids, 16, 1.